

Observed snow depth trends in the European Alps 1971 to 2019

Michael Matiu¹, Alice Crespi¹, Giacomo Bertoldi², Carlo Maria Carmagnola³, Christoph Marty⁴, Samuel Morin³, Wolfgang Schöner⁵, Daniele Cat Berro⁶, Gabriele Chiogna^{7,8}, Ludovica De Gregorio¹,
5 Sven Kotlarski⁹, Bruno Majone¹⁰, Gernot Resch⁵, Silvia Terzago¹¹, Mauro Valt¹², Walter Beozzo¹³,
Paola Cianfarra¹⁴, Isabelle Gouttevin³, Giorgia Marcolini⁸, Claudia Notarnicola¹, Marcello Petitta^{1,15},
Simon C. Scherrer⁹, Ulrich Strasser⁸, Michael Winkler¹⁶, Marc Zebisch¹, Andrea Cicogna¹⁷, Roberto
Cremonini¹⁸, Andrea Debernardi¹⁹, Mattia Faletto¹⁸, Mauro Gaddo¹³, Lorenzo Giovannini¹⁰, Luca
Mercalli⁶, Jean-Michel Soubeyroux²⁰, Andrea Sušnik²¹, Alberto Trenti¹³, Stefano Urbani²², Viktor
10 Weilguni²³

¹Institute for Earth Observation, Eurac Research, Bolzano, 39100, Italy

²Institute for Alpine Environment, Eurac Research, Bolzano, 39100, Italy

15 ³Univ. Grenoble Alpes, Université de Toulouse, Météo-France, CNRS, CNRM, Centre d'Etudes de la Neige, Grenoble,
38000, France

⁴~~Winter Sports and Climate, WSL~~⁴WSL Institute for Snow and Avalanche Research SLF, Davos, 7260, Switzerland

⁵Department of Geography and Regional Sciences, University of Graz, Graz, 8010, Austria

⁶Società Meteorologica Italiana, Moncalieri, 10024, Italy

⁷Chair of Hydrology and River Basin Management, Technical University Munich, Munich, 80333, Germany

20 ⁸Department of Geography, University of Innsbruck, Innsbruck, 6020, Austria

⁹Federal Office of Meteorology and Climatology MeteoSwiss, Zurich-Airport, 8058, Switzerland

¹⁰Department of Civil, Environmental and Mechanical Engineering, University of Trento, Trento, 38123, Italy

¹¹Institute of Atmospheric Sciences and Climate, National Research Council, (CNR-ISAC), Turin, 10133, Italy

¹²Centro Valanghe di Arabba, Arabba, 32020, Italy

25 ¹³Meteotrentino, Provincia Autonoma di Trento, Trento, 38122, Italy

¹⁴Dipartimento di Scienze della Terra, dell'Ambiente e della Vita - DISTAV, Università degli Studi di Genova, Genova,
16132, Italy

¹⁵SSPT-MET-CLIM, ENEA, Rome, 00123, Italy

¹⁶ZAMG, Innsbruck, 6020, Austria

30 ¹⁷ARPA Friuli Venezia Giulia, Palmanova, 33057, Italy

¹⁸ARPA Piemonte, Torino, 10135, Italy

¹⁹Assetto idrogeologico dei bacini montani, Region Valle d'Aosta, Aosta, 11100 Italy / Fondazione Montagna sicura,
Courmayeur, 11013, Italy

²⁰Météo-France, Direction de la Climatologie et des Services Climatiques, Toulouse, 31057, France

35 ²¹Meteorology Office, Slovenian Environment Agency, Ljubljana, 1000, Slovenia

²²Centro Nivometeorologico, ARPA Lombardia, Bormio, 23032, Italy

²³Abteilung I/3 - Wasserhaushalt (HZB), BMLRT, Vienna, 1010, Austria

40 *Correspondence to:* Michael Matiu (michael.matiu@eurac.edu)

Abstract

The European Alps stretch over a range of climate zones, which affect the spatial distribution of snow. Previous analyses of station observations of snow were confined to regional analyses. Here, we present an Alpine wide analysis of snow depth from six Alpine countries: Austria, France, Germany, Italy, Slovenia, and Switzerland; including altogether more than 2000 stations, of which more than 800 were used for the trend assessment. Using a principal component analysis and k-means clustering, we identified five main modes of variability and five regions, which match the climatic forcing zones: north ~~and~~ high Alpine, northeast, northwest, southeast, and ~~southwest~~ south & high Alpine. Linear trends of ~~mean~~-monthly mean snow depth between 1971 ~~to~~ and 2019 showed decreases in snow depth for ~~87% of the most~~ stations. ~~December to February trends were on for November to May. The~~ average ~~-1.1 cm~~ trend among all stations for seasonal (November to May) mean snow depth was -8.4 % per decade⁺ (min, max: -10.8, 4.4; elevation range 0–1000 m), -2, for seasonal maximum snow depth -5 (-25.1, 4.4; 1000–2000 m), 6 % per decade, and -0.1 (-23.3, 9.9; 2000–3000 m), with stronger trends in March to May: -0.6 (-10.9, 1.0; 0–1000 m), -4 for seasonal snow cover duration -5.6 (-28.1, 4.1; 1000–2000 m) and -7.6 (-28.3, 10.5; 2000–3000 m), % per decade. However, regional trends differed substantially after accounting for elevation, which challenges the notion of generalizing results from one ~~Alpine~~ region to another or to the whole Alps. This study presents an analysis of station snow depth series with the most comprehensive spatial coverage in the European Alps to date.

1 Introduction

In the European Alps, snow is pervasive throughout nature and human society. Snow is a major driver of Alpine hydrology by storing water during the winter season, which gets released in spring and summer and which is used for water supply, agriculture, and hydropower generation. Water stored in the snow cover also feeds alpine aquifers through the network of fault and fracture systems. Ecologically, the mountain flora and fauna depend on the timing and abundance of snow cover (Esposito et al., 2016; Keller et al., 2005; Lencioni et al., 2011). Snow is tightly linked to human culture in the European Alps and has brought economic wealth to previously remote regions through tourism (Beniston, 2012a; Steiger and Stötter, 2013). Since snow cover depends on temperature and precipitation, ongoing climate change in the Alps and especially rising temperatures and changing precipitation patterns affect the abundance of snow (Beniston and Stoffel, 2014; Gobiet et al., 2014; Steger et al., 2013). Snow cover extent decreased globally, while for snow mass some regions experienced increases (Pulliainen et al., 2020). Decreases are expected for the future, especially at low elevations, with more uncertain trends in observations and future projections at higher elevation (Beniston et al., 2018; Hock et al., 2019; IPCC, 2019).

~~To~~ Observations are needed to assess ongoing changes in snow cover, ~~observations of the snow cover are required~~. The most widespread snow cover measurements are snow depth (HS), depth of snowfall (HN, also denoted fresh snow or snowfall),

snow water equivalent (SWE), snow cover area (SCA), and snow cover duration (SCD). Snow depth and ~~fresh snow~~depth of snowfall measurements have been scientifically documented in the European Alps since the late 18th century (~~Leporati and Luea, 1994~~)(Leporati and Mercalli, 1994). Such measurements indicate the height of the snow cover relative to the ground (snow depth) or a reference surface, usually a board (depth of snowfall), are performed each morning by observers, and only require a graduated stake or rod and a meter stick. While automatic sensors have been developed in the recent decades, most European weather and hydrological services continue with manual observations. Although there is a trend towards automatization, missing standards on the processing of the data (even at national level) impedes their uptake (Haberborn, 2019; Nitu et al., 2018). The main limitation of snow depth and ~~fresh snow~~depth of snowfall measurements is that their number decreases sharply with elevation, and only with few stations ~~are~~ available above 3000 m in the European Alps. SWE is the mass of snow per unit surface area, which corresponds to the amount of water stored in the snow cover and thus is a hydrological key variable. However, its measurement is far more complicated and available with lower temporal frequency than snow depth, and thus not as widely observed ~~and available with lower temporal frequency~~. SCA and SCD identify the spatial extent and temporal duration of snow on the ground. SCD can be inferred from snow depth measurements using a threshold, or more recently from satellite observations, which also allow SCA retrieval at different spatial scales from tens of metres to several kilometres. The main benefit of satellite observations is that they cover the whole elevational gradient and are also available in data-scarcer regions. Satellite observations can identify SCA and SCD at high spatial resolutions (1 to 5 km for decadal length time periods), and less accurately SWE at coarser resolution (~25km) (Schwaizer et al., 2020), ~~though~~, However, they typically cover a relatively short time period and are hampered by cloud cover and rugged topography (Bormann et al., 2018), and the satellite orbit might not provide a worldwide cover. An application of global satellite imagery for 2000-2018 has shown ~~snow~~SCD declines for 78% of global mountain areas ~~with significant changes~~ and only a few regions with increasing SCD (Notarnicola, 2020), although the short time span of 19 years is a limiting factor in interpreting these trends.

The European Alps are densely populated and have a long history of manual snow depth and depth of snowfall observations, which makes them ideal to study long-term trends over a large spatial domain with complex topography and strong climate gradients. Not surprisingly, ~~a vast array of much~~ literature on the topic exists; ~~however~~ (see Table B1 in Appendix B for an overview). However, most studies are limited in their spatial extent to regions or nations, restricted by a lack of data sharing, harmonized data portals, and joint projects or initiatives fostering such analyses (Beniston et al., 2018). ~~Exceptions include an Alpine wide analysis of SWE trends showing stronger and more significant decrease in spring than winter (Marty et al., 2017), which, however, considered a relatively limited number of locations since SWE measurements are rare and unevenly distributed; a pan-European study showing accelerating negative trends for mean winter snow depth (Bach et al., 2018), which, however, does not cover France and Italy, and covers only sparsely Austria and Slovenia, thus missing large parts of the European Alps; and finally an Austrian-Swiss study, identifying seven snow regions, strongest trends at high elevation, and a regional dependence of the trends (Schöner et al., 2019).~~

105 Most of the published literature is on Switzerland. Results include a regime shift in snow days at the end of the 1980s and no
clear trend until 2008 (Marty, 2008); differences between north and south Switzerland, more pronounced trends at low and
mid elevation, and a shorter SCD mainly because of earlier snow melt (Laternser and Schneebeli, 2003); an analysis of
extreme values that shows significant decreases in 44% of the cases for maximum snow depth (Marty and Blanchet, 2012); a
110 long term (1864–2009) seasonal analysis of depth of snowfall that shows strong decadal variability with high values 1900–
1920 and 1960–1980 (Scherrer et al., 2013); a mean December to February snow depth decline between 10 to 50% with
differences between the moist north and the dry south (Beniston, 2012b); and a study based on 11 stations over the time
period 1970–2015, which has shown significant reduction in SCD, on average by 8.9 days decade⁻¹, largely driven by earlier
snowmelt (on average 5.8 days decade⁻¹) (Klein et al., 2016).

In Italy, literature on snow mostly confined to regional analyses or comparisons between the eastern and western Italian
115 Alps. For the provinces of Bolzano and Trento, different dynamics were observed above and below 1650 m, larger
reductions at lower elevations, and strong changes in the late 1980s (Marcolini et al., 2017b). An analysis of stations in
Veneto and Aosta Valley showed a breakpoint around 1990, stronger negative trends below 1500 m and in spring, and
negative trends related to precipitation decreases (Valt and Cianfarra, 2010), as well as decreases in snow cover of 14 days
when comparing the period 1991–2007 to 1960–1990 (Valt et al., 2008). In Piedmont, the analysis of six long term snow
120 depth stations located between 960 and 2177 m showed a significant decrease of snow depth in the period 1951–2010, with
the main contribution coming from spring months (Terzago et al., 2013). Another study comparing monthly snow depth at
middle elevations (960–1589 m) in the decade 2000–2009 with respect to 1971–2000 showed increased snow depth in
November and December, decreased snow depth in January to April, and almost no residual snow in May (Terzago et al.,
2010). In the case of Friuli Venezia Giulia, positive anomalies were observed in the 1980s, shifts to low snow amounts until
125 the beginning of the 2000s, and some recovery afterwards (Micheletti, 2008).

For France, an analysis at Col de Porte showed a decrease of mean seasonal (December to April) snow depth between 1960
to 1990 and 1990 to 2017 of 39 cm, which corresponds to 40% of the mean snow depth 1960–1990. (Lejeune et al., 2019).
Other studies have focused on a reanalysis driven snow model (Crocus), instead of directly analysing station observations.
For the French Alps, results indicated no trends in December to February snow depth above 2700 m during 1959 to 2005,
130 and decreases below, as well as decreases in snow days at all elevations (Durand et al., 2009).

The high elevation snow network close to the observatory at Sonnblick in Austria, a research station at 3100 m in the vicinity
of several glaciers, showed outstanding large snow depths in the 1940s and 1950s, strong decreases afterwards, and clear
links between winter precipitation and snow depth (Schöner et al., 2009).

135 The most relevant findings of the latest literature on snow cover trends (Table B1) can be summarized as follows. Snow
variables exhibited a strong temporal and spatial variability (e.g. Beniston, 2012b; Schöner et al., 2019). Long-term analyses
identified periods of high snow cover in the 1940s/50s, as well as in the 1960s/70s, followed by absolute minima in the
1980s and early 1990s, with some recovery afterwards, but not to the pre-1980s values (Marty, 2008; Micheletti, 2008;

Scherrer et al., 2013; Schöner et al., 2009; Valt and Cianfarra, 2010). Trends were strongly related to elevation (Latarnser and Schneebeli, 2003; Marcolini et al., 2017b; Valt et al., 2008) and were mostly negative at low elevations (Bach et al., 2018), while higher elevations showed no change or even increases (Marty et al., 2017; Terzago et al., 2010). Snow melt was identified as the main contribution to the decreasing trends (Klein et al., 2016), which explains the pronounced trends at low elevations and in spring (Marty et al., 2017). Finally, after accounting for elevation, regional differences between trends were observed (Beniston, 2012b; Latarnser and Schneebeli, 2003; Schöner et al., 2019; Terzago et al., 2013).

Quantitatively synthesizing all these studies into a common Alpine view is challenging and hampers the provision of quality-ensured information on snow cover climatology and trends at the regional scale (Hock et al., 2019). This starts from the different definitions of the studied seasons, which range from December–February to October–May, and thus sometimes include start, middle, and end of the season. Difficulties also arise in the selection of existing snow variables and indices, such as mean snow depth, maximum snow depth, snow days (based on thresholds from 1 to 50 cm), 3-day cumulative values, etc. Naturally, the station series are of different lengths, and the studied periods get longer for the more recent studies. And finally, the statistical methods differ from one study to another: linear regressions, Mann-Kendall tests, Sen slopes, moving window approaches (windows ranging from 5 to 20 years), breakpoint analysis, principal component analysis / empirical orthogonal function analysis (PCA/EOF) and more.

To overcome these limitations, we embarked on the effort to collect and analyse an Alpine wide data set of snow measurements from stations covering Austria, France, Germany, Italy, Slovenia, and Switzerland. The main aim is to understand how changes in snow cover vary over space and time by applying the same methods to an as homogenous as possible Alpine wide data set. This approach avoids sub-regional perspectives, inconsistencies from single data sources and different methods, and influences of artificial boundaries such as national borders. Since we wanted the data collection effort to be of use for the scientific community, we provide as much as possible of the data openly accessible (as far as data policies allow us to). The remainder of the paper is structured as follows: Section 2 introduces the data and the statistical methods, Section 3 presents results and discusses them, while Section 4 ~~concludes~~provides conclusions.

2 Data and methods

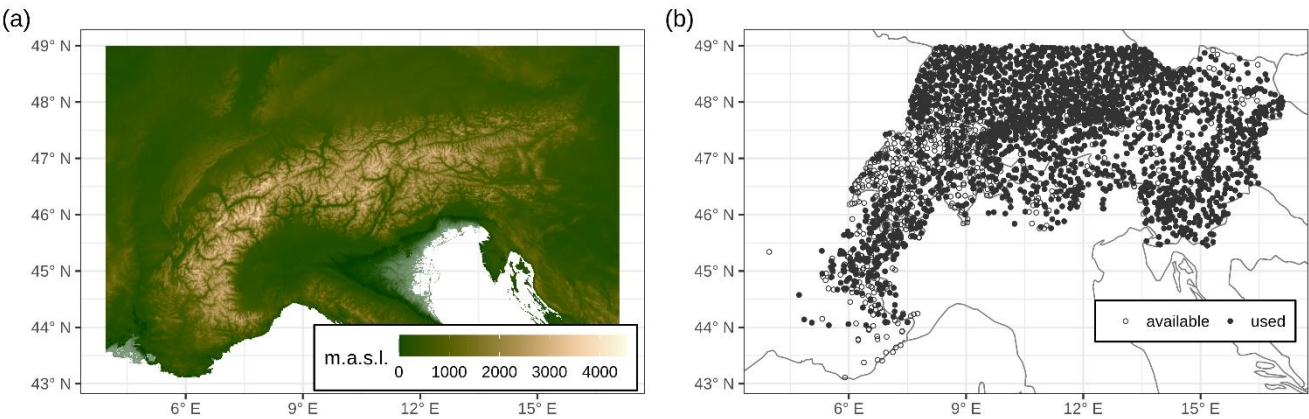
2.1 Study region

The European Alps extend, with their ~~typical~~ arc-shaped structure, over more than 1000 km from the French and Italian Mediterranean coasts to the lowlands east of Vienna, covering south-eastern France, Switzerland, northern Italy, southern Germany, Austria, and Slovenia (see Fig. 1 (a)). The Alpine ~~chain~~region is characterized by a very complex ~~physiography including sectors~~orography with ~~strong~~large elevation gradients ~~that contrast with~~and deep, ~~tectonically controlled~~ valleys. ~~These elongated depressions etch elevated rough ridges with~~ of different orientation intersecting the ridge and shaping numerous mountain massifs.

170 Regarding their climatic setting, the European Alps are located in a transitional area influenced by the intersection of three main climates: The zone impacted by the Atlantic Ocean with moderate wet climate, the zone linked to the Mediterranean Sea characterized by dry summers and wet and mild winters, and the zone characterized by European continental climate with dry and cold winters and warm summers. Elevational effects and very small-scale climatic features originating from the complex Alpine topography are superimposed on this large-scale climatic setting (Auer et al., 2005; Isotta et al., 2014).

175 The interaction of the three climate forcing zones together with the topography of the Alps results in climatic gradients along the north-south and west-east directions. The intersection of these two gradients can be characterized by four main climate regions ~~for the Alps~~, as shown by Auer et al. (2007). The first and sharpest climatic border is along the central main ridge, separating the temperate westerly from the Mediterranean subtropical climate. The second climatic border separates the western oceanic from the eastern continental influences.

180



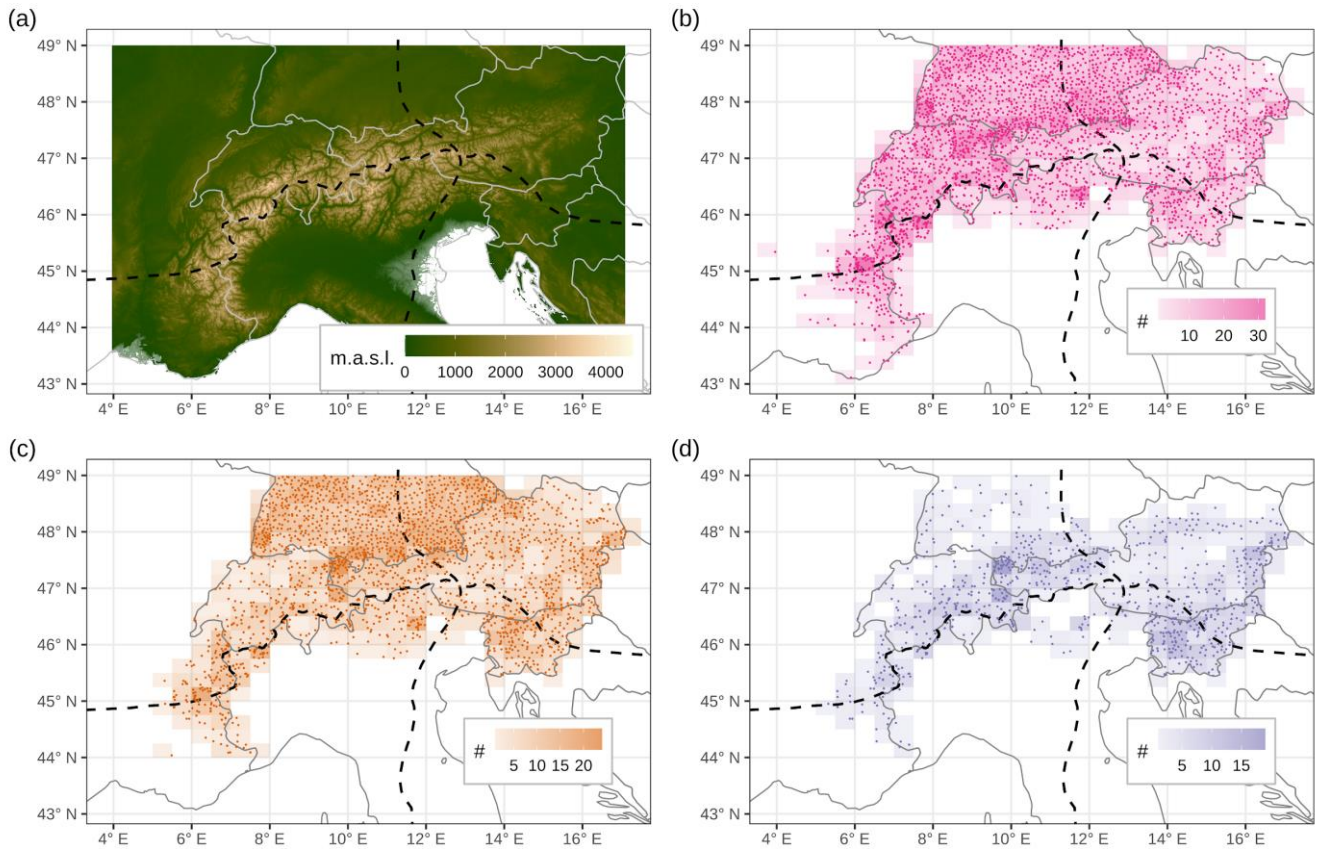


Figure 1: Topography of the European Alps (a) and overview of station locations (b-d). (a) shows the SRTM30 DEM (Shuttle Radar Topography Mission Digital Elevation Model) with ~1 km resolution. (b) shows the location of snow depth measurement locations that were available (provided) and used in the analysis (see Appendix A for quality checks and Sec. 2.4 for selection criteria). (c) shows the locations of stations used in the regionalization analysis. (d) shows the stations used for the long-term trend analysis. The station density for a 0.5x0.25 degree grid is shown underneath the points in (b)-(d). The main climatic divides from Auer et al. (2007) are shown as dashed lines in (a)-(d). See also Appendix A, Sec. 2.4 and Sec 2.5 for selection criteria.

2.2 Data sources

Acquisition of snow observation data was performed by using open data portals and by directly contacting data providers (see Table 1 for an overview). For Austria, the Austrian Hydrographical Service (HZB, Hydrographisches Zentralbüro) offers free download of their data for the recent decades, and additional historical data at the seasonal scale was kindly provided by the HZB. For France, data was kindly provided by the national weather service Météo-France. This includes data collected as part of the collaborative network (réseau nivo-météorologique) between Météo-France and mountain stakeholders (in particular Domaines Skiabiles de France, Association Nationale des Maires de Stations de Montagne, Association Nationale des Directeurs de Pistes et de la Sécurité de Stations de Sports d'Hiver). For Germany, data was

downloaded from the national weather service's (DWD, Deutscher Wetterdienst) open data portal using the R-package rdwd. For Germany, only stations below 49° N were downloaded. For Italy the data was kindly provided by many regional authorities:

- for the province of Bolzano from the hydrographical office of Bolzano (BZ)
- for Friuli Venezia Giulia (FVG) from the regional weather observatory (OSMER, Osservatorio meteorologico regionale), which is part of the ARPA (Agenzia regionale per la protezione dell'ambiente) FVG, and where the data was collected and cleaned by the Servizio foreste e corpo forestale struttura stabile centrale per l'attività di prevenzione del rischio da valanga
- for Lombardy from the ARPA Lombardia
- for Piedmont from the ARPA Piemonte
- for the province of Trento from Meteotrentino (TN), and with some additional long-term series previously analysed (TN_TUM, Marcolini et al., 2017a)
- for the Aosta Valley (VDA) from the civil protection office (CF: Centro funzionale, Regione Valle d'Aosta) and from the avalanche office (AIBM: Assetto idrogeologico dei bacini montani, Regione Valle d'Aosta)
- for Veneto from the avalanche office (Centro valanghe di Arabba), which is part of the ARPA Veneto
- finally, additional data for Piedmont and Aosta Valley was provided by the Italian meteorological society (SMI, Società Meteorologica Italiana)

For Slovenia, data was kindly provided by the Slovenian Environmental Agency (ARSO, Agencija Republike Slovenije za okolje). For Switzerland, data was downloaded from the IDAWEB portal of the national weather service MeteoSwiss, and additional data was kindly provided by the WSL Institute for Snow and Avalanche Research SLF. This dataset comprises the entire geographical range of the European Alps, yet we are aware of the existence of additional data sets (such as in the private sector, or public but not yet digitized), which unfortunately were not included in this analysis, and whose inclusion would be beneficial for even more robust results.

The data consists of daily measurements of snow depth (HS) and depth of snowfall (HN), ~~with a few exceptions of monthly/seasonal data from the HZB and SMI.~~ The largest part of the data are manual measurements; ~~some.~~ Some automatic measurements were ~~also~~ included only in the dataset provided for France ~~or, thanks to a close communication with the operating office, they were merged with manual series for.~~ For a few sites in the Aosta Valley, in Italy, manual series were merged to automatic series. This was done in order to extend up to the present some records that were dismissed at the beginning of the last decade, ~~and this was performed in close communication with the operating office.~~ While the observers follow slightly different guidelines in each country or network, the observation modalities are remarkably similar, thus allowing a combination of the different sources. For more detailed information on the measuring modalities, we refer to the European Snow Booklet (Haberkorn, 2019). Values of HS and HN were rounded to full centimetres. The further processing,

quality checking, and gap filling are described in Appendix A. For all the following statistical analyses the quality checked and gap filled data were used.

235 The fraction of stations used for the MeteoSwiss data is very low compared to the other networks. The MeteoSwiss data contains a large number of stations from the manual precipitation network which is not dedicated to snow. Many stations display a strong gap of digitally available snow contain an important data in gap for the period 1981–1997 (see also Fig. 2b). This long data break renders period that rendered a large fraction of the stations unusable for this study.

240

245

250

255

260

Table 1: Overview of the number of stations with daily data provided by the different data sources. The data source consists of a country abbreviation, followed by the data source. Country abbreviations are AT for Austria, CH for Switzerland, DE for Germany, FR for France, IT for Italy, and SI for Slovenia, respectively. For source abbreviations, please see Sec. 2.2. The Station numbers in the table are shown for fresh snow depth of snowfall (HN) and snow depth (HS) time series provided. See Appendix A, Sec 2.4 and Sec 2.45 for more details on station selection procedure for procedures associated with the number different types of HS stations used in the analysis analyses. HN was not analysed but only used for checking HS.

265

Data source	HN	HS	HS used (regionalization)	<u>HS used in(trend analysis)</u>
AT_HZB	653	652	588	<u>335</u>
CH_METEOSWISS	505	501	<u>157</u> <u>142</u>	<u>79</u>
CH_SLF	96	96	94	<u>84</u>
DE_DWD	956	964	<u>850</u> <u>830</u>	<u>104</u>
FR_METEOFRAANCE	239	286	<u>152</u> <u>145</u>	<u>45</u>

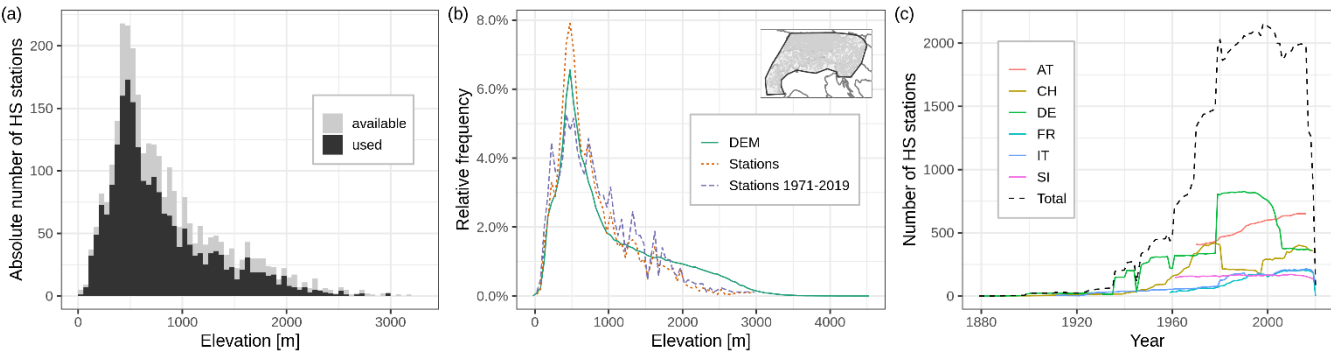
IT_BZ	60	64	48	<u>0</u>
IT_FVG	30	30	18	<u>8</u>
IT_LOMBARDIA	11	11	11	<u>0</u>
IT_Piemonte	34	34	24	<u>15</u>
IT_SMI	6	8	8	<u>7</u>
IT_TN	52	52	30 <u>29</u>	<u>8</u>
IT_TN_TUM	0	5	2 <u>1</u>	<u>0</u>
IT_VDA_AIBM	57	57	17	<u>5</u>
IT_VDA_CF	0	17	44 <u>11</u>	<u>3</u>
IT_VENETO	10	11	11	<u>9</u>
SI_ARSO	130	172	172	<u>152</u>
Total sum	2,839	2,960	2,496 <u>149</u>	<u>854</u>

270 2.3 Data overview

The locations of the stations are shown in Fig. 1-(b1 (b-d), the availability of stations in time in Fig. 2 (a), the elevational distribution in absolute terms in Fig. 2 (ab) and in relative in Fig. 2 (b), and the availability of stations in time in Fig. 2 (c). The stations cover the whole Alpine arc, but they are distributed with different station densities arising from the different national and regional networks. As expected, most stations ~~are were~~ found at lower elevations, the maximum number ~~is was~~ at ~500 m, and sharply declining for higher elevations. Above 2000 m, the number ~~is was~~ low, and no stations above 3200 m ~~are were~~ available. ~~for this study~~. The longest series ~~datedates~~ back to the ~~late 18th century for HN (Torino in Italy, starting 1787), and~~ late 19th century for HS (Passau_Maierhof in Germany, starting 1879). The total number of available HS stations ~~depends depended~~ on the availability of digitized data. It slowly ~~starts started~~ increasing around ~1900, with significant jumps in the 1960s and 1970s, when the French, Slovenian and ~~Austria Austrian~~ series ~~start started~~, and in the 1980s, when Germany ~~hashad~~ a large network increase. The highest number of stations ~~is was~~ available after the 1980s, with approximately 2000 stations. The total number of stations ~~drops dropped~~ significantly after 2017, because the data for Austria was only available until 2016, ~~and due to the delays induced from performing quality checks by the data provider. Moreover,~~ the data collection was performed between 2019 and 2020, thus some sources ended ~~sometime at some date~~ in between. ~~The main~~ We used two different periods for the two analyses that we performed. For the regionalization we aimed to have the largest possible spatial extent and density of the stations, so the period ~~studied for HS spans from 1961/1981 to 2010 was~~

chosen, because it is the period with the highest number of stations. For the trend analysis, we aimed to have as long as possible trends that sample the whole region, so the period 1971 to 2019, in order to have a complete Alpine view including all sources, some of which start only in the 1960s was chosen, because it offered the best tradeoff between station coverage and 1970s period length.

290



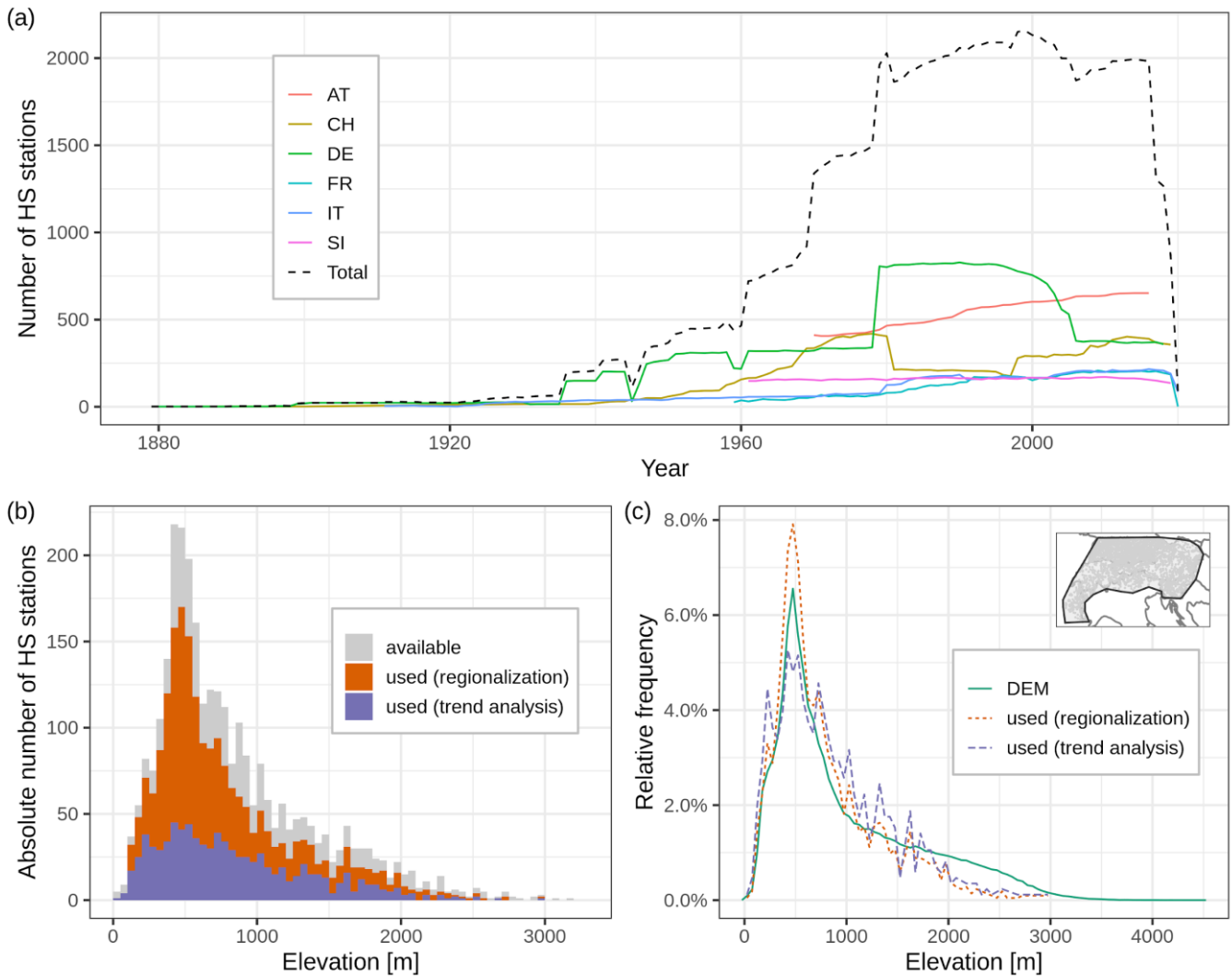


Figure 2: Overview of station elevations and temporal data availability. (a) The elevational distribution of snow depth (HS) stations in absolute numbers, both that were available and used. For the histogram 50 m bins were used. (b) Comparison of the relative elevational distribution of the station locations versus a digital elevation model (DEM). The frequency by elevation (50 m bins were used to calculate to proportion) is shown for the SRTM30 DEM (Shuttle Radar Topography Mission, ~1 km resolution) for the area spanned by the stations (see polygon in inset map). This is compared to the elevation frequency of the stations, both for all stations included in the analysis and for the subset used in the 1971 to 2019 analysis. (c) and station elevation. (a) The number of stations with daily data (before gap filling) is shown per year and country, and a total sum for the whole Alpine region. Stations are included in the count only, if they have at least one non-missing observation in the respective calendar year. Thus, This simple threshold was chosen, because the aim of this gives only a rough indication of figure is to show the availability and network abundance and not the effective usability. Country abbreviations are as in Table 1. (b) The elevational distribution of snow depth (HS) stations in absolute numbers. For the histogram 50 m bins were used. (c) Comparison of the relative elevational distribution of the station locations versus a digital elevation model (DEM). The distribution of the stations is shown in relative terms, using the same bin width (50m) as in the histogram in (b), but normalized to show the relative frequency instead of absolute numbers, and displayed as lines instead of bars. This is compared to the elevation for the whole area spanned by the stations (see polygon in inset map; area was outlined manually along the stations), which is extracted from the SRTM30 DEM (Shuttle Radar Topography Mission, ~1 km resolution).

310 2.4 Regionalization-and-trends

An empirical orthogonal function (EOF) analysis, also called principal component analysis (PCA), was conducted to determine the common modes of spatial variability. PCAs are widely employed in climatological studies to ~~study~~evaluate spatial modes of variability (Storch and Zwiers, 1999). They have been employed for meteorological records in the European Alps (Auer et al., 2007) and also for snow variables (López-Moreno et al., 2020; Scherrer and Appenzeller, 2006; Schöner et al., 2019; Valt and Cianfarra, 2010). ~~We~~For the PCA we used daily quality checked and gap filled data. However, the gap filling was only employed, when enough confidence in the filled value could be expected (see Appendix A for a detailed description). So some of the series still had gaps. Because the aim of this regionalization was to have a large spatial coverage, we did not want to exclude series with only few missing values. Consequently, we used a modification of the PCA algorithm that allows using data with gaps to estimate the principal components-~~(PCs)~~ (Taylor et al., 2013). ~~This~~

315 ~~The PCA was done using~~applied to the daily data from December to April for the hydrological years 1981 to 2010. The period was chosen, because it is long enough to provide a climatological reference (30 years), and it is the period that has the largest number of stations available. A hydrological year is defined here as starting in October, and it is designated as the calendar year of the ending month (e.g. December 1998 to April 1999 ~~have~~belong to the hydrological year 1999). ~~Stations~~Only those stations were selected ~~which that~~ had at least 70% of daily data available in this period. Each series was

320 scaled to zero mean and unit variance before applying the PCA. We retained the first five ~~PCs~~principal components (PCs), as additional PCs explained only less than 2.6% of the variance and the regions became noisy.

In order to identify spatially homogeneous regions within the Alpine domain, we performed a k-means clustering on the estimated PCA matrix. ~~We tested using 2 to 8 clusters on the PCA matrix with 2 to 8 PCs, as well as clustering directly on the daily observations. The best results were obtained using the PCA matrix for clustering and with the same number of~~

330 ~~clusters as PCs. Five clusters were chosen, because they showed the best results in terms of silhouette values and visual interpretability.~~We tested configurations with 2 to 8 clusters with the PCA matrix and with 2 to 8 PCs as input. We also applied k-means clustering directly on scaled daily observations of snow depth for comparison. To identify the best number of clusters, we used the “elbow-method”, average silhouette coefficients, and visual interpretation. For the “elbow-method”, the fraction of explained variance is plotted against the number of clusters, and the “elbow” of this curve is the point where

335 the increase in explained variance becomes marginal. This is a semi-objective method, because an elbow cannot always be clearly identified. The silhouette is a measure of how well an observation fits into its own cluster versus the others. For an observation i in cluster C_i , the silhouette coefficient is $1 - a(i)/b(i)$ if $a(i) < b(i)$, $b(i)/a(i) - 1$ if $a(i) > b(i)$, and 0 if $a(i) = b(i)$, where $a(i)$ is the mean distance between i and all other points in the same cluster, and $b(i)$ is the smallest mean distance of observation i to all other clusters. Specifically, $a(i) = \frac{1}{|C_i|-1} \sum_{j \in C_i, i \neq j} d(i, j)$ and $b(i) = \min_{k \neq i} \frac{1}{|C_k|} \sum_{j \in C_k} d(i, j)$,

340 where $d(i, j)$ is the Euclidean distance between observations.

Trend analysis was performed using linear regression (OLS, ordinary least squares) with two approaches. The first was to determine the long term changes in the longest period with the densest station coverage, which is 1971 to 2019. Linear trends were computed separately for each month from November to May. Only stations with complete 49 years were considered. The predicted variable was the mean monthly HS and the only predictor the year (shifted to 0).

The second approach was a moving window approach that aims at identifying the short term changes in trends. For this, linear trends were computed on all 30 year windows from 1961 to 2019. A 30 year time was identified optimal in the sense that it is short enough to appreciate the changes of trends over time and, at the same time, it is long enough to filter out natural cyclic fluctuations of hydrometeorological variables in the Alps (Mallucci et al., 2019). Again, trends were calculated separately by month (November to May) and station, and only if no year was missing in each window.

Both approaches resulted in different numbers of analysed stations per month (and per moving window), because low elevation stations have no snow early or late in the season, not all stations record the complete winter season, and, in the case of the moving window approach, the network density changes over time. The significance of trends was assessed using assessed using a 95% confidence level.

Some of the previous studies used the Theil Sen estimator to identify trends in snow cover variables (Marty et al., 2017; Schöner et al., 2019). The Theil Sen estimator is a robust estimator of trends, which works better than OLS for heteroscedastic data and in the presence of outliers. However, for the monthly snow depth series we did not detect any heteroscedasticity, significant outliers, or other evidence against the assumptions of OLS.

2.5 The optimal number of clusters varied between 2 and 5 depending on the input (observations or PCA matrix) and depending on the metric (elbow in variance explained or average silhouette coefficients). After looking at the clustering results on maps (see Fig. S1), all 2 to 5 clusters made sense. They simply highlight different aspects of the snow depth spatial variability, such as the gradients along elevation, north-south and west-east. Finally, five clusters based on the PCA matrix were chosen, because they provide the best trade-off between the semi-objective metrics and the patterns expected from the climatic drivers.

2.5 Trend analysis

For the trend analysis monthly and seasonal indices were used, which are indicative for different aspects and times of the snow season: monthly mean HS for November to May, mean winter HS (December to February, DJF), mean spring HS (March to May, MAM), mean seasonal HS (November to May), maximum HS from November to May (maxHS), early season snow cover duration (SCD, November to February), late season SCD (March to May), and full season SCD (November to May). SCD was the number of days with HS above 1 cm (Brown and Petkova, 2007). Indices were calculated from the quality checked and gap filled daily snow depth observations, if more than 90% of the daily values in the respective period were available. Trends of all indices were calculated for the period 1971 to 2019 for stations with complete data in the period. For the monthly mean HS values only, April and May series displaying mean HS less than 1 cm in all years were

discarded, because these are insignificant snow amounts and divert attention from the other sites. The number of series available for each snow variable differs: the largest number of series is available for the monthly mean HS, less for the half-seasonal (three to four months) and the fewest number for the full-season indices.

Trend analysis was performed using two different approaches: ordinary least squares (OLS) and generalized least squares (GLS) regression. GLS was used because it allows accounting for changes in the variance (Pinheiro and Bates, 2000). This was employed because the monthly snow depth series exhibited a change in the inter-annual variability, especially at the end of the season, where monthly snow depths approached zero. The regression formula was $y_t = \beta_0 + \beta_1 t + \epsilon_t$, where y_t is the value of the respective snow variable in year t (centred such that year 1971 becomes year 0), β_0 and β_1 are the estimated regression coefficients and ϵ_t are the errors, which are normally distributed with mean zero and variance σ^2 . For OLS, σ^2 is assumed to be constant. For GLS, we allowed the variance to depend on the year t with $Var(\epsilon_t) = \sigma^2 * \exp(2 * \gamma * t)$, where γ is a coefficient to be estimated in the inference procedure that indicates the change in variance associated to t . Estimated trends (β_1) did not differ substantially between OLS and GLS (see supplementary material, Fig. S8 and S9, Table S8 and S9). The GLS regressions for monthly mean HS showed a significantly improved goodness-of-fit ($p < 0.05$, likelihood ratio test) for 40% of all cases, and, specifically for November, April and May, even for more than 60%. For consistency, GLS was used for all monthly mean HS trends. For seasonal values, GLS regressions improved goodness-of-fit especially for spring mean HS and to a moderate extent also for the other seasonal HS indices. Consequently, in order to be consistent with the monthly analysis, GLS regressions were used for all seasonal HS indices. For the SCD variables, only a small fraction of models ($< 10\%$) were better with GLS, so OLS was used instead. The significance of trends was assessed using a 95% confidence level. For the fraction of variance explained by the trend, we used the R squared statistic. To determine the magnitude of the interannual variability after accounting for the trend, we used the standard deviation of the model residuals. The SCD variables are bounded counts, which can pose problems to the assumption of OLS. However, this was only problematic for very low and very high elevation sites, which display many SCD values at the minimum or maximum. For MAM this concerns series below 500 m and above 2000 m, while for NDJF and NDJFMAM this is problematic below 250 m and above 2500 m. In these cases, a different model, such as Poisson or negative-binomial, might be more appropriate. However, we decided to still use OLS in order to keep results comparable across sites and snow variables, and because OLS is estimating the coefficients robustly even in misspecified models, although the standard errors should be considered cautiously.

2.6 Air temperature and precipitation data

In order to study the relationship of snow depth with temperature and precipitation, we extracted temperature and precipitation series for each station from available gridded products. While gridded data sets clearly have some shortcomings, e.g. comparisons to point observations need a cautious interpretation (Salzmann and Mearns, 2011), their strength is the spatial and temporal coverage ~~as well as their homogeneity with respect to interpolation methods.~~

Two types of products were considered, the first is a reanalysis and the second is an observation-based spatial analysis. For the reanalysis, we used temperature and precipitation from the MESCAN-SURFEX data set (Bazile et al., 2017), which was produced during the UERRA (Uncertainties in ensembles of regional reanalyses) project and which is available via the Copernicus data store (CDS). It covers the period from January 1961 to July 2019 on a 5.5 km grid. Precipitation is available as total daily sum and temperature at 6-hour intervals (00, 06, 12, 18 UTC). For the observational based data, we chose E-OBS v20.0e for mean daily temperature (Cornes et al., 2018), and the Alpine precipitation grid dataset (EURO4M-APGD) for total daily precipitation (Isotta et al., 2014; Isotta and Frei, 2013). E-OBS v20.0e spans the period from January 1950 to July 2019 on a 0.1° grid. APGD covers the period January 1971 to December 2008 on a 5 km grid. It should be noted that the observation-based precipitation grids do not account for undercatch, which can lead to uncertainties at high elevations and in winter (Prein and Gobiet, 2017).

In order to assign grid cells to stations for temperature and precipitation, we selected those grid cells which contain the stations. Consequently, some nearby stations could have the same series of temperature and precipitation. The daily (or 6-hour for temperature MESCAN-SURFEX) series were aggregated to monthly means for temperature and monthly sums for precipitation.

The gridded products have a reference orography that, in complex mountain terrain, can differ significantly ~~to~~from the elevation of the point observation, thus e.g. introducing biases in temperature. Thus, temperatures were adjusted using a constant lapse rate of ~~6.4~~5 °C km⁻¹.

Monthly temperature and precipitation can be considered largely independent from one month to the next, while snow cover is a cumulative process across the snow season. Because of this, seasonal comparisons were performed with average seasonal temperature and precipitation for winter (December to February), spring (March to May), or the whole snow season (November to May). The time period 1981 to 2010 was used, which had the densest station coverage. Climatological averages were computed for all seasons: using the quality-checked and gap filled snow depth data. Since EURO4M-APGD ends in 2008, the time period 1981 to 2008 was used for the observation-based products. The manuscript contains results from the comparison with the reanalysis product (MESCAN-SURFEX), and the results from the observation-based products are shown in the supplementary material as sensitivity analysis.

~~2.6 Code and data~~

~~All computations were performed with R statistical software version 4.0.2 (RCoreTeam, 2008). Colors for the figures were taken from scientific color scales (Crameri, 2019) and colorbrewer. Code is available at Matiu et al. (2020), which includes scripts to read in the different data sources, perform all data pre processing, quality checks, gap filling, and do all statistical analyses (i.e. all of Sections 2.3 to 2.5).~~

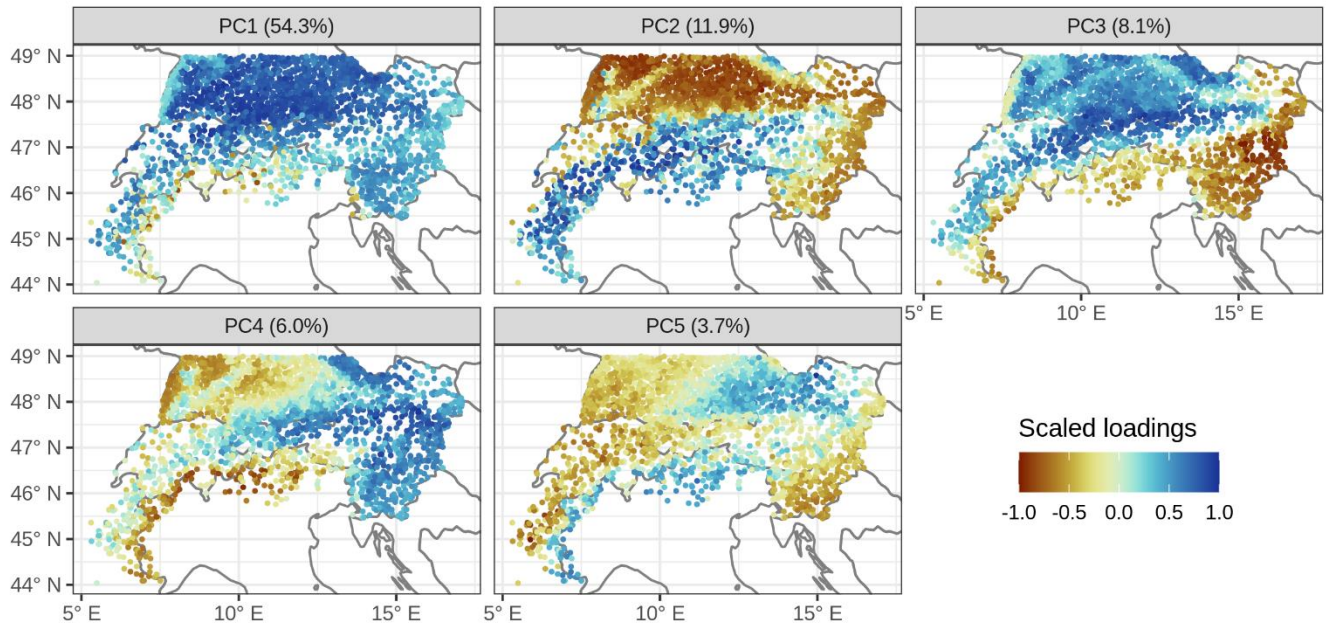
~~Most data providers agreed to share their data: see Table C1 for the availability of daily and monthly values. For the full data set, please contact the main authors (MM or AC); the usage is generally free for research purposes, though explicit consent is~~

required from some data providers, which want to keep track of the usage of the data. The data is available at an open repository (Matiu et al., 2020).

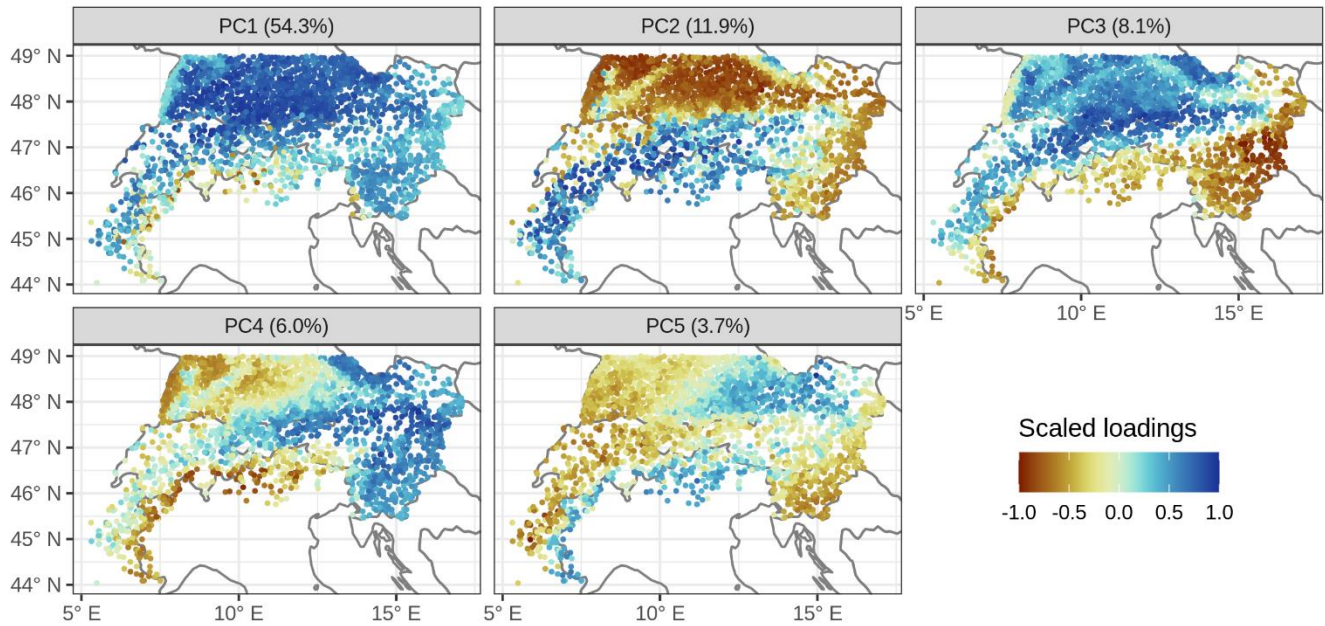
3 Results and discussion

3.1 Regionalization of daily snow depths 1981 to 2010

The PCA of daily snow depth series yielded five main modes of spatial variability, which explained in total 84% of the variance in the period December to April from 1981 to 2010 (Fig. 3). The first PC ~~explainsexplained~~ 54.3% of variance and ~~distinguishesdistinguished~~ between high to middle and low elevation stations (approximate threshold 500–1000 m, Fig. ~~B1-4~~). ~~It explained the variability in snow depth for stations above 1000 m,~~ and ~~iswas~~ probably also partly linked to the permanence (or permanent absence) of snow cover, which is why also some low elevation sites ~~havepresented~~ similar loading ~~asto~~ the high sites (a PC loading can be considered the correlation of the original series with the principal component). The second PC ~~explainsexplained~~ 11.9% of variance and ~~is highly correlatedwas also linked~~ to elevation ~~up to,~~ ~~but captured the variability below~~ 1000–1500 m, (Fig. 4). ~~Consequently, PC1 and mostly constant above PC2 together captured the variability across the whole elevation range.~~ The third PC ~~explainsexplained~~ 8.1% of variance and ~~separatesseparated~~ the stations into north and south of the main ridge. The fourth PC ~~explainsexplained~~ 6.0% of variance and ~~separatesseparated~~ east from west. The fifth PC ~~explainsexplained~~ 3.7% of variance and ~~separatesseparated~~ the south–eastern and north–western stations from the rest. ~~See also Fig. B1 for scatterplots of the PCs by elevation and region (from clustering below).~~



Some gradients in the PC loadings map (Fig. 3) could give the impression that data artefacts between the different data providers exist, such as at the Austrian-German border in PC2 and PC5, or at the French-Italian border for PC3-5. However, this is caused by the fact that the administrative borders in the Alps are tied to topography, and thus closely located near elevational borders (Fig. 1(a)). A version of Fig. 3 subdivided by data provider highlights clearly that the gradients were not associated with the administrative borders (Fig. S2 in the supplementary material).



465 **Figure 3: Main modes of variability in daily snow depth series.** The plots show scaled loadings for the first five principal components (PCs), which can be considered the correlation of the original series with the respective PC. The title in each panel contains the amount of variance explained by the respective PC. The principal component analysis was applied on daily snow depth data from December to April for the hydrological years 1981 to 2010, for stations that had at least 70% of available data.

470 **Based on**

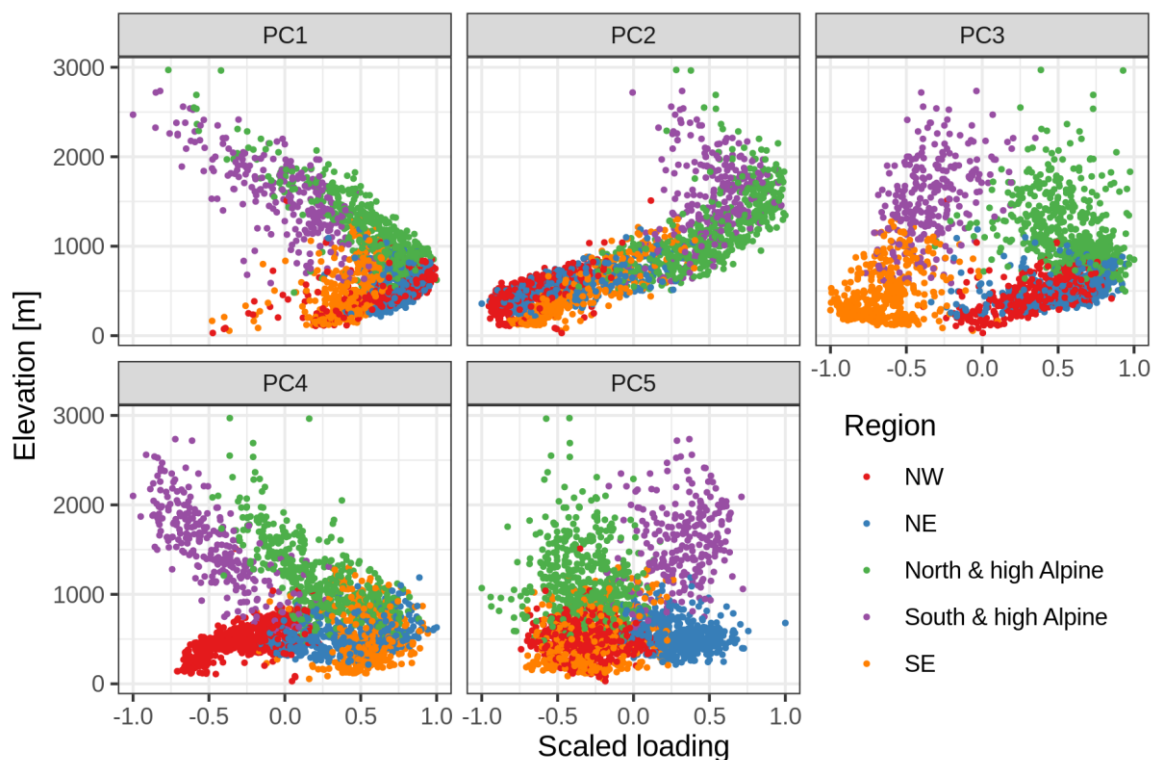


Figure 4: Scatterplots of principal component (PC) loading versus elevation and region. The PC loading can be considered the correlation of the original series with the respective PC. See Fig. 3 for a map of the PC loadings, and Fig. 5 for a map of the regions.

The PCA loadings, from the five PCs were used as input for a clustering algorithm (k-means), which divided the stations into five clusters or regions using a k-means clustering (Fig. 4). This yielded three regions in the north: northwest (NW) with a median elevation of 472 m (min-max: 30–1510 m), which contains stations from southwest Germany, northwest Switzerland, few from France, and a few from eastern Austria; northeast (NE) with a median elevation of 515 m (215–1188 m), which contains stations from southeast Germany and north Austria; North & high Alpine with a median elevation of 1050 m (482–2970 m), which contains stations mainly located in France, Switzerland, and Austria, but also includes the high-elevation sites in Germany, such as in the Black forest and Bavarian forest. South-Two regions emerged south of the main ridge, there were two regions: southwest (SW): South & high Alpine with a median elevation of 1530 m (588–2735 m), which contains stations from the southern French Alps, almost all of Italy, few of southern Switzerland, and some of south Austria and east Slovenia; and finally southeast (SE) with a median elevation of 420 m (55–1300 m), which contains almost all stations from Slovenia and parts of eastern Austria.

Consequently, clusters NW, NE, and SE ~~contain~~contained lower elevation sites, while North & high Alpine and ~~SW~~South & high Alpine contained the higher elevations. The spatial coverage of the stations in this study ~~includes the~~included low elevations sites for Switzerland, Germany, Austria, and Slovenia, but not in France and Italy, where the available stations ~~are were~~ mostly high elevation sites. For a future analysis, it would be interesting to include more low elevation sites from France and Italy, and see whether a third cluster would emerge south ~~as has in~~analogue to the north, because, as of now, the division into ~~SW~~South & high Alpine and SE is surely also caused by the different station elevations.

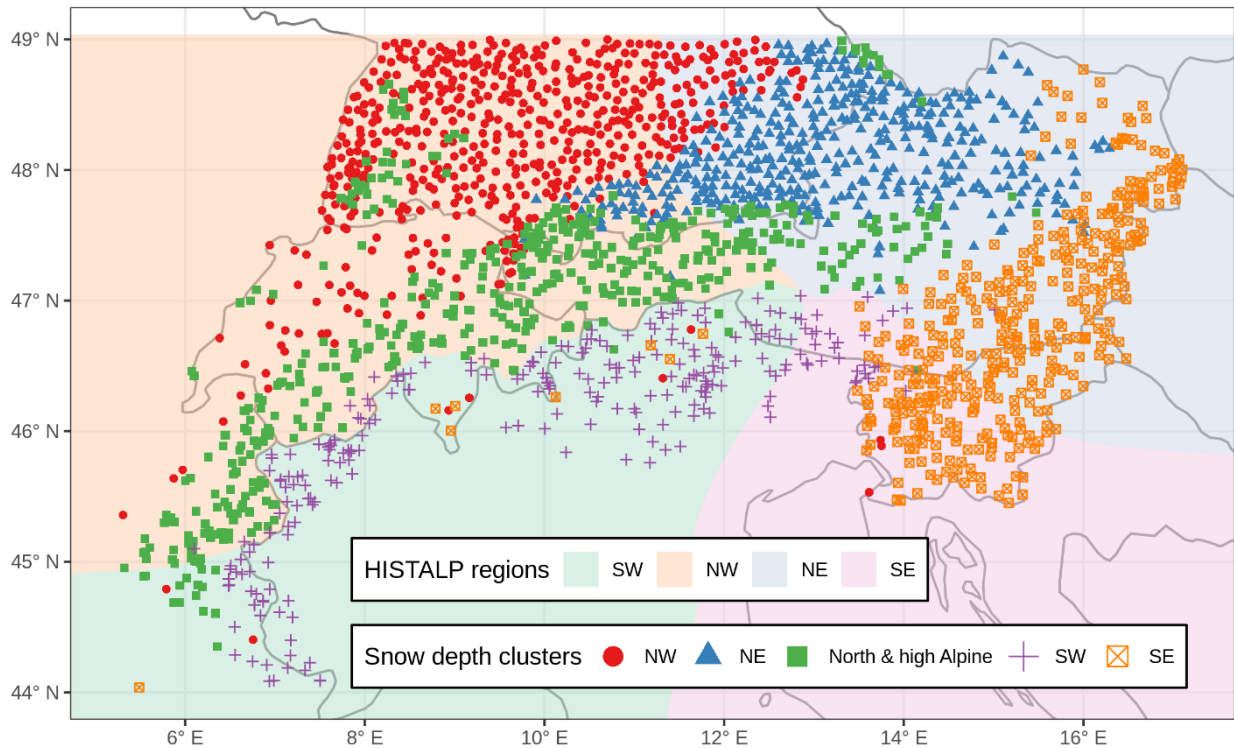
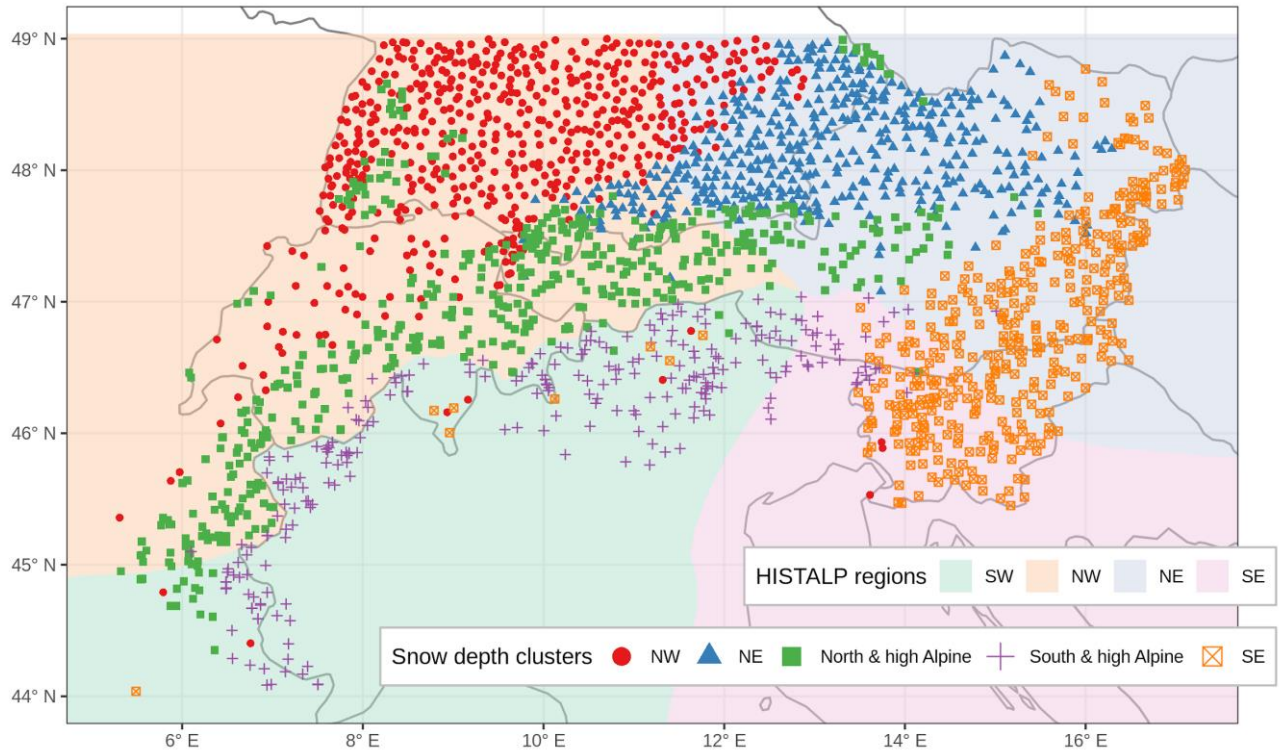


Figure 4: Clustering of stations based on daily snow depth data. Map of regions from applying a k-means clustering on the first five principal components. Underlaid are the HISTALP coarse resolution subregions, which were derived using a semi-automatic principal component analysis of climate variables (temperature, precipitation, air pressure, sunshine, and cloudiness).



505 **Figure 5: Clustering of stations based on daily snow depth data. Map of regions from applying a k-means clustering on the first five principal components. Underlaid are the HISTALP coarse resolution subregions (Auer et al., 2007), which were derived using a semi-automatic principal component analysis of climate variables (temperature, precipitation, air pressure, sunshine, and cloudiness).**

The results from the clustering were ~~estimated data driven and based solely on~~ obtained automatically and no manual post-processing or modification of the cluster assignments was performed. Additionally, the only input into the clustering algorithm was daily snow depth series; and no information on location or elevation ~~entered the input matrices~~ was included.

510 Given this absence of location information in the clustering process, the estimated modes of variability and the resulting regions ~~are were~~ very homogenous in space. However, in the clustering, some stations ~~seem seemed~~ off, such as ~~e.g.~~ the few “northwest” stations around Lugano in Switzerland, northern Italy, and at the Adriatic coast in Slovenia, as well as the SE stations in France, Switzerland, and northern Italy. This ~~is was~~ not related to the used PCA algorithm that ~~allows allowed~~ gaps in data, since the results ~~look looked~~ almost identical to a standard PCA (see Fig. B2S3 and B3S4), where the clustering ~~agrees agreed~~ in 98.5% of the stations ~~in common~~, and the same ~~common~~ stations ~~seem seemed~~ mis-clustered. Instead, this

515 might be related to special local climatic conditions affecting ~~the~~ snow cover or ~~unique to the fact that these~~ stations ~~did not have any similar neighbours~~ in the estimated clusters. For example, the five stations in Ticino, located in Switzerland south of the main ridge, are low elevation stations, which ~~have had~~ no correspondence in the ~~SWS~~ South & high Alpine cluster,

which ~~contains~~contained middle to high elevations. Thus, the next best clusters were SE and NW, which, however, ~~dedid~~ not fit well: ~~Thesethese~~ sites and all other seemingly mis-clustered stations ~~havehad~~ low silhouette values (Fig. ~~B4B1~~), which is a measure of how well a point matches its cluster compared to the others. Low silhouette values were also found along the borders of the different clusters, especially between NW and NE, which implies a smoother transition between NW and NE compared to the north–south boundary.

The estimated modes of variability of snow ~~matchare similar to~~ previous estimates on climatic subregions in the Alps, as identified in the HISTALP project (Auer et al., 2007), and which are underlaid in Figure 45. The HISTALP regions were based on temperature, precipitation, air pressure, sunshine and cloudiness, and the division into north, south, east and west matches what we found for snow depth. Since the four regions were a ~~comprise~~compromise between all variables, they do not match perfectly to what we found for snow depth, because the individual atmospheric variables exert different controls on surface snow cover. While the north–south boundary is almost identical in the central–western part, the eastern part has large mismatches. However, if the single element boundary for precipitation were considered as main factor (cf. Fig. 8 from Auer et al., 2007), then the agreement with snow depth would be almost perfect. This finding confirms a consistent picture of the Alpine climate, in which snow depth is ~~highlystrongly~~ related to precipitation and air temperature patterns.

The amount of variance explained in the PCA with five PCs (84%) might seem surprisingly high, given that snow cover is hypothesized to have a high spatial and temporal variability. The value is higher than recent estimates for the Swiss Alps, where the first three PCs explained 78% (Scherrer and Appenzeller, 2006), or for Austria and Switzerland, where the first three PCs explained 70% (Schöner et al., 2019). However, since here we included more stations and also stations from regions with different climatic influences, such as south of the main ridge, an increase in the amount of explained variance could be expected.

3.23.2 Snow depth climatology 1981 to 2010 and links to temperature and precipitation

Besides differences in trends, the regions also demonstrated different snow depth climatologies (Fig. 6). Looking at average winter (December to February) snow depth 1981–2010, the northern regions had higher snow depths than their southern counterparts. These differences became larger with increasing elevation: While below 750 m no substantial differences were observed, southern stations had ≈30% less snow than northern stations until 1750 m, and ≈20% less until 2250 m; above the number of stations is too low to obtain robust results (Table S1).

Average winter temperatures were higher in NW compared to NE and SE, and the latter two were similar. In North & high Alpine and South & high Alpine temperatures were also comparable, although northern stations were colder at 1500–2000 m. However, precipitation amounts were significantly lower south than north, and South & high Alpine stations received ≈100 mm less winter precipitation than North & high Alpine stations up to 2000 m, which amounts to ~1/3 of the precipitation north. These results suggest that the difference in December to February snow amounts north versus south are predominantly driven by precipitation differences and not temperature.

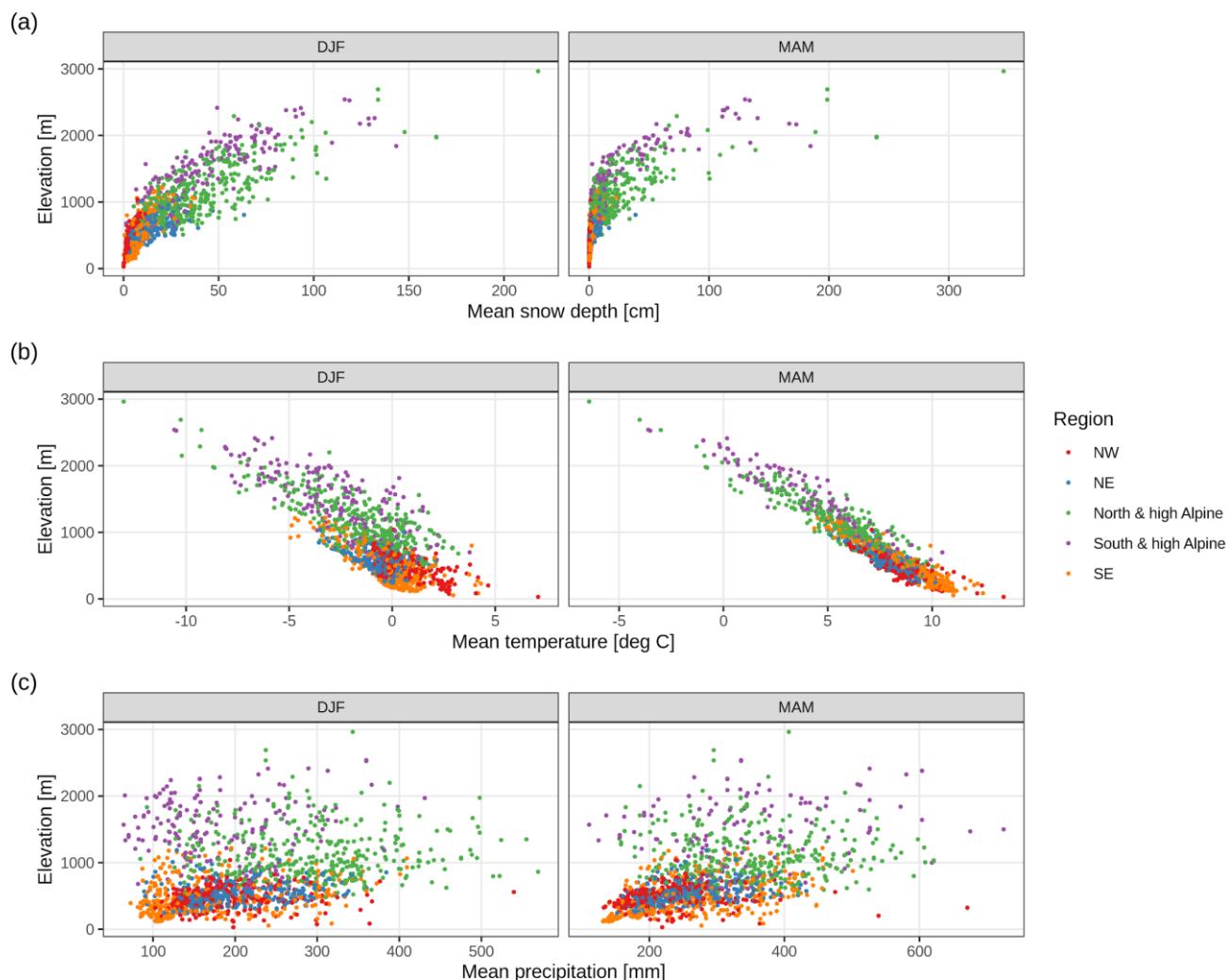


Figure 6: Climatology of (a) snow depth, (b) temperature, and (c) precipitation across regions and elevations for the winter season (December to February, DJF) and spring season (March to May, MAM). Average values are for the period 1981–2010. Each point represents one station. The temperature and precipitation values were extracted from MESCAN–SURFEX reanalysis, while the snow depths are based on station data. See also Table S1 and S2 for summary values.

Seasonal snow depth was correlated to temperature and precipitation extracted from a gridded reanalysis (MESCAN–SURFEX). Results indicated negative correlations with temperature, decreasing strongly with elevation, and positive correlations with precipitation, mildly increasing with elevation (Fig. S5). The magnitude of temperature correlations was between -0.8 and -0.5 below 1000 m, and the correlation decreased to about -0.2 up to 2000 m. For precipitation, correlations were between -0.2 and 0.7, with much higher variability than temperature. Correlations of snow depth with temperature did not differ by region. However, the stations in SE exhibited stronger (more negative) correlations with precipitation than the NE and NW regions.

The findings on the correlations agree with previous estimates for Swiss and Austrian stations (Schöner et al., 2019) in terms of signs and elevation patterns. However, our estimates are of higher magnitude for both temperature and precipitation. While the climatological and correlational results do not suffice to formally attribute changes in snow cover to temperature and precipitation, they highlight temperature and precipitation as likely drivers of variability and change, consistent with the physical understanding of snow processes (Hock et al., 2019). The lower precipitation amounts and the concurrent higher temperatures south of the main ridge and higher correlations (at least for SE) could be causing the higher variability of snow depth trends in the southern regions, because this implies less chances that precipitation falls concurrent with low temperatures.

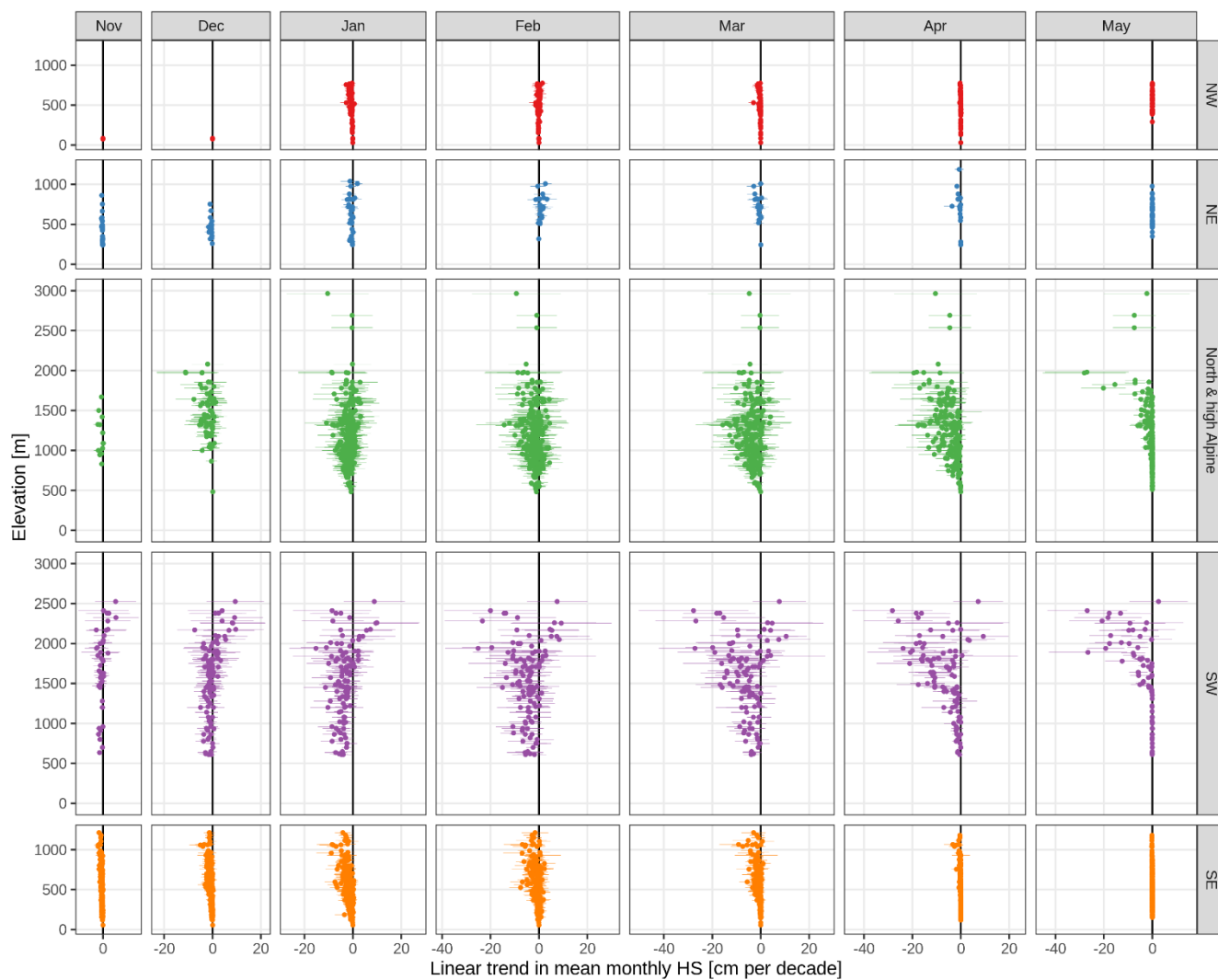
As sensitivity analysis, we repeated the climatology and correlational analysis using observation based spatial analyses instead of reanalysis for extracting temperature and precipitation (Fig. S6, Fig. S7, Table S3, Table S4), but results did not differ substantially from above.

3.3 Long-term trends for the period 1971 to 2019

Trends of monthly mean snow depth from November to May were mainly negative with some exceptions (Fig. 57 and Table 2). Over all stations and all months, 87.85% of the trends were negative and 12.15% positive; 48.23% significantly negative and 0% (only 34 station month combinations) significantly positive- (for significance, p-values had to be less than 0.05). The percentage of significant negative trends was substantially higher in the spring months (March to May) and at lower elevations, irrespective of region, and it could reach 40–89.70% (see also Table 2).

In the low elevation regions (NE, NW, SE), snow depth was decreasing much stronger in SE than in NE or NW- across all months. The mean trend of December snow depth below 1000 m in NE was -0.67 cm per decade⁺ (all further trends in the same unit) and -0.8 in SE- and NE, while in January it was -0.75 in NW- and, -0.6 in NE, but -1.76 in SE (Table 2). In February, NE stations even had increasing snow depth with +0.8, while NW and SE decreased. In the middle elevation (1000 to 2000 m), differences between north and south were even stronger and variable in amplitude during the snow season: While in December the negative mean trend was stronger in mean-North & high Alpine (N&hA) (-2. stations was stronger negative (-1.9) than compared to SWSouth & high Alpine (S&hA) stations (-0.8), but for January and February we observe the opposite behaviour, with a less pronounced negative trend in N&hA (-1.76 and -2.32) compared to SWS&hA (-3.9 and -5.1).

In the spring months March and April, trends in snow depth were again more negative south than north. For example, in the middle elevations (1000 to 2000 m), the mean March snow depth trend was -3.9 in N&hA compared to -6.97.0 in SWS&hA, in April -5.97 compared to -7.76.6, and in May -1.84 compared to -4.02.7. Notably, stations in SWS&hA above 2000 m exhibited strong variability in trends, and there were stations with increasing snow depth in all months (November to May). While mean trends were positive until January (November 4.52.7, December 4.20, January 0.40), mean trends were negative otherwise (February -21.9, March -52.6, April -8.73, May -40.89.5).



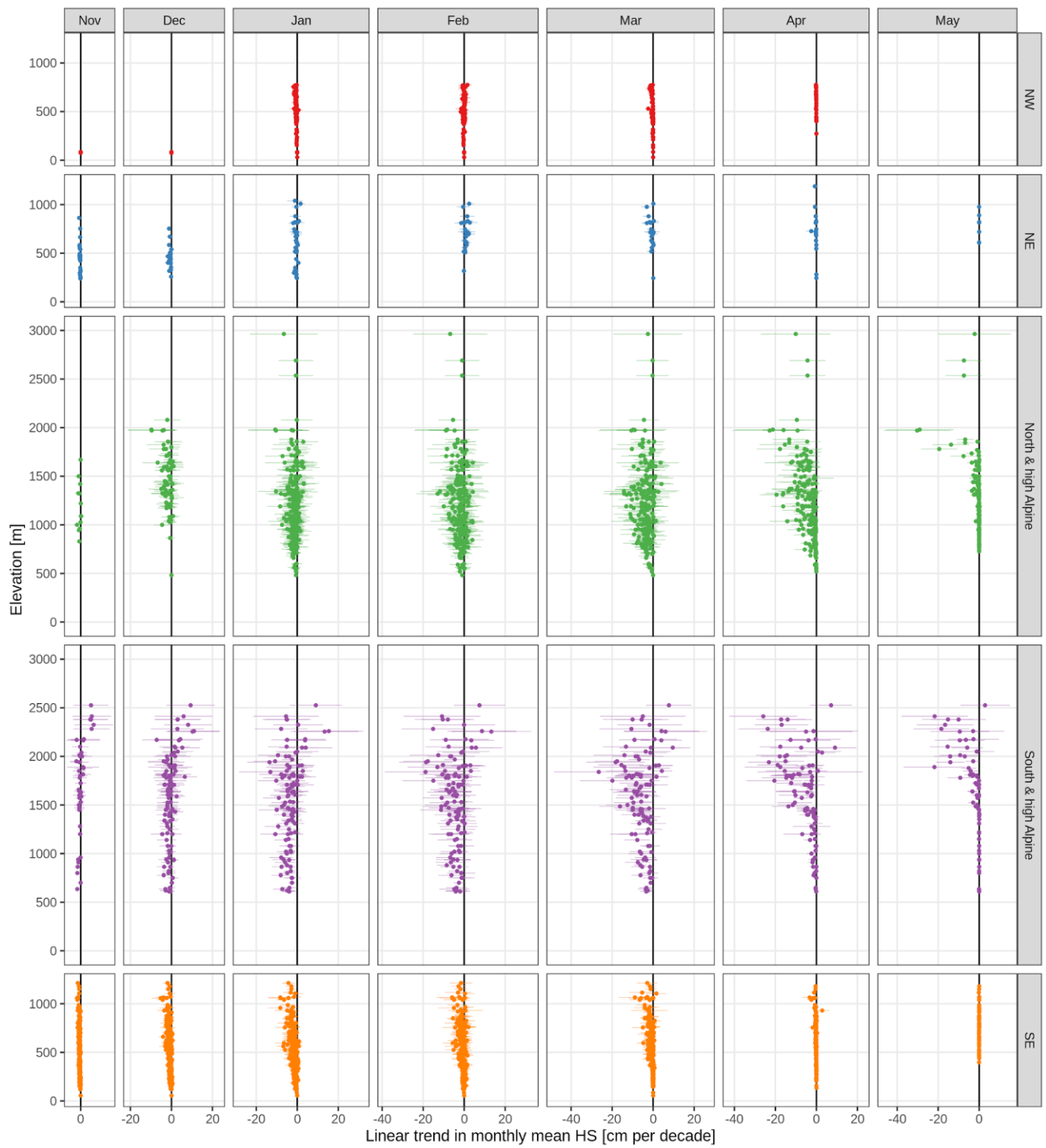


Figure 57: Long-term (1971 to 2019) linear trends in mean monthly snow depth (HS). Trends are shown separately by month (columns) and region (rows). Each point is one station. ~~Points with lines~~The points indicate the trend and ~~the lines~~ the associated 95% confidence interval.

605

610

Table 2: Overview of long-term (1971 to 2019) trends in mean monthly snow depth. Summaries are shown by month, region, and 1000 m elevation bands (0 to 1000, 1000 to 2000, and 2000 to 3000 m). Cell values are the number of stations (#), the mean trend (mean, in cm ~~per~~ decade⁻¹), and percentages of significant negative (sig-) and positive (sig+) trends; the remaining percentage (not shown) corresponds to the total of non-significant negative and positive trends. Empty cells denote no station available (for # and mean), and no stations with significant negative or positive trends (sig- and sig+). Trends were considered significant if p < 0.05. See also Fig. 5. ~~A version of the table with 500 m bands instead of 1000 m is available as auxiliary material (Matiu et al., 2020): 7. A version of the table with 500 m bands instead of 1000 m is available in the supplementary material (Table S5).~~

Month	Region	Elevation: (0,1000] m				Elevation: (1000,2000] m				Elevation: (2000,3000] m			
		#	mean	sig-	sig+	#	mean	sig-	sig+	#	mean	sig-	sig+
Nov	NW	2	-0.01	50.0%									
	NE	34	-0.2532	8.841.2%									
			-										
	N&hA	4	1.050.9	2550.0%		9	-0.6731	22.2%					
	SWS&h A	7	-1.0302	57.171.4%		23	-0.8022			1 2	1.522.68		
	SE	218	-0.4550	11.952.3%		8	-1.3421	50.0%					
Dec	NW	2	-0.0001										
	NE	24	-0.6268	8.329.2%									
	N&hA	3	-1.5472	33.3%		67	2.061.9	41.5%		1	-2.02		
	SWS&h A	17	-1.4734	11.85.9%		67	-0.8589	1.5%	1.5%	1 7	4.213.98		
	SE	221	-0.6177	7.724.9%		9	-2.2738	22.244.4%					
Jan	NW	81	-0.7251	27.212.3%									
	NE	32	-0.7055	3.1%		2	0.3223						

Month	Region	Elevation: (0,1000] m				Elevation: (1000,2000] m				Elevation: (2000,3000] m			
		#	mean	sig-	sig+	#	mean	sig-	sig+	#	mean	sig-	sig+
	N&hA	83	-1.9859	93.6%		154	-1.7259	45.2%		4	-2.8302		
	SWS&hA	19	-5.034.9	73.7%		76	-3.9194	22.421.1%		17	0.0850		
	SE	243	-1.6659	32.129.6%		10	-4.5832	70.0%					
Feb	NW	78	-0.0709	11.5%									
	NE	24	0.7775		4.2%	1	2.6744		100.0%				
	N&hA	84	-1.3536	3.64.8%		153	-2.3024	97.2%		4	-4.093.56		
	SWS&hA	19	-4.7610	15.810.5%		78	-5.09	16.715.4%		17	-21.91	23.5.9%	
	SE	228	-0.6663	4.84%		12	-2.7350	8.3%					
Mar	NW	65	-0.3033	1.54.6%									
	NE	20	-0.9093	10.0%		1	-0.0410						
	N&hA	75	-2.823.1	21.330.7%		151	-3.94	21.29%		4	-2.441.91		
	SWS&hA	18	-3.6852	38.933.3%		73	-6.907.0	41.146.6%		17	-52.55	29.411.8%	5.9%
	SE	212	-0.6465	3.85.2%		12	-3.2522	16.7%					
Apr	NW	6434	-0.0608										
	NE	4918	-0.5833	63.238.9%		1	-0.6473						
	N&hA	7069	-1.9948	84.368.1%		133	-5.9370	61.765.4%		4	-7.2207	25.0%	
	SWS&hA	1514	-1.250.9	46.750.0%		6665	-7.736.6	68.256.9%		17	-8.6628	47.141.2%	

Month	Region	Elevation: (0,1000] m				Elevation: (1000,2000] m				Elevation: (2000,3000] m			
		#	mean	sig-	sig+	#	mean	sig-	sig+	#	mean	sig-	sig+
	SE	<u>24813</u> <u>6</u>	-0.4 <u>013</u>	<u>6.938.2</u> %	<u>0.7</u> %	7	-1.3 <u>942</u>	14.3%					
May	NW	<u>46</u>	-0.00										
May	NE	<u>477</u>	-0.01										
	N&hA	<u>8036</u>	-0.0 <u>503</u>	<u>5.06</u> %		<u>44711</u> <u>4</u>	-1.7 <u>742</u>	<u>42.728.1</u> %		3	-5.7 <u>069</u>		
	SWS&h A	<u>439</u>	-0.0 <u>301</u>	<u>11.1</u> %		<u>4341</u> <u>8</u>	- 3.9 <u>72.6</u>	<u>55.839.0</u> %		1 5	- 40.8 <u>09.4</u>	<u>46.740.0</u> %	
	SE	<u>47452</u>	-0.02	<u>0.6</u> %	<u>1.9</u> %	7	-0.4 <u>402</u>	<u>14.3</u> %					

3.3 Short-term trend 4 Interannual variability from 1961 to 2019

Complementing the analysis over the entire time period from 1971 to 2019 in the previous section, this section analyses the trends within thirty year time periods in order to show the short term variability of trends over a slightly longer time period starting 10 years earlier (1961–2019 compared to 1971–2019 before). Between 1961 and 2019, mean monthly snow depth exhibited strong temporal variability, as evidenced by the variability in 30 year trends (Fig. 6). In general, the winter months December to February showed negative snow depth trends across all regions in the periods 1961–1990 to 1976–2005, and positive trends in the periods 1981–2010 to 1990–2019. However, there were regional deviations from this general picture. High elevation stations in SW showed strong increases already in the period 1981–2010, while North & high Alpine stations were decreasing. The periods 1976–2005 and 1981–2010 showed increasing snow depth in NW, but no change in NE and decreases in SE.

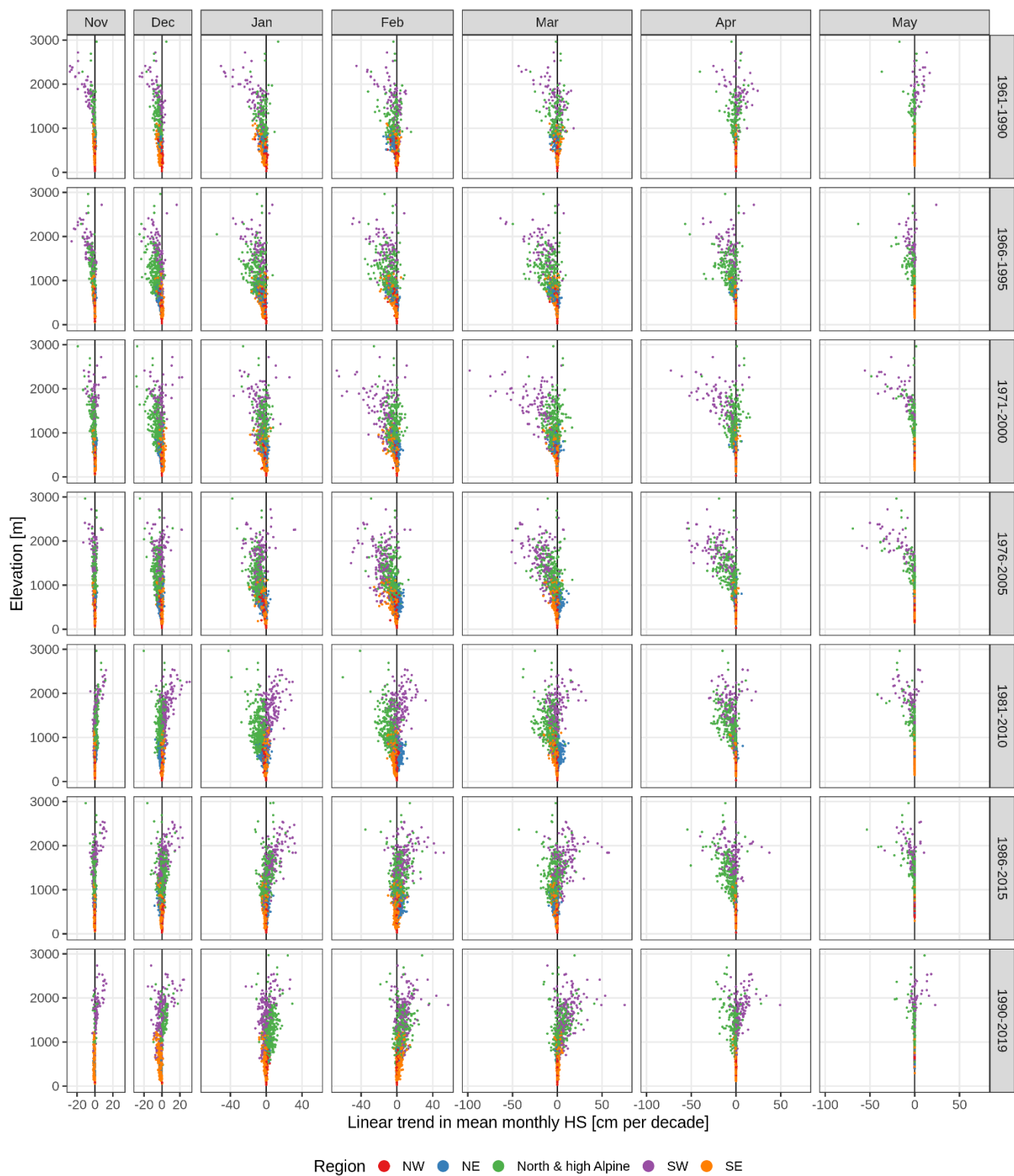
trend analysis, this section presents an evaluation of the interannual variability of snow depth series. Figure 8 highlights that mean snow depth exhibited a strong interannual variability in the analysed period. Because of the large number of stations, only time series that average over all stations in 500 m elevation bands are shown; however, individual station behaviour was well represented by the 500 m averages, see also auxiliary plots at the repository (Matiu et al., 2020). In the 1970s and 1980s high snow depths were observed, followed by a period of extreme low snow depth in the 1990s. Since the 1990s, snow depths in winter have partly recovered, while in spring snow depths have continued to decline. At the end of the snow season and for lower elevations, average snow depths approached zero, such as in April for 500 to 1000 m

or in May for 1000 to 1500 m. The different regions showed similar large-scale patterns, and, for example, the 1990s drop can be seen across the whole Alps. Particular years, especially extreme ones, show concurrent behaviour, for example February 1986 or 2009. Otherwise, there is mixed coherence across regions.

~~In March, high variability of trends was observed for the SW stations. Similar to before, trends were mostly negative in the periods from 1961–1990 to 1976–2005, both positive and negative in the period 1981–2010, and mostly positive in the periods 1986–2015 and 1990–2019. While North & high Alpine stations exhibited the same pattern, the magnitude of the positive and negative trends was smaller. This implies much stronger short-term variability in the southern Alps compared to the north.~~

~~In April and May, the pattern across the 30-year periods remains similar, however, all trends are more negative. Trends are negative across all periods for almost all stations in the three northern regions. Only some high-elevation SW stations show positive trends in April and May in the periods 1961–1990 and 1981–2010 to 1990–2019.~~

~~All these~~These patterns ~~fit the~~are generally in line with those presented in previous studies, which showed high snow amounts in the 1960s and ~~1970s~~1980s and negative anomalies in the ~~1980s~~1970s and 1990s, i.e. snow scarce winters, regime shifts or breakpoints in that period in France, Switzerland, Italy, and the western and southern part of Austria, and a recovery afterwards (Durand et al., 2009; Laternser and Schneebeli, 2003; Mallucci et al., 2019, 2019; Marcolini et al., 2017b; Marty, 2008; Micheletti, 2008; Scherrer et al., 2013; Schöner et al., 2019; Valt and Cianfarra, 2010). In an Alpine wide view, this temporal variability is also accompanied by a strong spatialregional variability, ~~especially comparing stations north versus south of the main ridge.~~



655

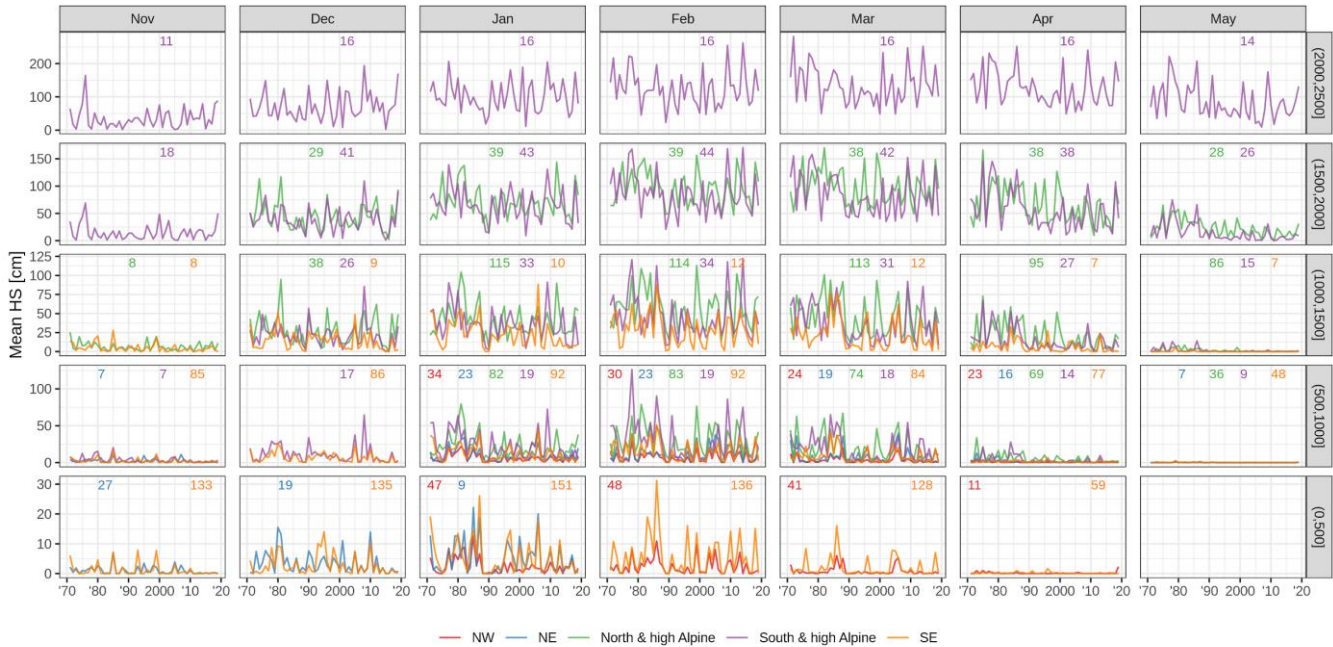
Figure 6: Thirty year linear trends in mean monthly snow depth (HS) from 1961 to 2019. Each point represents one station, the rows denote the 30 year period used to calculate the trend, and the columns the months. Larger plots and all intermediate windows are available as auxiliary material (Matiu et al., 2020).

3.4 Representativeness of the stations in an Alpine wide context

660

Most of the analysis was performed with the aim to maximize the number of available observations per month. While this results in unbalanced station sets across months, it should provide better areal estimates than significantly reducing the station set to complete seasonal series only. Moreover, we assume that most of this seasonal imbalance is because there is no or no significant snow cover in that month, and not because the stations have missing observations.

Station observations generally



665

Figure 8: Time series of mean monthly snow depth averaged by 500 m elevation bands. The rows indicate elevation band and the columns the months. The small numbers at the top of each panel denote the number of stations included in the average. Lines are only shown if more than 5 stations were available. Time series of all single stations are available at the repository (Matiu et al., 2020).

670

In order to put the trends from Sec. 3.3 into context of interannual variability, we examined their relationship by looking at the ratio between the 1971 to 2019 trend and the standard deviation of residuals (Fig. B2(a)). This gives an indication of the relative contribution of the trend to interannual variability. The highest ratios were observed in November to January below 1000 m, in March between 500 and 2000 m, in April between 0 and 2500 m, and in May between 1500 and 2500 m.

As expected from the high temporal variability of the snow depth series, the fraction of explained variance from the linear trends was low. The average R^2 over models with significant trends ($p < 0.05$) was 10%. However, R^2 increased with elevation and in the last months of the snow season, reaching up to 32%. Such low R^2 values do not cover the full elevational gradient and are supposed to diminish the significance of trends or the relevance of their magnitude, they simply highlight the strong interannual variability.

From Figure 8 a decrease in the variability of the snow depth series can be more densely located at observed, especially at the end of the season and for lower elevations. This is confirmed by the large fraction of negative time coefficients for the error variance in April and May (Table B2), where approximately 40-80% of the stations presented significantly decreasing variability, depending on the region. Notable decreases in variability were also observed in November and in January for NE, NW, and SE. Considerable significant increases of variability, on the other hand, were only observed in December for 27% of the South & high Alpine series.

3.5 Seasonal snow indices of snow depth and snow cover duration

In addition to the analysis of monthly mean snow depth from Sec. 3.3 and 3.4, this section gives a summary of trends in seasonal indices of mean and maximum snow depth as well as snow cover duration (Table 3, Appendix C). The results of seasonal mean HS agree with the monthly analysis and show generally decreasing snow depths in winter up to 2000 m and in spring for all elevations. Maximum snow depth across the whole season (November to May) decreased stronger than mean snow depth, e.g. the average trend of mean HS for stations in the north (N&hA, NE, NW) between 1000 and 2000 m was -2.8 cm per decade and -5.2 cm per decade for maximum HS, which corresponds to -6.2 and -4.2 % per decade, respectively. Again, stations south (S&hA, SE) had more negative trends: e.g. -4.1 cm per decade for mean HS and -9.8 cm per decade for maximum HS for the same elevations (1000 to 2000 m), which corresponds to -8.9 and -7.1 % per decade, respectively. Average relative trends below 1000 m were more negative than average trends between 1000 and 2000 m for meanHS (DJF and NDJFMAM) and all SCD indices, but not that obviously for meanHS in MAM and maxHS.

Seasonal SCD also decreased for almost all stations below 2000 m, while above no consistent or significant changes were observed. The average trend in November to May SCD over all stations below 1000 m was -4.4 days per decade in the north and -4.8 in the south, and over all stations between 1000 and 2000 m, -5.3 in the north and -6.7 in the south, respectively. The fact that above 2000 m no changes in SCD were observed might also be caused by our season definition (November to May), which is not always enough to capture the full season above 2000 m. In addition, our changes per decade for mean HS, maximum HS and SCD are clearly smaller than the ones found by Klein et al. (2016) for a similar time period but a small number of stations in Switzerland. In relative terms, mean HS decreased stronger than maximum HS in our study, which is consistent with previous findings (Bach et al., 2018). However, in absolute terms, the opposite was true for our study.

710

Table 3: Summary of 1971 to 2019 trends in seasonal snow indices. The five regions were collapsed into two (north and south). The number of stations differs by season and the range of available series is indicated in the third column. Average trends (with minimum, maximum in parentheses) are given for seasonal indices of mean snow depth (meanHS), maximum snow depth (maxHS), and snow cover duration (SCD). The season is indicated in the second row with the first letter of the included months (e.g. NDFJ is November, December, January, and February). Absolute trends are in cm per decade for meanHS and maxHS, and in days decade⁻¹ for SCD. Relative trends are expressed as % per decade (a few stations south below 1000m were removed, because their low and insignificant snow amounts caused unlikely high relative trends).

Elevation [m]	Region	# series	meanHS	meanHS	meanHS	maxHS	SCD	SCD	SCD
		(range)	DJF	MAM	NDJFMAM	NDJFMAM	NDJF	MAM	NDJFMAM
Absolute changes			cm per decade			days per decade			
(0,1000]	North	141-190	-0.9 (-5.3, 1.0)	-0.8 (-6.4, 0.1)	-0.8 (-4.7, 0.4)	-2.4 (-11.2, 3.1)	-2.7 (-10.0, 2.8)	-1.7 (-5.9, 0.1)	-4.4 (-12.7, 2.8)
	South	224-241	-1.2 (-6.0, 0.9)	-0.3 (-3.2, 0.3)	-0.7 (-3.6, 0.2)	-3.2 (-15.3, 3.1)	-3.6 (-10.8, 1.1)	-1.1 (-5.3, 0.3)	-4.8 (-14.6, 0.1)
(1000,2000]	North	122-155	-2.1 (-11.0, 3.1)	-3.7 (-21.9, 0.8)	-2.8 (-15.6, 1.6)	-5.2 (-19.9, 3.0)	-2.2 (-8.3, 5.0)	-3.0 (-7.4, 0.7)	-5.3 (-13.7, 0.8)
	South	61-84	-3.5 (-12.6, 2.3)	-4.9 (-18.7, -0.3)	-4.1 (-14.0, 1.6)	-9.8 (-29.2, 2.6)	-2.5 (-7.4, 1.9)	-4.0 (-8.2, 1.3)	-6.7 (-14.1, -0.5)
(2000,3000]	North	3-4	-4.3 (-9.9, -2.2)	-4.5 (-5.2, -4.1)	-5.0 (-8.2, -3.3)	-8.1 (-15.8, -4.2)	0.0 (-0.1, 0.1)		0.0 (-0.1, 0.1)
	South	16-17	-0.1 (-9.2, 11.3)	-6.7 (-18.2, 6.6)	-2.9 (-11.5, 6.8)	-9.4 (-29.2, 6.1)	-0.3 (-2.7, 1.5)	-0.6 (-4.6, 1.3)	-0.9 (-4.8, 1.2)
Relative changes			% per decade						
(0,1000]	North	141-190	-7.2 (-20.4, 12.1)	-11.2 (-20.6, 18.0)	-8.7 (-20.4, 10.0)	-4.7 (-19.4, 8.6)	-5.1 (-19.7, 7.8)	-9.9 (-28.5, 3.4)	-6.1 (-16.3, 6.8)
	South	220-238	-8.7 (-18.6, 22.7)	-7.5 (-21.7, 28.0)	-10.0 (-19.0, 10.6)	-6.8 (-16.7, 10.4)	-6.7 (-14.5, 14.1)	-7.9 (-22.0, 14.8)	-7.2 (-14.2, 10.1)
(1000,2000]	North	122-155	-3.6 (-17.6, 23.3)	-9.5 (-20.0, 3.1)	-6.2 (-18.3, 5.1)	-4.2 (-13.8, 3.9)	-2.1 (-8.6, 10.6)	-6.0 (-19.2, 4.2)	-3.5 (-11.9, 0.8)
	South	61-84	-6.5 (-14.1, 5.1)	-11.4 (-17.2, -1.0)	-8.9 (-14.8, 4.9)	-7.1 (-12.0, 3.0)	-2.6 (-8.7, 2.0)	-7.7 (-17.5, 4.5)	-4.6 (-10.4, -0.4)
(2000,3000]	North	3-4	-2.5 (-4.0, -1.5)	-1.8 (-2.0, -1.4)	-2.4 (-2.9, -2.1)	-2.1 (-3.1, -1.6)	0.0 (-0.1, 0.1)		0.0 (-0.1, 0.0)
	South	16-17	0.2 (-8.0, 11.7)	-4.2 (-11.9, 13.2)	-2.4 (-10.1, 6.7)	-3.4 (-9.1, 4.6)	-0.2 (-2.4, 1.4)	-0.7 (-5.3, 2.0)	-0.5 (-2.4, 0.6)

715

3.6 Representativeness of the stations in an Alpine wide context

Since we aimed to give an Alpine wide assessment, the spatial and elevational representation coverage of the station observations is crucial in determining the confidence in the results. For this, we compared the elevation distribution of our station set with a digital elevation model (DEM) at 1 km resolution for the area spanned by the stations (Fig. 2(bc)). In relative terms, the elevations of the stations used in this study oversampleoversampled the elevations up to 1000 m, arewere similar from 1000 to 2000 m, significantly underrepresentunderrepresented 2000 to 3000 m, and dedid not cover elevations above 3000 m.

720

If the absolute number of stations used in this study is deemed sufficient to describe the spatial coverage, then the confidence of statements would be high for elevations up to 2000 m, while between 2000 and 3000 m, the results should be taken more cautiously. The elevations above 3000 m are only local features, but in an Alpine wide view they only cover a minimal area

725

(0.7% of the area studied here, see Fig. 2(bc)), and thus their significance is limited for hydrological applications, yet they remain relevant for mountain ecosystems, glacier dynamics and mountain (ski) tourism.

Spatial variability of snow increases with elevation (see also Fig. 76), and thus the absolute number of stations required for comparative assessments would be even higher for high elevations compared to low elevations. This limitation could be tackled with automatic snow depth sensors, which better sample high elevations; however, their historical time series are yet too short for assessing long-term trends, besides their issue of harmonized data processing (see also Sec. 1).

~~3.5 Snow depth climatology and links to temperature and precipitation~~

~~Besides differences in trends, the regions also demonstrate different snow depth climatologies (Fig. 7). Looking at average winter (December to February) snow depth 1981–2010, the northern regions had higher snow depths than their southern counterparts. These differences became larger with increasing elevation: While below 750 m no substantial differences were observed, southern stations had ~30% less snow than northern station until 1750 m, and ~20% less until 2250 m; above the number of stations is too low (Table C2).~~

~~Average winter temperatures were higher in NW compared to NE and SE, and the latter two were similar. In North & high Alpine and SW temperatures were also comparable, although northern stations were colder in 1500–2000 m. However, precipitation amounts were significantly lower south than north, and SW stations received ~100m less winter precipitation than North & high Alpine stations up to 2000 m, which amounts to ~1/3 of the precipitation north. These results suggest that the difference in December to February snow amounts north versus south are driven by precipitation differences and not temperature.~~

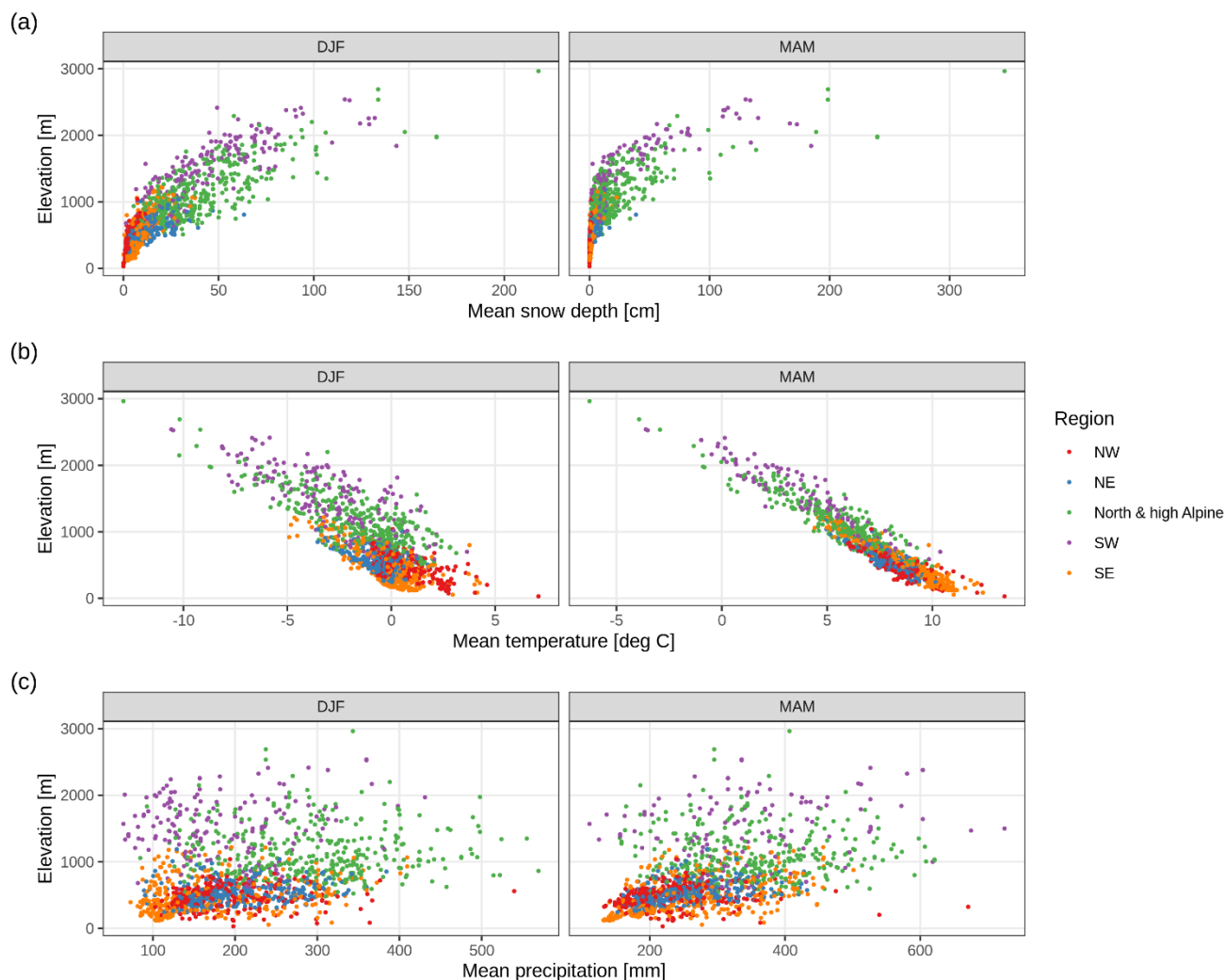


Figure 7: Climatology of (a) snow depth, (b) temperature, and (c) precipitation across regions and elevations for the winter season (December to February, DJF) and spring season (March to May, MAM). Average values are for the period 1981–2010. Each point represents one station. The temperature and precipitation values were extracted from MESCAN–SURFEX reanalysis, while the snow depths are based on station data. See also Table C2 and C3 for summary values.

Seasonal snow depth was correlated to temperature and precipitation extracted from a gridded reanalysis (MESCAN–SURFEX). Results indicate negative correlations with temperature, decreasing strongly with elevation, and positive correlations with precipitation, mildly increasing with elevation (Fig. B5). The magnitude of temperature correlations was between -0.8 and -0.5 below 1000 m, and the correlation decreased to about -0.2 up to 2000 m. For precipitation, correlations were between -0.2 and 0.7 , with much higher variability than temperature. Correlations of snow depth with temperature did not differ by region. However, the stations in SE exhibited stronger (more negative) correlations with precipitation than the NE and NW regions.

The findings on the correlations agree with previous estimates for Swiss and Austrian stations (Schöner et al., 2019) in terms of signs and elevation patterns. However, our estimates are of higher magnitude for both temperature and precipitation. While the climatological and correlational results do not suffice to formally attribute changes in snow cover to temperature and precipitation, they highlight temperature and precipitation as likely drivers of variability and change, consistent with the physical understanding of snow processes (Hock et al., 2019). The lower precipitation amounts south of the main ridge and higher correlations (at least for SE) could be causing the higher variability of snow depth trends in the southern regions, because this implies less chances that precipitation falls at the “right” time. As sensitivity analysis, we repeated the climatology and correlational analysis using observation-based spatial analyses instead of reanalysis for extracting temperature and precipitation (Fig. B6, Table C4, Fig. B7), but results did not differ qualitatively from above.

3.6 An alternative method to derive spatially representative results is to transform the station point observations into a gridded area, by e.g. deterministic or geostatistical interpolation (i.e., kriging). However, in the complex topography of the European Alps with strong elevation gradients, it is challenging to determine an appropriate horizontal resolution that represents elevation well. Moreover, a high enough station density would be needed to perform interpolation. An observation-based grid of snow depth for the Alps would have many potential use cases, from hydrological applications to evaluation of remote sensing and climate models, but it is beyond the scope of this study.

3.7 Outlook

The scope of this study was primarily the detection of snow depth trends, thereby contributing to better understanding and quantification of the state and evolution of the mountain cryosphere in the European Alps (Beniston et al., 2018; Hock et al., 2019). The formal attribution of the trends to climatic drivers, such as temperature and precipitation, as well as the influence of anthropogenic climate change on snow trends (Najafi et al., 2017; Pierce et al., 2008) is not explicitly addressed, although the collation of this unique dataset allows the scientific community developing such studies ~~to develop~~ in the future.

The homogenization of series, which is the removal of non-climatic parts in the time series, such as e.g. caused by instrumentation changes or station relocations, is a standard practice in long-term temperature and precipitation records (Auer et al., 2007). Applying the same tools to snow depth is not straightforward. There is discussion ongoing on the appropriate homogeneity tests and suitable observation frequency, such as daily, monthly, or seasonal (~~Marcolini et al., 2017a; Schöner et al., 2019~~); (Marcolini et al., 2017a, 2019; Schöner et al., 2019). An analysis of a data set with parallel snow measurements indicates that SCD and maxHS are one of those indicators which are least affected by inhomogeneities (Buchmann et al., n.d.). Current research tries extending existing approaches with new innovations (Resch et al., 2020). Homogenization could improve the robustness of estimated trends, and be especially useful for areas with sparse observations, such as for elevations above 2000 m. ~~However, Given the use large extent of such an extended our dataset based on several thousands of individuals observation stations reduces the impact of non-climatic changes in some stations, hence~~

~~the explicit need of, it was not possible to apply a common homogenization here framework for our study and we leave this for future studies.~~

Besides snow depth, also observations of the depth of snowfall (HN) were collected for this study. However, analysing the HN series and comparing results to those obtained for snow depth would have exceeded the scope of this study. In the future, we plan to continue with the analysis of HN series, for which we are also aware of other data sources, in particular for low elevation sites in Italy (Pifferetti et al., 2017).

4 Conclusions

We presented the first Alpine wide assessment of snow depth trends based on in-situ measurements in the European Alps. This enabled the identification of five distinct snow regions, whose spatial gradients are related to the known diverse climatic influences for the Alps.

The trend analysis, based on measurements from 1971 to 2019, ~~highlights the overall reduction in snow cover. Decreases in snow depth were observed for 82% of the stations from December to February (15% of these significant) and 90% for March to April (27% significant), while only 18% and 10% showed increases, respectively (0.6% of the increases significant, in both cases).~~ highlights the overall reduction in snow cover. Decreases in monthly mean snow depth from November to May were observed for 85% of the station-month combinations (of which 26% significant, $p < 0.05$), while only 15% showed increases (of which $<1\%$ significant). Stronger negative trends with higher significance were observed in spring, and in the case of low elevations during the whole season (Table 2). Seasonal maximum snow depth decreased stronger than seasonal mean snow depth in absolute terms, while in relative terms the opposite was true (Table 3). Snow cover duration decreased below 2000 m, while above no consistent change was observed. The magnitude of trends differed by region and the decreases in the south were on average stronger than in the north (Table 2, Table 3). Combined with the lower snow depths south than north (Fig. 6, Table S1 and S2), this resulted in an even stronger relative decrease south than north. The number of stations analysed here gives high confidence to the changes up to 2000 m, while above this elevation the changes have to be interpreted more carefully, especially in the north, where only few stations were available.

~~The magnitude of trends differed by region and the number of stations analysed here gives high confidence to the changes up to elevations of 2000 m, while above 2000 m the changes have to be interpreted more carefully, especially in the north, where only ~10 stations were available. The decreases in the south were on average stronger than north (Table 3). Combined with the lower snow depths south than north (Fig. 7, Table C2 and C3), this results in even stronger relative decreases south than north.~~

Table 3: Summary of monthly snow depth trends. The five regions were collapsed into two (north and south) and the months into seasons. Trends are given in cm decade^{-1} for winter (December to February, DJF) and spring (March to May, MAM), along with the number of stations (#) in the respective spatial and temporal subset.

Elevation	Region	DJF mean (min, max)	DJF #	MAM mean (min, max)	MAM #
(0,1000]	North	-0.9 (-7.3, 4.4)	411	-0.8 (-10.9, 0.4)	486
	South	-1.2 (-10.8, 2.3)	747	-0.4 (-8.7, 1.0)	647
(1000,2000]	North	-2.0 (-14.3, 4.4)	377	-4.0 (-28.1, 4.0)	403
	South	-3.4 (-25.1, 3.3)	252	-5.9 (-27.2, 4.1)	208
(2000,3000]	North	-3.3 (-10.4, 0.2)	9	-5.1 (-10.5, 0.3)	11
	South	0.5 (-23.3, 9.9)	51	-8.2 (-28.3, 10.5)	49

825 The orography of the Alps clearly manifests as ~~athe~~ main impact on ~~the~~ snow climatology ~~thus defining. It defines~~
boundaries for subregions in north versus south, followed by west versus east. The location of a ~~stations~~station with respect
to the climatic forcing zones defines the snow depth climatology, ~~and~~ impacts the variability of snow depth at ~~a~~ daily scale,
~~and. Additionally, it~~ can result ~~not only~~ in different trend ~~strength but~~magnitudes ~~and~~ also trend signs. Besides these larger
scale features, substantial variability exists at higher elevations within the estimated snow depth ~~clusters~~regions. In summary,
830 the assumption that results from one region are valid in another or for the whole European Alps needs to be evaluated
cautiously.

This study provides a clear and harmonized picture ~~relevant to~~for the detection of observed snow depth trends across the
European Alps, ~~thereby. Thereby it~~ contributes to ~~bridging~~bridge a scientific gap, which exists for many mountain areas in
the world (Hock et al., 2019). We anticipate that the dataset developed for this study, ~~and~~ from which a large part is made
835 available to the broader scientific community, will provide support for further studies ~~and in. In~~ particular ~~to~~ formal
attribution studies, ~~to physical drivers of changes as well as~~which quantify the ~~quantification of their~~ anthropogenic
component, ~~in the physical drivers of change, and~~ which remain extremely limited regarding snow cover trends (Najafi et al.,
2017; Pierce et al., 2008).

A large community effort and open data sharing for research purposes has made this study possible. We ~~hope to~~ have shown
840 the benefits of ~~having such a~~ data set that spans many nations and institutions ~~and. We~~ expect this dataset to be used, ~~and~~
~~perhaps expanded thanks to additional contributing organizations, in for~~ further studies addressing various sectoral
applications or for the evaluation of remote sensing or reanalysis products. ~~Perhaps it might be expanded in the future thanks~~
~~to additional contributing organizations.~~ However, we currently lack the opportunity to have a continuously updated version.
With ECA&D (European Climate Assessment & Dataset), a harmonized station data collection portal exists at the European
845 scale for many meteorological variables. But while the coverage of e.g. temperature and precipitation is balanced across
Europe, snow depth is only limited or not at all available for many European mountain regions, such as the European Alps,
Carpathians, Balkan Mountains, or Dinaric Alps. It would be desirable to have an updated harmonized station dataset for ~~the~~
snow cover, given its importance in mountains and further downstream. This would enable ~~tea~~ better ~~monitor~~monitoring of

the changes, their consequences and impacts, and contribute more quantitatively ~~than at the present to regional and global~~
850 climate change, ecosystems and environmental assessments than is possible at the moment. However, such an endeavour
requires a more formal umbrella and long-term commitment, e.g. in the framework of the Copernicus Earth monitoring
programme of the European Commission.

855

Appendices

Appendix A: Data Processing

860 After collecting the data, the series from different data providers were harmonized and put into a common data format. This included converting all station coordinates into latitude and longitude. In a few cases, where only station name and elevation were available but no coordinates, the missing coordinates were extracted from Google Maps using the approximate location (with correct elevation) based on the station name. Most data providers ~~used~~ station identifiers along with station names. We chose to have unique identifiers for all stations based on the station name. Station names were standardized by replacing
865 blanks and apostrophes with underscores, and by removing accents. If multiple stations had the same name within one ~~network~~ data source i.e. by data provider, the names were suffixed with the ~~data-provider~~ station identifier: from the data provider. If multiple stations had the same name across ~~networks~~ data providers, the names were suffixed with the data provider identifier.

A.1 Merging of records

870 The final database included several cases in which snow measurements for the same location were stored as separate records since they covered different periods and/or a slight relocation of the same station site occurred. In some cases, different records were available at very close locations where snow data were collected at the same time or over partially overlapping periods for different operative or research purposes. In order to maximize the temporal continuity and extent of available HS and HN series, the records referring to the same site or to very close locations were merged: ~~One~~ series was created from
875 the multiple series by replacing missing values or missing periods. In particular, the merging was performed only if the sites were closer than 3 km and their vertical distance was less than 200 m. In the case of overlapping periods, the data from the series with the fewest gaps was retained. The merging was evaluated and performed on HS series first. In the case that HN series for the same sites were also available, the data were merged by following the same criteria used for HS, in order to preserve consistency between HS and HN measurements. The metadata of the most recent series included in the merging
880 was assigned to the resulting record. About 60 merged series were obtained in total and the duplicated records for the same site were discarded.

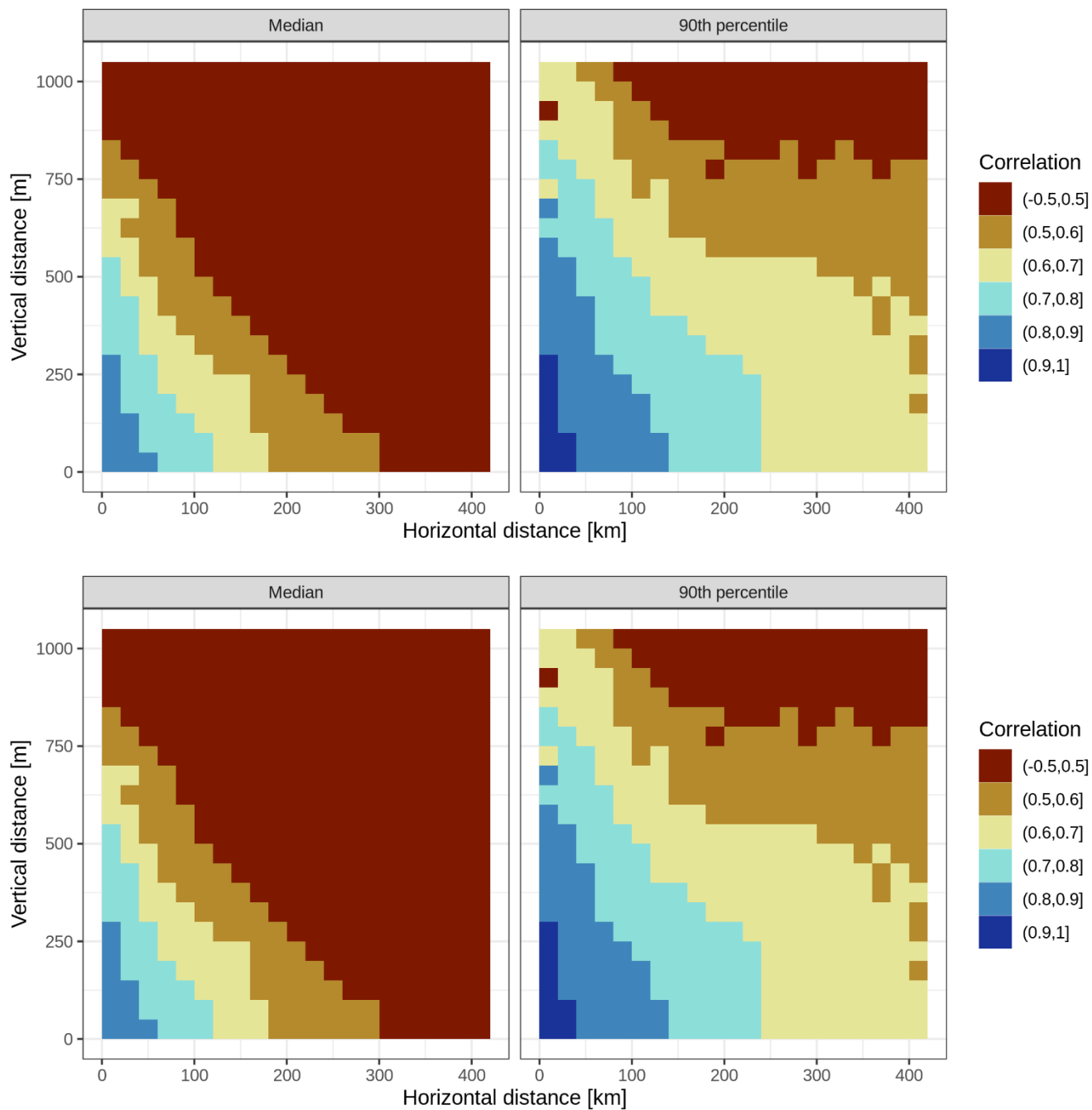
A.2 Quality control

The series were quality checked in order to remove recording errors. First, below zero HS or HN values were replaced with
885 missing values. Then a temporal consistency check was applied to HS to identify recording errors. Series were screened for jumps larger than 50 cm (up and down in two consecutive days; or vice versa). This criterion identified 680 values from the daily observations from all series, which were checked manually, and recording errors were replaced with missing values. Another issue with HS series is that missing observations might falsely be recorded as 0 cm. To identify suspicious series,

mean winter (December to February) HS and the fraction of 0 cm values were calculated per station. Then, looking at a
890 surrounding elevation band per station (200 to 500 m, depending on the elevation and station availability), series were
marked if the mean HS was less than the 5th percentile or the fraction of 0 cm values was higher than the 95th percentile of all
stations in the elevation band. The horizontal distance was not considered for this step. This resulted in 181 suspicious series,
which were checked manually. For 32 stations, there were periods where 0 cm were obviously missing values, and in these
periods the 0 cm values were replaced with missing values; the remaining 149 stations had no missing values denoted as 0
895 cm. Finally, during all previous manual checks, series that showed “dubious” ~~behavior~~behaviour were marked, which were
in total 48 series. Dubious ~~behavior~~behaviour was e.g. inconsistency between HN and HS, unlikely values, improbable
temporal variability, multiple seasons with no snow, or excessive gaps. From these 48 series, 29 were considered usable, 11
had some periods removed, and 8 were completely removed.
These procedures could identify some errors, but ~~definitively~~definitely not all. Because of the large number of series, it was
900 not feasible to manually quality check all of them, and fully automatic checks are often not feasible. Instead a spatial
consistency check was applied (see Appendix A.4), and the rest of remaining errors could be considered noise given the
large amount of data.

A.3 Gap filling

905 Most series contained gaps ranging from some days up to whole seasons. In order to conduct climatological or trend
analyses, gaps in the series needed to be filled. For this we employed a spatial interpolation approach, similar to the one used
for temperature and precipitation records (see e.g. Brunetti et al., 2006; Crespi et al., 2018; Golzio et al., 2018). The
approach is based on correlations between the series, and because snow strongly depends on elevation, we first performed a
spatial analysis to identify which correlations can be expected depending on horizontal and vertical distances between
910 stations. For this, pairwise correlations (Pearson) between the daily HS series were performed for December to April from
1981 to 2010, only if the series had at least 70% valid data, and only if each pair had at least 50% of data in common. As
expected, correlations decreased with both horizontal and vertical distance (Fig. A1). But correlations remained high even
for large distances, e.g. correlations higher than 0.7 were found up to vertical distances of 500 m (with less than 100 km
horizontal distance) or up to horizontal distances of 200 km (with less than 250 m vertical distance). It should be noted that
915 correlations can be high even if there are large differences in amounts or ratios between the series, as long as the differences
and ratios are constant across the range of values.



920 **Figure A1: Summary of pairwise correlations between HS series for December to April, 1981 to 2010. Shown is the average (median, left) and 90th percentile (right) of all pairwise correlations in bins of 20 km horizontal distance by bins of 50 m vertical distance. The correlations were only calculated if each series had at least 70% valid data in the period and if each pair had at least 50% of data in common.**

925 The chosen approach fills a gap based on finding highly correlated ~~neighboring~~neighbouring series to the one with gaps. The
~~correlation is calculated on gap filling algorithm works as follows. For each gap:~~

1. Find temporally surrounding non-missing values in the gap series around the gap date (“window data, by crossing
”), see also Fig A2 (a calendar day window with a year window. Specifically, for each gap,)
 - 1.1. Take 15 days before and after ~~are considered, and the same calendar days are taken the gap.~~ This results in
930 31 days of the year: e.g. for Jan 15, this would be Jan 01 to Jan 31; for Jan 01, this would be Dec 16 to Jan
16.
 - 1.2. Repeat step 1.1. for 10 years before and ~~40 years~~ after the gap. ~~Thus, in~~ This results in 21 years. E.g. for
1996, this would be 1986 to 2006.
 - 1.3. This window data potentially contains 651 values (21*31), but likely has missing values. If there are more
935 than 150 non-missing values continue to step 2. If there are less than 150 non-missing values, increase the
day window by 5 days in both directions, and repeat from 1.1. If the day window has reached 45 in one
direction (i.e. total, including the gap day/year, this results in a window of 31 days by 21 years (651
potential values). ~~The 91 days), and still there are less than 150 non-missing dates, stop. Note: only the day~~
window is increased ~~up to 91 days, until sufficient non-missing values,~~ the year window from 1.2. stays
940 constant at 10 years before and after.
2. Pre-select potential reference series (Fig. A2 (b)) based on the following criteria: vertical distance to gap series
below 500 m, horizontal distance below 200 km, and the value at the date of the gap is not missing.
3. For each potential reference series:
 - 3.1. Identify dates with values available for both gap and reference series in the window identified in step 1.
945 (Fig. A2 (c)). Continue only if more than 80% of the minimum 150 non-missing values (i.e. 120) are
available in common.
 - 3.2. For the common dates: calculate mean of gap series and mean of reference series; calculate correlation
between gap series and reference series. If all values of gap and reference series are zero, set the
correlation to the minimum threshold ~~used here was 150 values). Based on the previous spatial analysis,~~
950 ~~reference stations were searched for in a 200 km horizontal radius with less than 500 m vertical distance.~~
~~The (see step 4.) plus 0.001 (in order to be able to fill also zero periods).~~ If only one of the series has all
zero values, i.e. either gap or reference but not both, set the correlation to zero.
 - 3.3. Calculate ratio between mean of gap series divided by mean of reference series. If the mean of the
reference series (divisor) is zero, set the ratio to zero (in order to be able to fill also zero periods).
4. Sort potential reference series by correlation with gap series (from step 3.1.). Remove all candidates with a
955 correlation below 0.7. ~~This threshold for minimum correlation was set to 0.7, was chosen~~ as it is used e.g. in the
homogenization of snow depth (Marcolini et al., 2017a). ~~One to five reference stations were selected if they passed
all of these criteria (within spatial distance, minimum correlation, enough common data in window, and no missing~~

value on gap day); if more than five stations were available, then the five with the highest correlation were selected. Based on the same window as above, the ratio between candidate and each reference series was calculated by dividing the mean of the daily values from the candidate series with the mean of each reference series. The final filled value is a weighted average of the reference series values at the gap date multiplied with the ratios, and the weights were based on the vertical distance between candidate and reference station.

5. Select the first 5 best correlated reference series, or up to 5, depending on how many available.
6. Calculate weights based on vertical distance (exponential decay with halving distance 250 m).
7. Fill the gap value with a weighted (step 6.) average of the reference series values adjusted by the ratios between gap and reference series (step 3.3.): $HS_t^{gap} = \frac{1}{n} \sum_{i=1}^n w_i * HS_t^{ref_i} * \frac{HS_{mean}^{gap}}{HS_{mean}^{ref_i}}$, where t is the date of gap, i is the index of reference series, n is the number of reference series 1...5, and w_i are the weights with $\sum_i w_i = 1$.

The filled value was rounded to the nearest integer value in cm. Since the method requires finding suitable ~~referencees~~reference stations, it was only performed for the period 1961 to 2020, because the station density was too low before. The gap filling was applied to all gaps in all series considering all available data; afterwards thresholds were applied to select usable series (see end of this section).

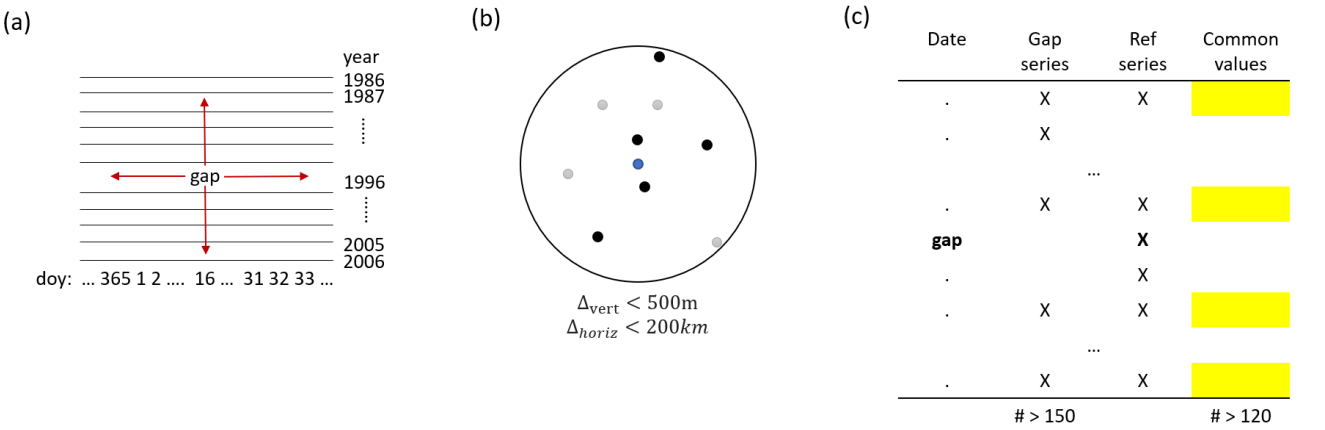


Figure A2: Visualization of some steps of gap filling algorithm. (a) shows how the window data in the gap series around the gap is determined (step 1.); day is day-of-the-year. (b) shows the selection of potential reference series by horizontal and vertical distance (step 2.). (c) shows how common dates for gap and reference series are identified (step 3.); the dates come from the window in (a).

The chosen limits of 200 km horizontal distance and 500 m vertical distance might seem very high in the Alpine context with the complex topography. Since we were interested in larger scale snow ~~pattern~~patterns and not local snow peculiarities, such large distances ~~were useful~~are justified. Moreover, the correlation threshold should exert control on selecting only

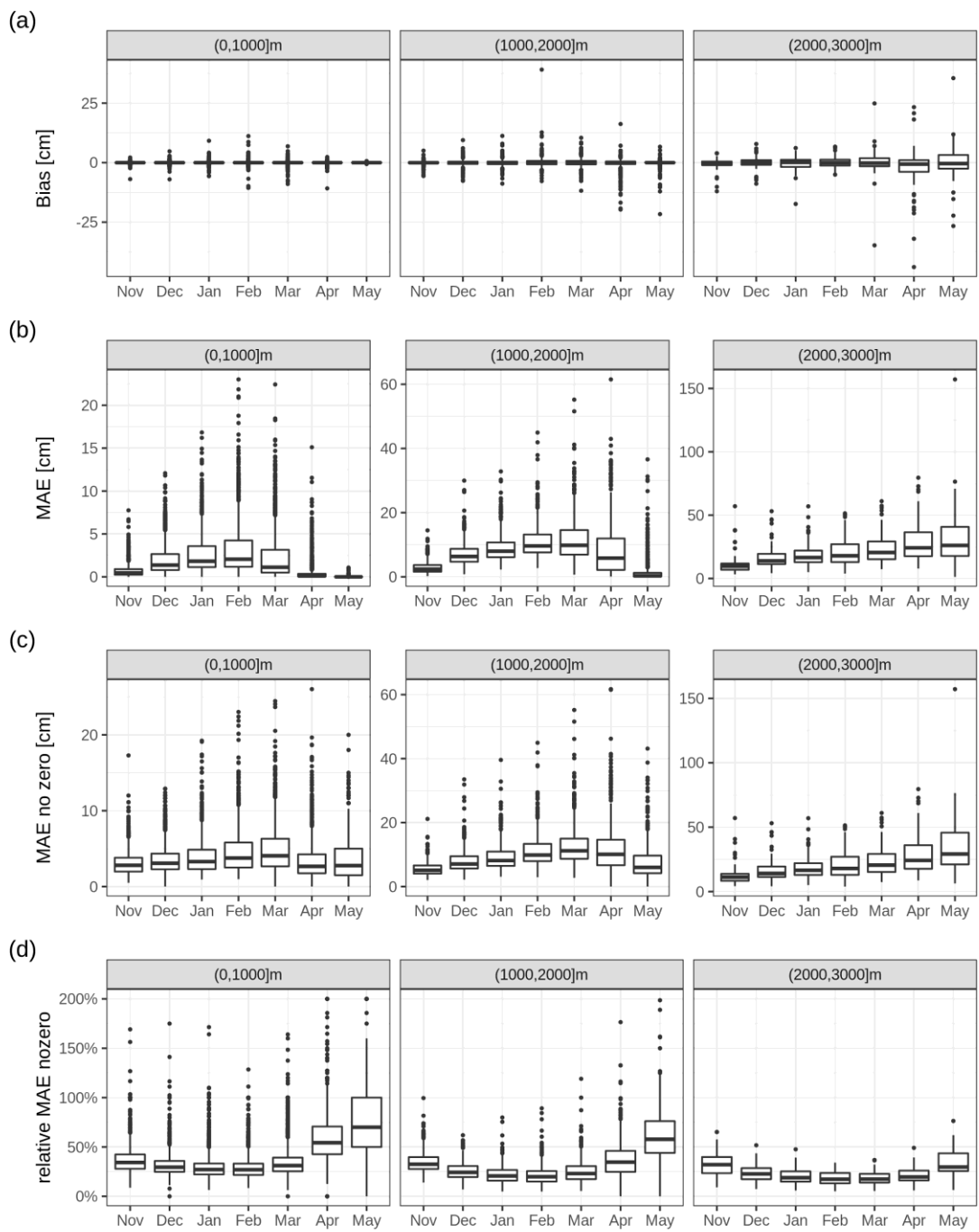
stations that share the same snow cover evolution, and high correlations were found up to these horizontal and vertical limits (Fig. A1). On the other hand, a nearby station might also be a worse predictor than a more distant one, if, e.g., it differs in its local climate.

Since this gap filling approach has not ~~yet~~ been ~~yet~~ used for snow depth, we performed a cross-validation analysis to identify the gap filling errors. For this, we used data from November to May in the period 1981 to 2010. For each station and each year, one month at a time was held out, but only if at least 10 days were available. Thus, for each month, a maximum potential of ~900 values were cross-validated; however, the effective number was lower, because of missing values, and because not all gaps could be filled, if no suitable reference stations were available. In order to test the effect of shorter period gaps, we also applied the cross-validation on subsets (to reduce computation time): 1) 100 random samples of 1 day and 2) 20 random samples of 5 consecutive days. Then, the held-out values were filled using the above approach, and metrics calculated based on the filled and held-out values. Metrics include the bias, the MAE (mean absolute error), the MAE for non-zero true values only, and a modified version of relative MAE. The relative MAE is based on the MAE for non-zero values only, and this non-zero MAE is divided by the average of true non-zero values. This is then not a “true” relative error, which would divide each error by the true value ~~-, i.e. $\frac{1}{n} \sum_{i=1}^n \left| \frac{y_i - x_i}{x_i} \right|$, but our modification is $\frac{1}{n} \sum_{i=1}^n \frac{|y_i - x_i|}{|x|}$, where x is the average of all x_i .~~ This was done to remove the large influence of errors close to zero, which are not that relevant in this case. The metrics were only calculated if more than 50 values were available per month and station (out of potentially ~900 for the month-long gaps, and 100 for the 1 and 5 day gaps), in order to provide robust estimates.

The cross-validation showed that the gap filling is unbiased (Table A1) with the overall average daily bias for the ~~month-~~ month long gaps being -0.04 cm. Average daily MAE for filling whole months was 1.6 cm (averaged over stations located in 0–1000 m), 7.7 cm (1000–2000 m), and 22.0 cm (2000–3000 m). MAE was lower for 1 and 5 day long gaps compared to month long gaps, but almost no differences were observed comparing 1 day or 5 days, e.g. for the 1000–2000 m band, MAE for 1 day gaps was 6.2 cm, for 5 day gaps 6.4 cm, compared to 7.7 cm for 1 month gaps. The relative MAE of month-long gaps decreased with elevation from 39.4% (0–1000 m) to 32.7% (1000–2000 m) to 22.8% (2000–3000 m). Additionally, there was also a seasonal dependence of MAE, while bias remained largely constant across the season (Fig. ~~A2A3~~). MAE below 2000 m peaked in February, while above 2000 m MAE increased throughout the season. Relative MAE decreased with higher snow depths, both temporally and with elevation, that is, relative MAE was lowest in February and at high elevations. It is to be expected that errors at the end of the season are related to the ablation scheme (i.e. local climatic and topographic characteristics that influence ablation) of the different stations; however, at this stage we did not check this issue further.

Table A1: Cross-validation (CV) metrics for the gap filling approach: Bias (the difference between gap filled and observed values), the mean absolute error (MAE), mean absolute error only for non-zero observed values (MAE no zero), and MAE no zero divided by the average of all true non-zero values (Rel. MAE no zero).

Elevation band [m]	CV period	Bias [cm]	MAE [cm]	MAE no zero [cm]	Rel. MAE no zero
(0,1000]	1 day	-0.0	1.3	3.1	30.1%
	5 days	-0.0	1.4	3.3	34.0%
	1 month	-0.0	1.6	3.9	39.4%
(1000,2000]	1 day	-0.1	6.2	7.9	26.1%
	5 days	-0.1	6.4	8.2	28.5%
	1 month	-0.1	7.7	9.7	32.7%
(2000,3000]	1 day	-0.6	18.2	18.6	18.9%
	5 days	-0.8	18.3	18.7	19.2%
	1 month	-0.4	22.0	22.5	22.8%



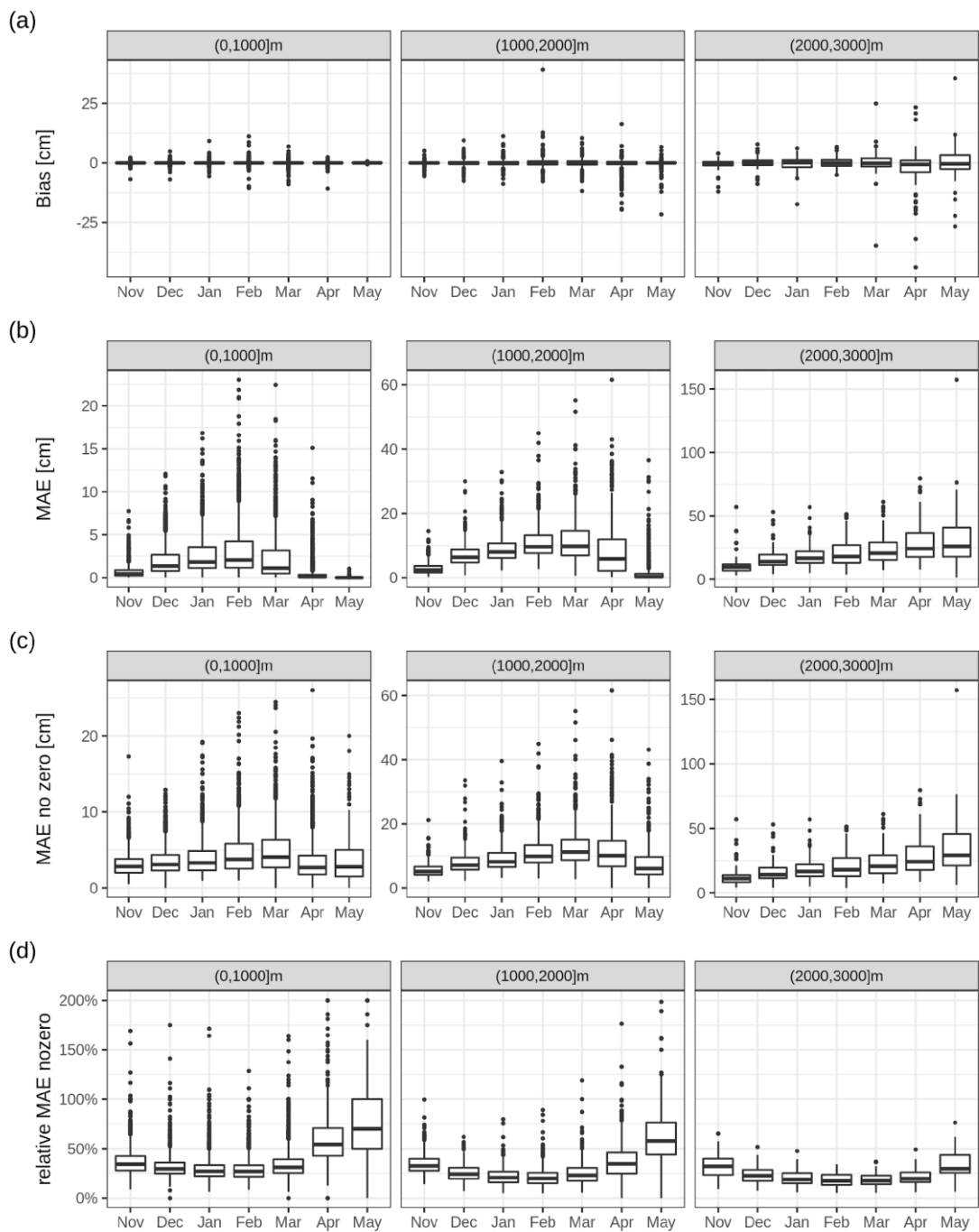


Figure A2A3: Cross-validation metrics for the gap filling approach: (a) bias, (b) mean absolute error (MAE), (c) mean absolute error for non-zero values (MAE no zero), (d) non-zero MAE divided by the true non-zero mean (relative MAE no zero). Panels show the 1000 m elevation bands indicated in the title. The boxplots represent statistical quantities: the box indicates the first and third quartile; the bold line inside the box is the median; the vertical lines outside the box extend up to the most extreme point but

at most 1.5 times the interquartile-range (IOR; height of the box); finally, points below/above 1.5*IOR of the first/third quartile are shown as separate points.

Moreover, we compared our proposed gap filling approach to results from gap filling snow depth series using simulations of the Crocus snow model for the French Alps. The Crocus simulations with meteorological forcing were performed independently of this study, but we found it useful to compare the two approaches - albeit only exploratively. The observed snow depths with gaps were assimilated into the Crocus modelling scheme, using SAFRAN reanalysis data as forcing (López-Moreno et al., 2020). The two gap filling approaches were compared only for existing gaps in the French Alps. This was intended as a preliminary companion evaluation, and no cross-validation was performed. ~~Thus, there was no ground truth to evaluate the two gap filling approaches with formal metrics, and we only performed a visual assessment (figures for comparison available at Matiu et al., 2020)~~ Thus, there was no ground truth to evaluate the two gap filling approaches with formal metrics, and we only performed a visual assessment (figures for comparison available at Matiu et al., 2020). Time series of both gap filling procedures looked remarkably similar, even for reconstructions of complete missing seasons: the different snowfall events were visible in both and snow depths averaged over multiple days were comparable. Differences emerged in the snow settling ~~behavior~~behaviour and for the spring snow melting periods. More information on this exercise is available from the authors on request.

For Switzerland, a comparison of gap filling methods for HS was performed, which aimed at reconstructing complete missing seasons, and which included regression based methods and snow models (Aschauer et al., 2020). While our proposed method was not explicitly used in that comparison, it can be assumed to be similar to the regression-based and distance weighted methods used there. The errors reported in their study (root mean squared error less than 20 cm) are in the same order of magnitude as those found in our cross-validation.

Altogether, the abovementioned (the cross-validation results, the comparison to Crocus, and the preliminary findings of the Swiss study) convinced us that the gap filling procedure is also suitable for reconstructing whole seasons, and not only some intermediate gaps, considering the fact that we only used it to derive monthly means (see below) and ~~havedid not useduse~~ the daily values directly. Further research would be required to check the suitability of the daily reconstructions, in our opinion, also considering the temporal distance to the last existing observations. For the final analysis, all gap filled data within the recording period was used, and we also allowed extending the period up to five years before the start or after the end of the recordings – but only if the total number of gap filled observations was less than the ~~total~~ number of ~~original~~ observations without gap filling. The main reason for this extension was to have series covering the complete period until 2019, because some series stopped just a few years earlier. As sensitivity analysis, we repeated ~~the statistical analysis also for the original data without gap filling and provide results as auxiliary material (Matiu et al., 2020). The gap filling was able to significantly increase the temporal availability, but its aim was not to fill all gaps most of the statistical analysis also for the original data without gap filling and provided results in the supplementary material: the estimated modes of variability matched (Fig. S12); the magnitude and variability of monthly trends was similar, although a lot less stations were available (Fig. S10); and~~

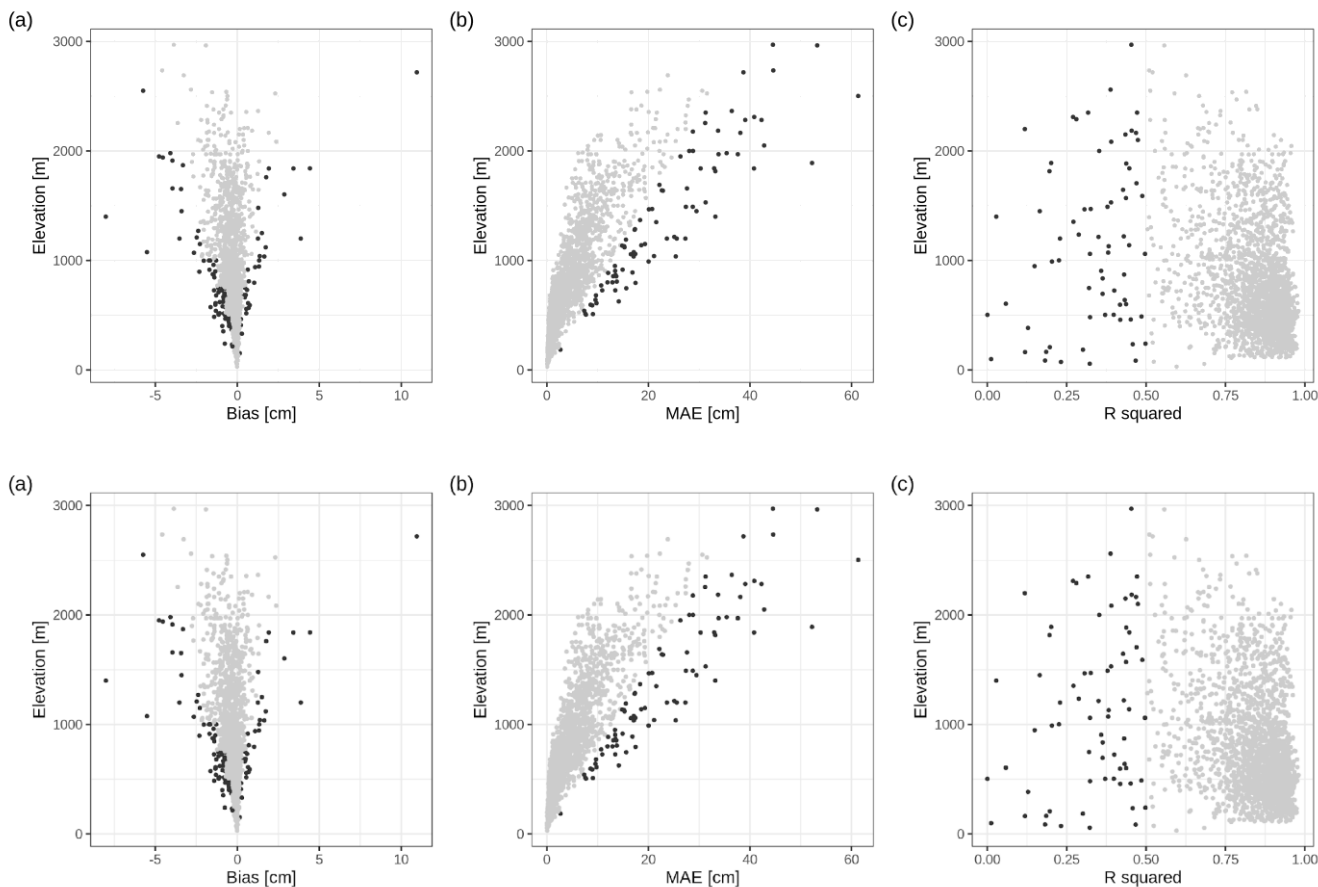
1060 ~~finally the time series of 500 m average HS also showed similar behaviour (Fig. S11). The gap filling was able to~~
~~significantly increase the temporal availability, but its aim was not to fill all gaps.~~ Gaps were not filled, for example, if no
suitable reference station was found or if not enough common data was available.

A.4 Aggregation and spatial consistency

1065 The daily snow depth (HS) values were ~~aggregate~~aggregated to mean monthly HS, if at least 90% of the daily values were
available in the respective months after the gap filling (~~monthly time series plots available at Matiu et al., 2020~~)(monthly
time series plots available at Matiu et al., 2020).

Based on the monthly series, a consistency check was performed (Crespi et al., 2018), which identifies dubious values/series,
(but can also identify series with strong local influences on snow depth). Each monthly HS series of the tested station was
reconstructed from up to five reference stations by a spatial interpolation approach. The reference series were selected if the
1070 monthly record was available and if at least 10 monthly records were in common with the tested station. If more than five
~~neighbors~~neighbours were available, the ones with the highest weights were selected with weights being derived from the
horizontal distance and elevation difference, similar to the gap filling procedure described above. Each reference station
value was rescaled by the ratio between tested and reference mean HS for the month under reconstruction. Finally, the
monthly simulation of the tested series was defined as the median of the up to five rescaled ~~neighboring~~neighbouring values.
1075 The comparison between simulated and observed monthly HS series for each station was evaluated by computing bias,
MAE, and R^2 (squared correlation) from December to February, in order to avoid unreliable low error values due to zeros in
HS records outside of winter.

The mean bias over all stations was -0.3 (min, max: -8.0, 10.9) cm, average MAE was 4.8 (0.1, 61.3) cm, and average R^2
was 0.83 (0.0, 0.98). However, there was a strong elevational dependency, and station metrics deteriorated with elevation
1080 (Fig. ~~A3A4~~). A semi-automatic approach was considered to look for suspicious series. The following criteria were used to
screen stations: bias outside the 95% confidence interval per elevation bands (250 m bands up to 1500 m, then 1500 to 2000
m, and 2000 to 3000 m) or MAE above a manually defined threshold line (see Fig. ~~A3A4~~ (b)) or R^2 below 0.5 or simulation
not successful because of too many gaps. This yielded 225 stations, which were checked manually by looking at monthly
simulated and observed series, and daily series. Only 14 stations were found suspicious and 18 partly suspicious; all 32
1085 series were removed from the ~~following~~-statistical analyses. More detailed results and time series comparing simulated with
observed snow depths are available as auxiliary material (~~Matiu et al., 2020~~)(Matiu et al., 2020).



1090 **Figure A3A4:** Metrics for spatial consistency: (a) bias, (b) mean absolute error (MAE), and (c) R squared (squared correlation). Metrics were derived from statistical simulations of the monthly series from December to February using spatial neighbours. Black points indicate stations which were further analysed with manual checks.

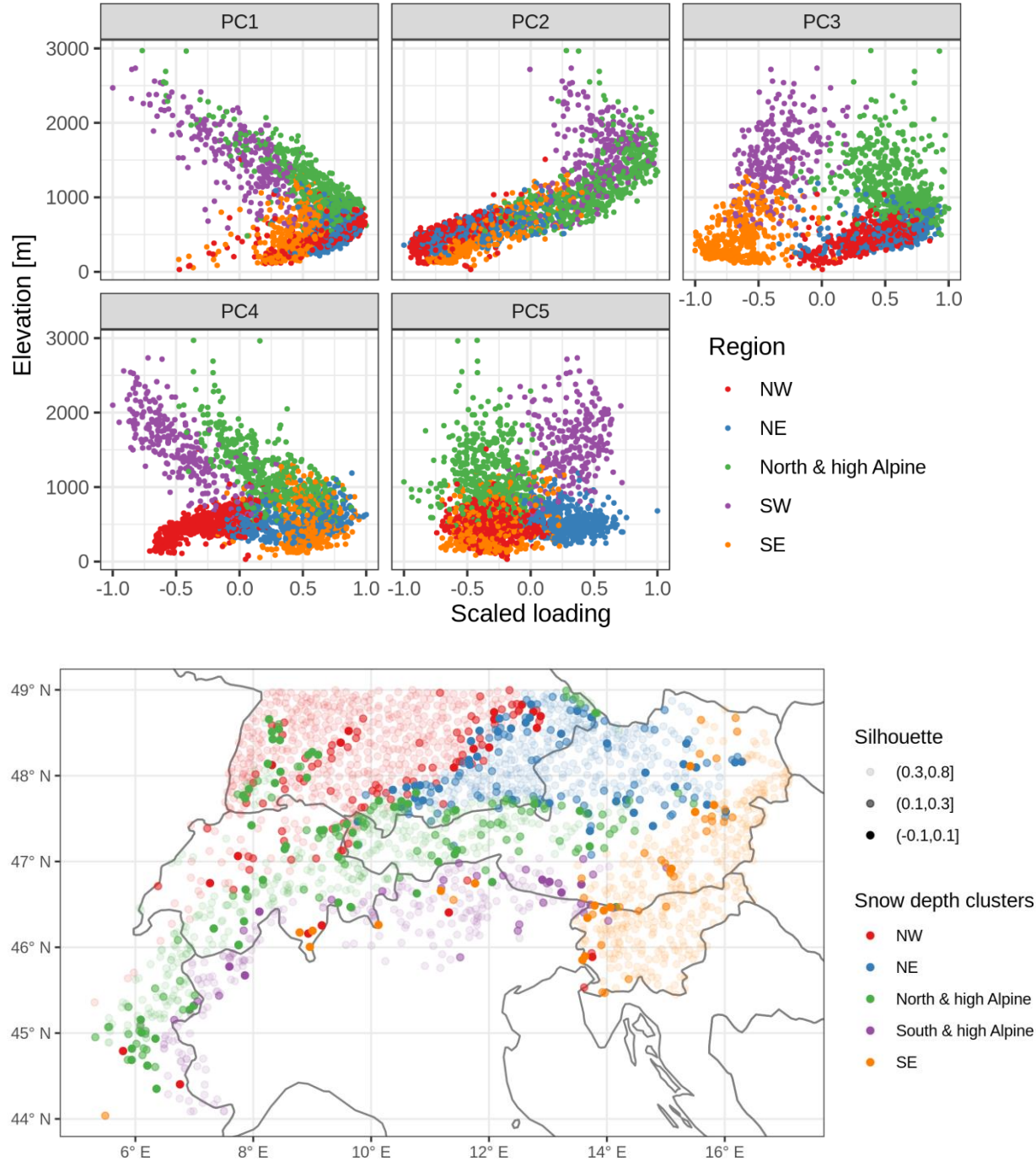


Figure B1: Scatterplots of principal component (PC) loading versus elevation and region. The PC loading can be considered the correlation of the original series with the respective PC. See Fig. 3 for a map of the PC loadings, and Fig. 4 for a map of the regions.

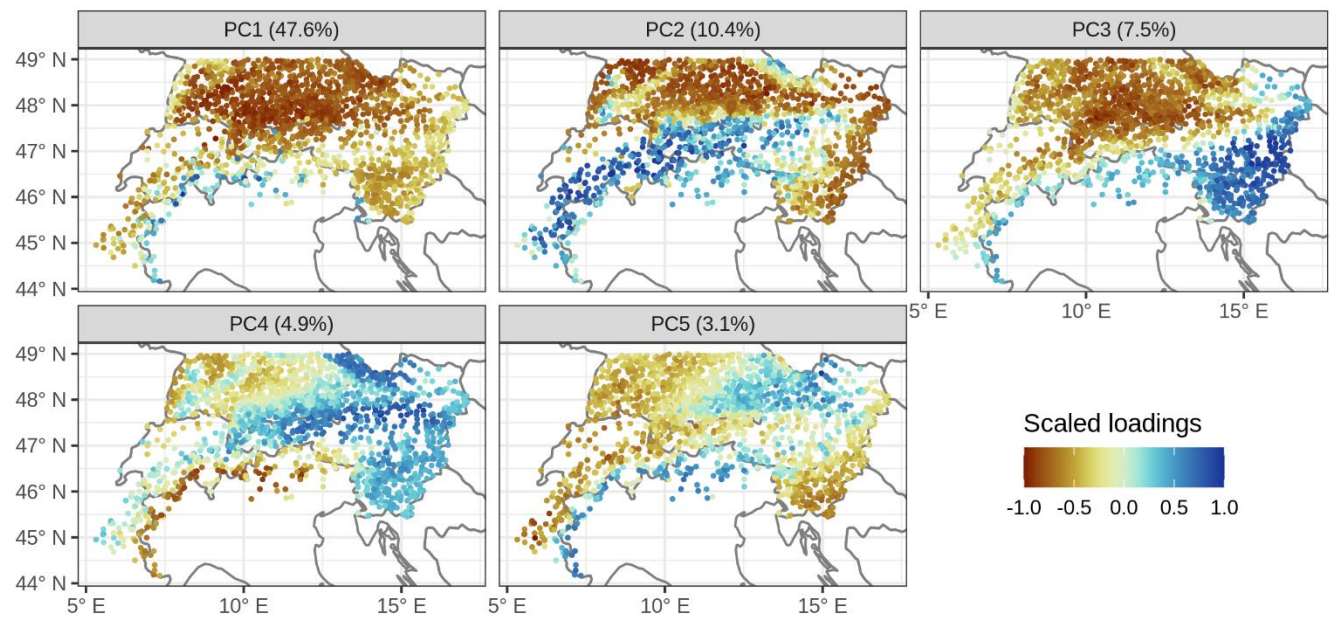


Figure B2: Same as Fig. 3 but using a standard principal component analysis (PCA) and only stations which had complete data. Main modes of variability in daily snow depth series. The plots show scaled loadings for the first five principal components (PCs). The title in each panel contains the amount of variance explained by the respective PC. The principal component analysis was applied on daily snow depth data from December to April for the hydrological years from 1981 to 2010, for stations that had no missing observations.

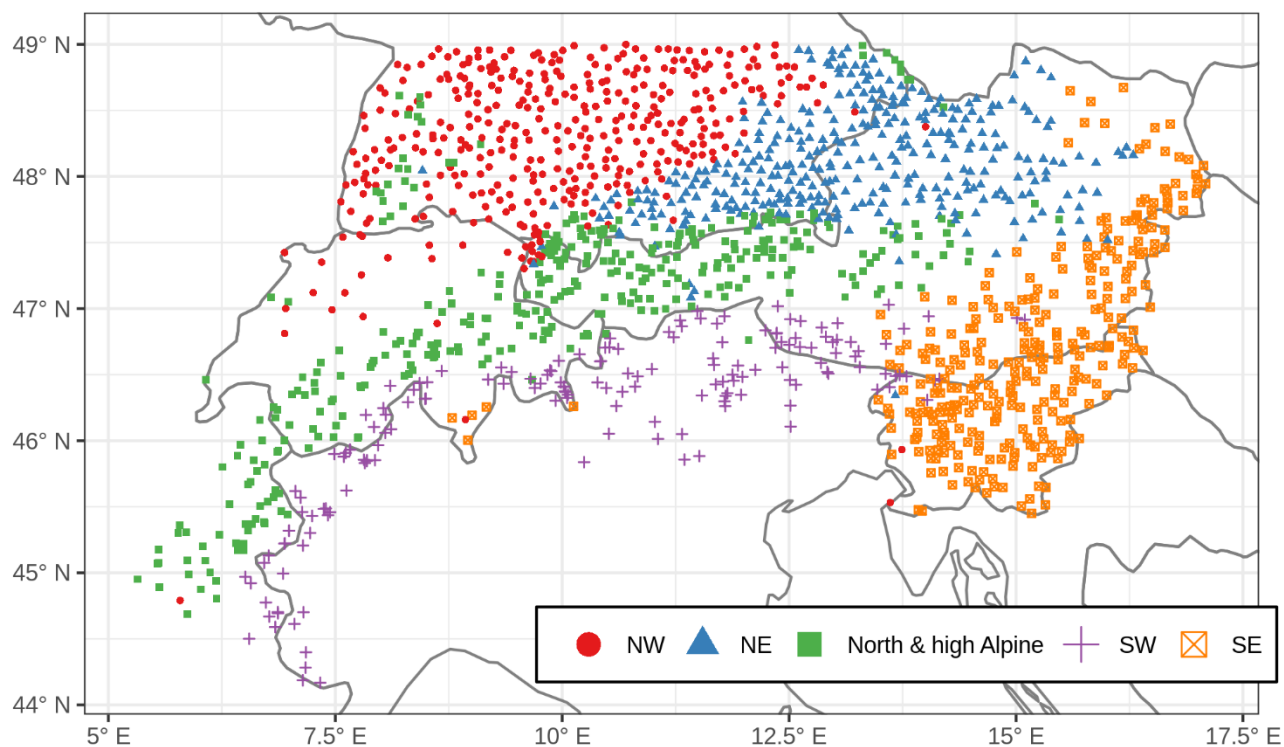


Figure B3: Same as Fig. 4, but based on the PCA from Fig. B2, which is for stations with no missing observations. Clustering of stations based on daily snow depth data. Map of regions from k-means clustering on the first five principal components. See Fig. B2 for the values of the clustering matrix (loadings of the stations).

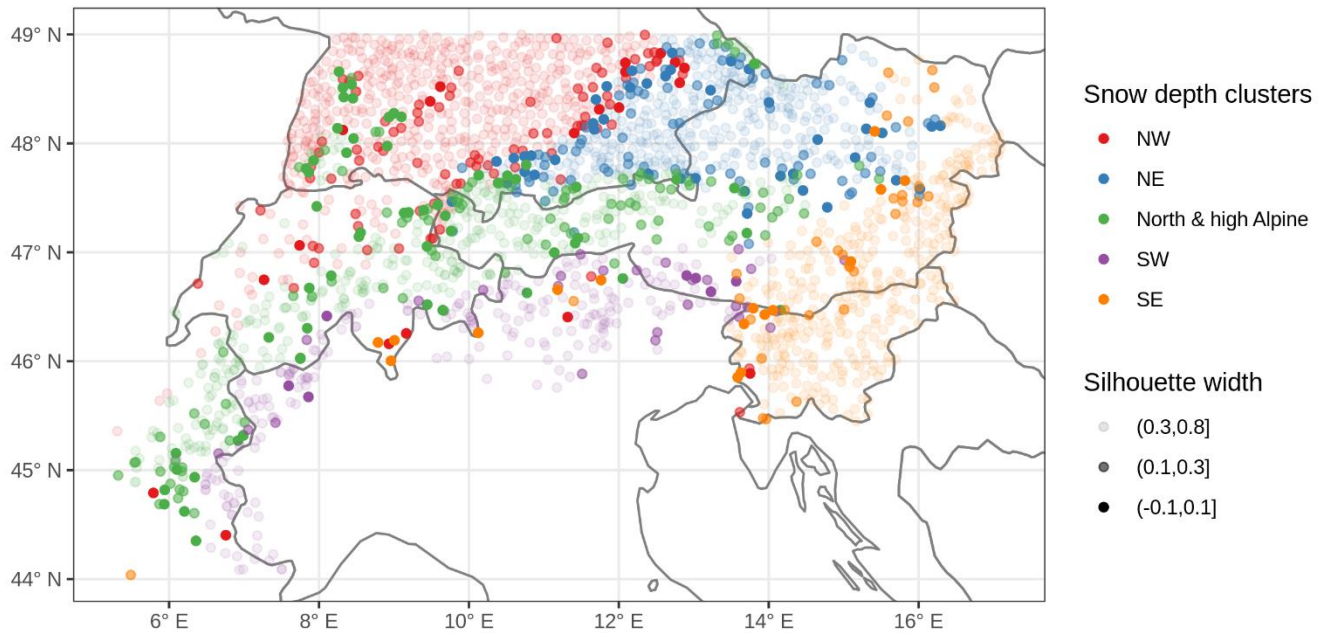


Figure B4: Silhouette values of the stations, which show consistency of clustering. The silhouette is a measure of how similar the station is to its own cluster compared to the other clusters. [\(see methods for formula\)](#). High values indicate a good match, while low and negative values indicate a poor match.

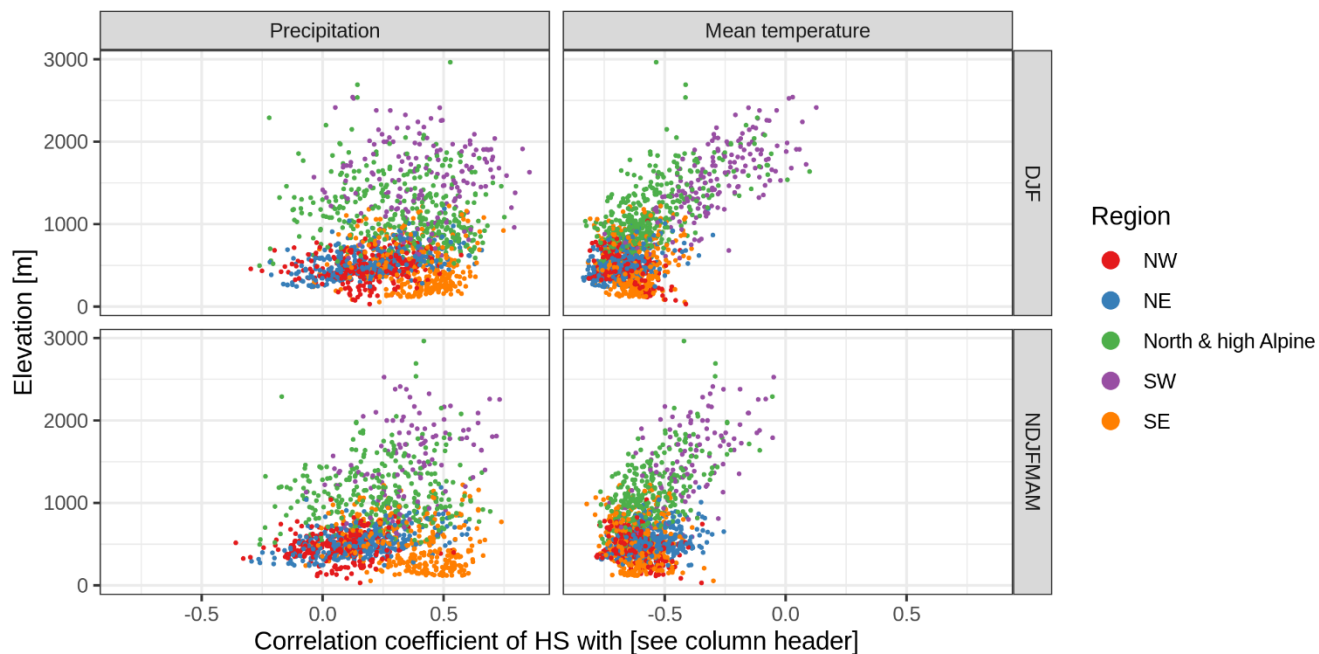


Figure B5: Correlation of station snow depth (HS) with precipitation and temperature extracted from gridded products. Each point shows the Pearson correlation coefficient of seasonal HS with the seasonal sum of precipitation (left column) and with the seasonal mean temperature (right column) for one station. The top row shows the season December to February (DJF), and the bottom row the season November to May (NDJFMAM). The temperature values used in the correlations are extracted from the reanalysis MESCAN SURFEX.

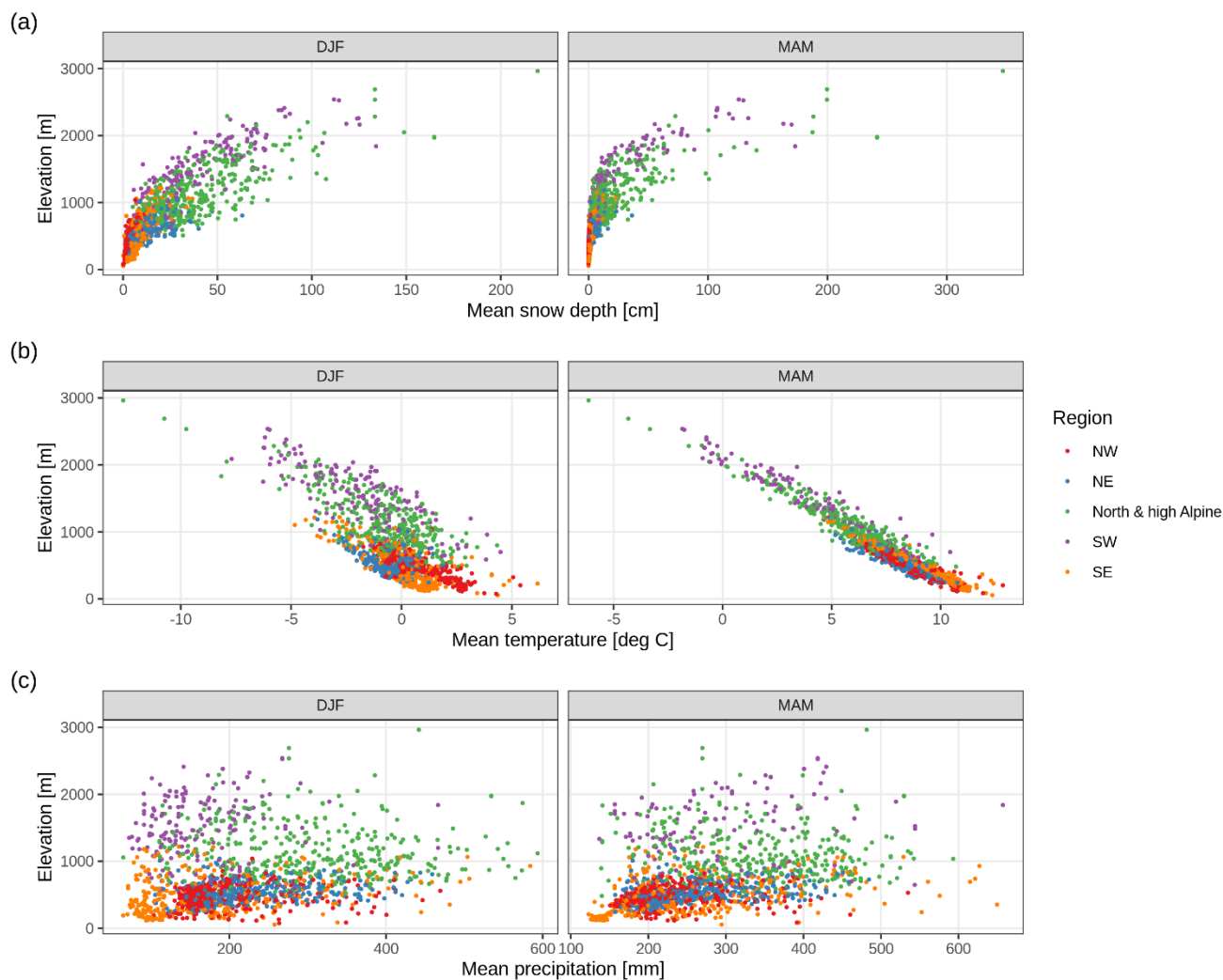


Figure B6: Same as Fig. 7 but using observation based spatial analysis data for temperature and precipitation and the period 1981–2008. Instead of MESCAN-SURFEX reanalysis, here the temperature and precipitation values were extracted from E-OBS and EURO4M-APGD, and the period slightly shortened from 1981–2010 to 1981–2008, because of the shorter availability of EURO4M-APGD.

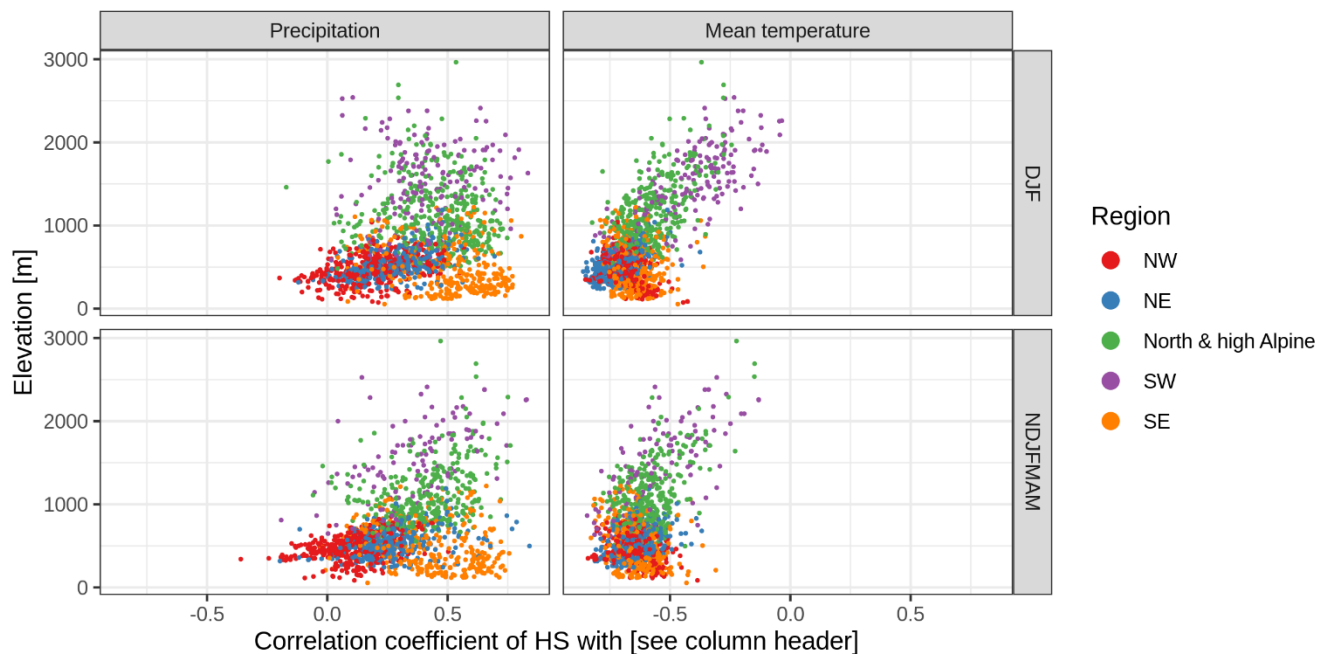


Figure B7: Same as Fig. B5 but using observation-based spatial analysis data for temperature and precipitation and the period 1981–2008. Instead of MESCAN-SURFEX reanalysis, here the temperature and precipitation values were extracted from E-OBS and EURO4M-APGD

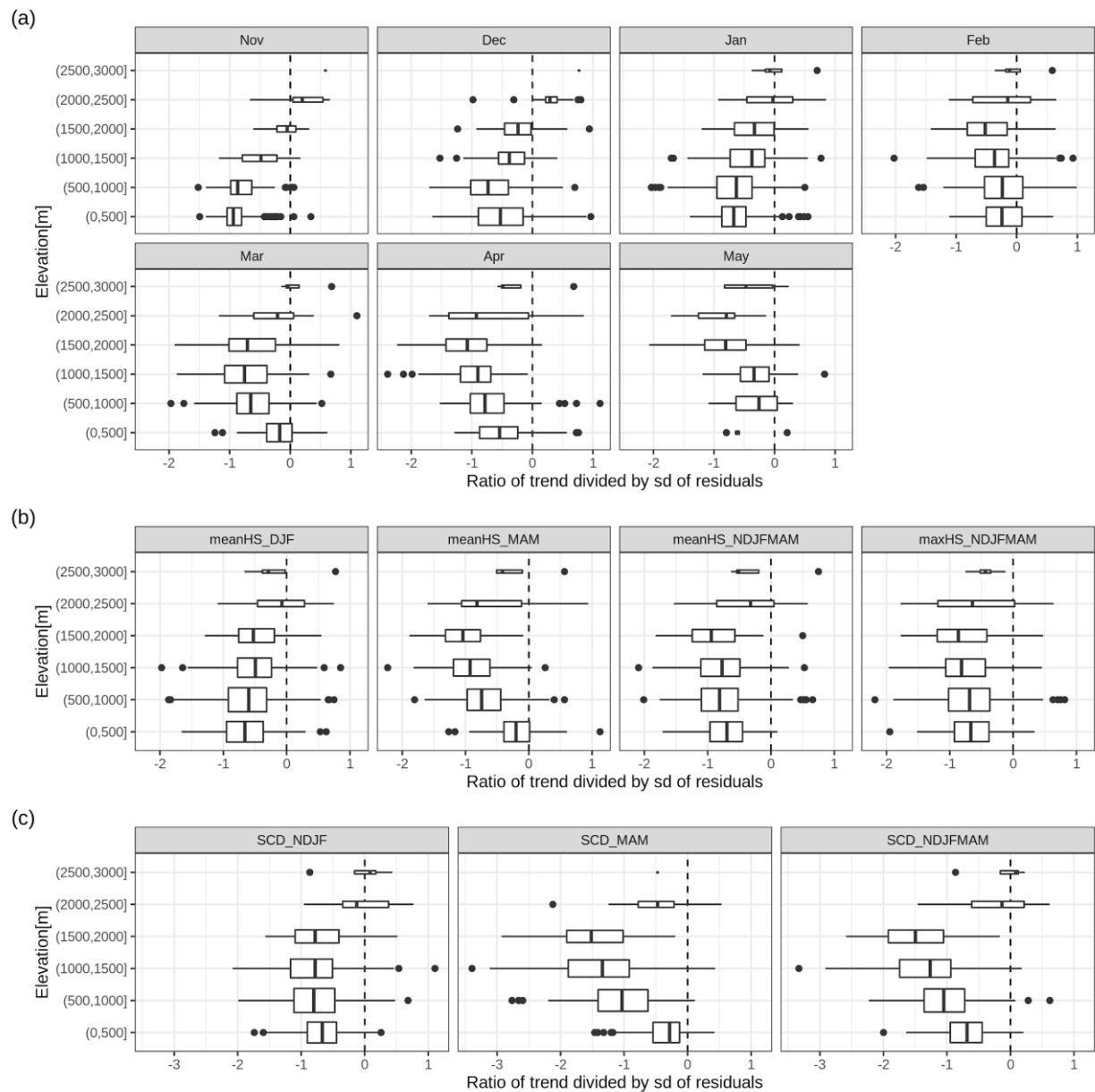


Figure B2: Ratio between the trend over the full period (1971 to 2019) and interannual variability (standard deviation of the residuals). (a) shows the values for monthly mean HS (snow depth), (b) for seasonal indices of HS, and (c) for seasonal indices of SCD (snow cover duration). The boxplots represent statistical quantities: the box indicates the first and third quartile; the bold line inside the box is the median; the vertical lines outside the box extend up to the most extreme point but at most 1.5 times the interquartile-range (IQR; width of the box); finally, points below/above 1.5*IQR of the first/third quartile are shown as separate points. The height of the box is proportional to the number of observations in each group.

Table B1: Overview of literature on snow cover trends in the European Alps.

<u>Area</u>	<u>Number stations</u>	<u>Time period</u>	<u>Season</u>	<u>Snow variable</u>	<u>Methods</u>
<i>(Bach et al., 2018)</i> <i>Mean HS -12.2%/10y (40% stn $p<0.05$); max HS -11.4%/10y (36% stn $p<0.05$); except coldest climates.</i>					
pan-Europe: mostly Germany, Benelux, AT-Tirol, Czech Republic, Slovakia, Finland; partly UK, Balkan, part E of Baltic Sea	(not specified)	1951-2017	DJF	Mean HS; Max HS (95pctl)	OLS if trend pos.; OLS (exp) if trend neg.; Significance: Mann-Kendall
<i>(Beniston, 2012b)</i> <i>10-50% decline in DJF HS (less decline moist north vs. dry south)</i>					
Switzerland	10	1930-2010	DJF; NDJFMA	mean HS, snow days (10cm)	visual; 5yr moving window
<i>(Durand et al., 2009)</i> <i>HS no trend at 2700m, decreases below; n0 negative trends</i>					
French Alps	Modelling: ERA-40, SAFRAN, Crocus	1959-2005	DJF	Mean HS n0 (Number of days with snow) HS100d (minimum 100day snow depth)	300m elevation steps (1500-2700); Spearman correlation (year-n0); Step-year (n0); Linear trend (n0)
<i>(Klein et al., 2016)</i> <i>SCD shorter 8.9days/decade; more because of earlier snow melt (5.8days/decade); decrease in maxHS, and earlier date of maxHS</i>					
Switzerland	11	1970-2015	Sep-Aug	maxHS; date of snow onset, snowmelt, maxHS; SCD; snow days (1,20,50,100)	Theil-Sen, Mann-Kendall; stepwise regression
<i>(Kreyling and Henry, 2011)</i> <i>150 stations showed decrease ($p<0.05$ for 69), 22 positive ($p<0.05$ for 1); decrease accelerated over the last 15yr, -0.48 to -0.89d/yr</i>					
Germany	177	1950-2000	Aug-July	SD (1cm)	OLS; random effects with stations
<i>(Laternser and Schneebeli, 2003)</i> <i>All variables show increase until 1980, followed by significant decrease. Trends more pronounced at mid and low elevation. South != North. Shorter SCD because earlier melt in spring.</i>					
Swiss alps	140 (HS) 120 (HN)	1931-1999	NDJFMA; two-month splits	Mean seasonal HS; SCD (start, end, length); Days with HN > 0, 10, ...; HN3max (max 3 day HN)	Trend analysis; relative to long-term mean; Trend short period equal long period
<i>(Lejeune et al., 2019)</i> <i>39cm less 1990-2017 vs. 1960-1990</i>					
France	1 (Col de Porte)	1960-2017	DJFMA	mean HS	moving window (15yr) and comparison 30yr

<u>Area</u>	<u>Number stations</u>	<u>Time period</u>	<u>Season</u>	<u>Snow variable</u>	<u>Methods</u>
<i>(Marcolini et al., 2017b)</i> <i>different dynamics above and below 1650m; larger reductions at lower elevation; strong change late 1980s</i>					
<u>Italy (BZ+TN)</u>	<u>37</u>	<u>1980-2009</u>	<u>NDJFMA</u>	<u>SCD (>30cm); seasonal HS</u>	<u>homogenization; hovmöller plots; wavelet analysis</u>
<i>(Marty, 2008)</i> <i>Regime shift at end of 1980s, no clear trend since then.</i>					
<u>Switzerland</u>	<u>34</u>	<u>~1931-2008</u>	<u>DJFM</u>	<u>Snow days (5, 30, 50cm)</u>	<u>Mann-Kendall; shift detection</u>
<i>(Marty and Blanchet, 2012)</i> <i>44% of stations show sig decrease in HSmax, 32% for HN3max; decrease in spread of HSmax</i>					
<u>Switzerland</u>	<u>18 (HSmax) 25 (HN3max)</u>	<u>1931-2010</u>	<u>annual</u>	<u>HSmax (annual max HS); HN3max (annual max sum HN 3day)</u>	<u>GEV with time-dependent location and shape</u>
<i>(Marty et al., 2017)</i> <i>SWE decline (independent of lat or long); stronger and more significant decrease in spring (-80% to -10% low to high elevation / 60 years) than winter; winter: some pos non-significant at high elevation.</i>					
<u>alpine wide (AT, FR, DE, IT, CH)</u>	<u>54</u>	<u>1968-2012</u>	<u>index values (spring and winter)</u>	<u>SWE (not continuously measured)</u>	<u>Mann-Kendall; Theil-Sen</u>
<i>(Micheletti, 2008)</i> <i>pos anomalies until end 80s, then shift to low snow amounts until beginning 2000; some recovery, but still below level of 80s</i>					
<u>Italy (FVG)</u>	<u>8</u>	<u>1972-2007</u>	<u>seasonal</u>	<u>sumHN, max of monthly meanHS</u>	<u>timeseries (only descriptive); % anomalies w.r.t. 1972-2007</u>
<i>(Scherrer et al., 2013)</i> <i>strong decadal variability; high values 1900-1920 and 1960-1970/80; lowest values end 1980/1990; increases/plateau 2000s linked to temperature evolution</i>					
<u>Switzerland</u>	<u>9</u>	<u>1864-2009</u>	<u>annual</u>	<u>MAXNS (max annual HN); NSS (sum annual HN); DWSF (days with snowfall)</u>	<u>plots; 20yr smooth; comparison to 71 other stations</u>
<i>(Schöner et al., 2009)</i> <i>largest HS in 1940s/50s; summer snow decreasing; interannual variability of winter precipitation closely related to HS (highest in 40s/50s, strong decreases since -> less extremes)</i>					
<u>Austria</u>	<u>1 (Sonnblick)</u>	<u>1928-2005</u>	<u>monthly</u>	<u>HS</u>	<u>(visual)</u>
<i>(Schöner et al., 2019)</i> <i>EOF groups AT-CH in 7 regions; trend analysis based on first PC; strong trends south ~2000m: up to -12cm/10y; strongest trends at highest elevations; regional dependence of trends</i>					
<u>Switzerland and Austria</u>	<u>196 (139 passed QC)</u>	<u>1961-2012</u>	<u>NDJFMA</u>	<u>seasonal HS and HN</u>	<u>MK-test with lag1 pre-whitening; running trend approach; Sen slope; EOF for regionalization</u>

<u>Area</u>	<u>Number</u> <u>stations</u>	<u>Time period</u>	<u>Season</u>	<u>Snow variable</u>	<u>Methods</u>
<u>(Terzago et al., 2010)</u> <u>more snow Nov-Dec, less Jan-Apr, disappeared in May</u>					
<u>Italy (Piemonte)</u>	<u>3</u>	<u>1971-2009</u>	<u>monthly</u>	<u>HN, HS, snowy days</u> <u>(HN>=1cm)</u>	<u>1971-2000 vs 2000-2009</u>
<u>(Terzago et al., 2013)</u> <u>some maxima 1940,50,60, absolute 1970, absolute minima 1990, then recovery; significant decrease seasonal HS 2-14cm/decade; stronger decreases in North (considering elevation); changes not driven by precip changes; snowfall anticorrelated to NAO</u>					
<u>Italy (West)</u>	<u>6</u>	<u>1926/1951 -</u> <u>2010</u>	<u>DJF, MAM,</u> <u>NDJFMAM</u>	<u>precip, days with precip, solid</u> <u>precip fraction, HN, snowy</u> <u>days (HN>0), HS</u>	<u>trend analysis; Mann-kendall; spectral</u> <u>analysis</u>
<u>(Valt et al., 2008)</u> <u>snow cover decreased 14 days (1991-2007 vs 1960-1990), stronger <1600m (16d) vs >1600m (11d); fresh snow decreased 1990-2000, then stationary (for all altitudes and months)</u>					
<u>Italy (east and west)</u>	<u>5 (west); 6</u> <u>(east)</u>	<u>~1920/1960-</u> <u>2007</u>	<u>Oct-May</u>	<u>snow days (>=1cm); sumHN</u>	<u>(visual)</u>
<u>(Valt and Cianfarra, 2010)</u> <u>NDJFMA CSF shows -3 to -40 cm/10yr for all 18 stations 1960-2009, SCD also all negative; breakpoint ~ 1990, before decrease, after increase; strongest negative trend in spring and below 1500m; neg trend related to precipitation decrease; PCA shows long-term negative trend</u>					
<u>Italy (east and west)</u>	<u>18</u>	<u>1950-2009</u>	<u>DJFMA; DJF;</u> <u>MA</u>	<u>SCD (>1cm); CSF (sum of</u> <u>new snow)</u>	<u>split by 1500m alt; OLS, Mann-Kendall;</u> <u>changepoint; PCA</u>

160 **Table B2: Fraction of models with significantly positive or negative changes in the error variance by time. The remaining percentage (not shown) corresponds to the total of non-significant negative and positive changes. Empty cells no stations with significant negative or positive trends (sig- and sig+). Changes were considered significant if the GLS model with a time coefficient for the error variance showed significantly improved goodness-of-fit compared to the OLS model with constant error variance ($p < 0.05$).**

Region	Nov		Dec		Jan		Feb		Mar		Apr		May	
	sig-	sig+	sig-	sig+	sig-	sig+	sig-	sig+	sig-	sig+	sig-	sig+	sig-	sig+
NW					86.4%		24.4%	5.1%	30.8%	3.1%	76.5%	11.8%		
NE	47.1%	2.9%	16.7%		47.1%	2.9%	4.0%	8.0%	28.6%	4.8%	78.9%		80.0%	
N&hA	53.8%		4.3%		28.9%	0.4%	5.5%	0.4%	22.4%		72.8%		75.3%	4.7%
S&hA	43.9%	4.9%		26.7%	8.0%	8.0%	9.1%	6.4%	14.0%	6.5%	41.1%	1.1%	76.6%	1.6%
SE	72.4%	0.4%	22.6%	2.2%	40.5%	2.4%	18.4%	2.9%	29.1%	2.7%	55.2%	6.3%	100.0%	

165 **Table B3: Overview of shareable data. Column daily indicates if the original daily data can be shared, and monthly if the derived monthly data can be shared.**

Code	Country	Data provider	Daily	Monthly
AT_HZB	Austria	HZB	no	yes
CH_METEOSWISS	Switzerland	MeteoSwiss	no	yes
CH_SLF	Switzerland	SLF	no	yes
DE_DWD	Germany	DWD	yes	yes
FR_METEOFRACTANCE	France	MeteoFrance	yes	yes
IT_BZ	Italy	Bolzano	yes	yes
IT_FVG	Italy	Friuli Venezia Giulia	yes	yes
IT_LOMBARDIA	Italy	Lombardia	yes	yes
IT_PIEMONTE	Italy	Piemonte	no	no
IT_SMI	Italy	SMI	no	no
IT_TN	Italy	Trentino	yes	yes
IT_TN_TUM	Italy	Trentino (TUM)	no	no
IT_VDA_AIBM	Italy	Valle D'Aosta (AIBM)	no	no
IT_VDA_CF	Italy	Valle D'Aosta (CF)	yes	yes
IT_VENETO	Italy	Veneto	no	yes
SI_ARSO	Slovenia	ARSO	no	yes

Appendix C: Seasonal snow indices

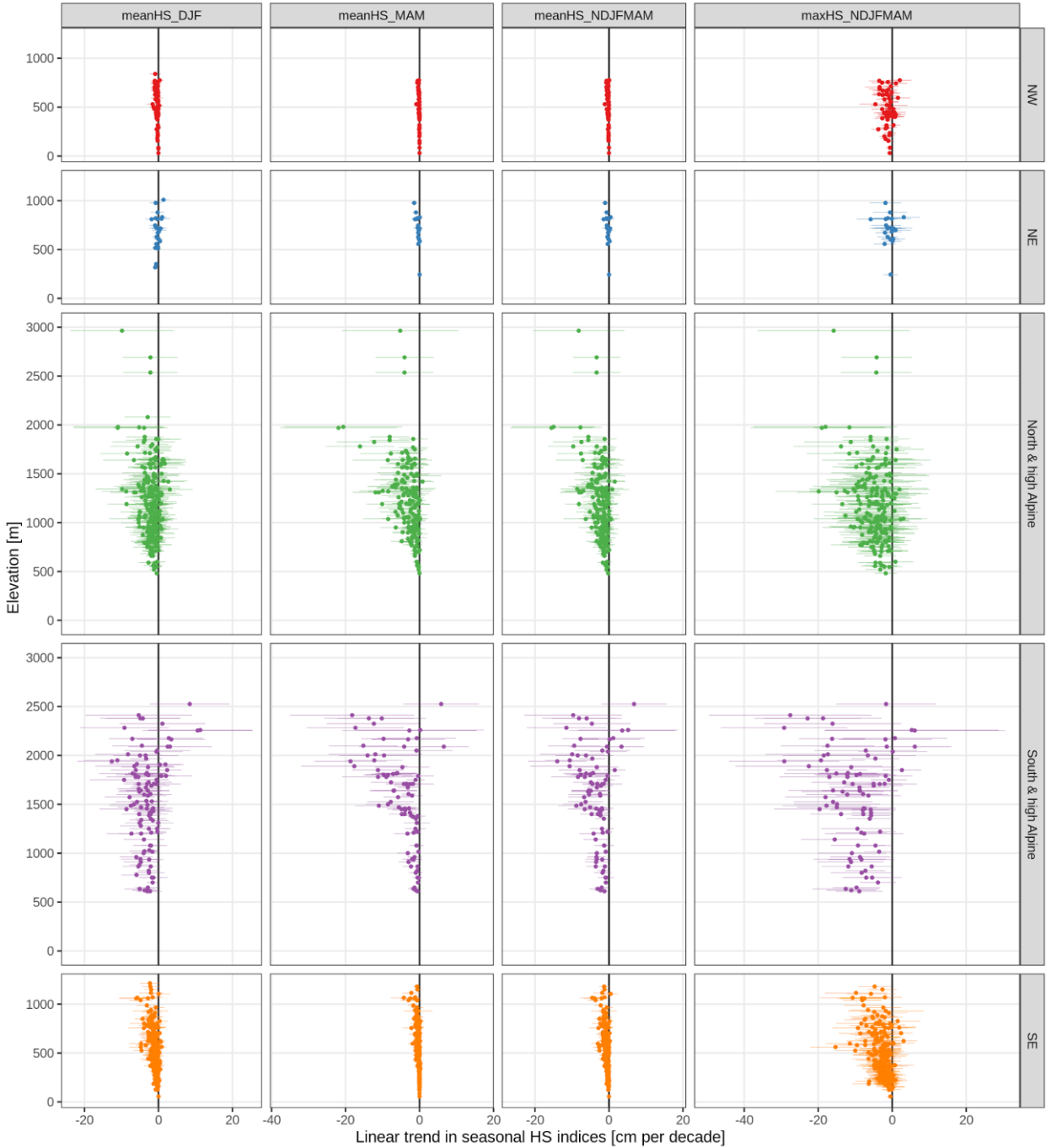
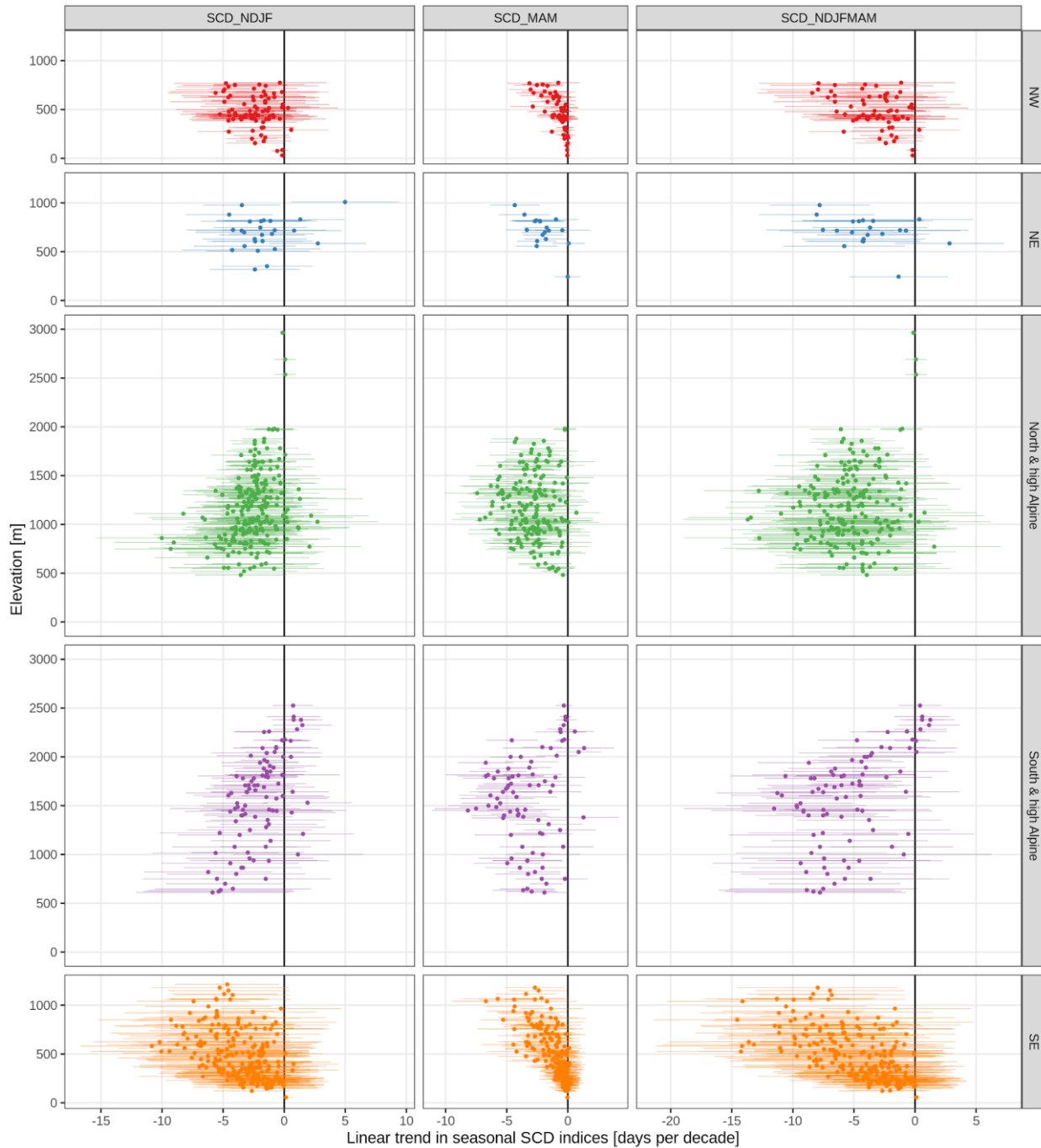
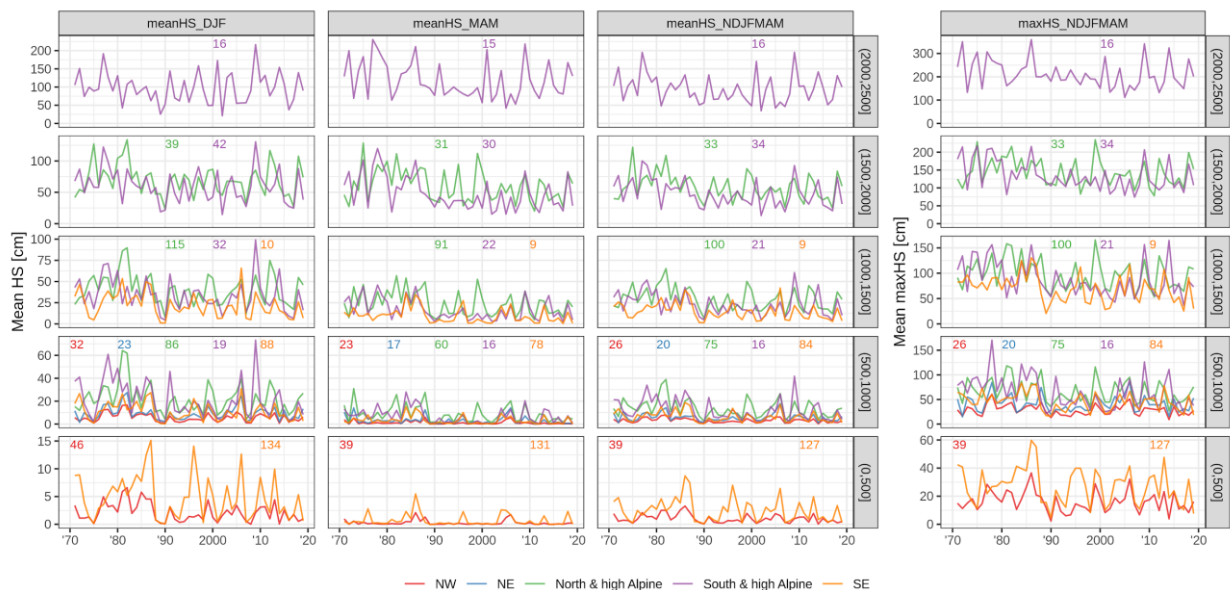


Figure C1: Long-term (1971 to 2019) linear trends in seasonal snow depth (HS) indices. Trends are shown separately by index (columns) and region (rows). The season is indicated in the columns with the first letter of the included months (e.g. DJF is December, January, and February). Each point is one station. The points indicate the trend and the lines the associated 95% confidence interval.



180

Figure C2: Long-term (1971 to 2019) linear trends in seasonal snow cover duration (SCD) indices. Trends are shown separately by index (columns) and region (rows). The season is indicated in the columns with the first letter of the included months (e.g. NDFJ is November, December, January, and February). Each point is one station. The points indicate the trend and the lines the associated 95% confidence interval.



185

Figure C3: Time series of mean seasonal snow depth (HS) indices averaged by 500 m elevation bands. The rows indicate elevation band and the columns the index. The season is indicated in the columns with the first letter of the included months (e.g. DJF is December, January, and February). The small numbers at the top of each panel denote the number of stations included in the average. Lines are only shown if more than 5 stations were available.

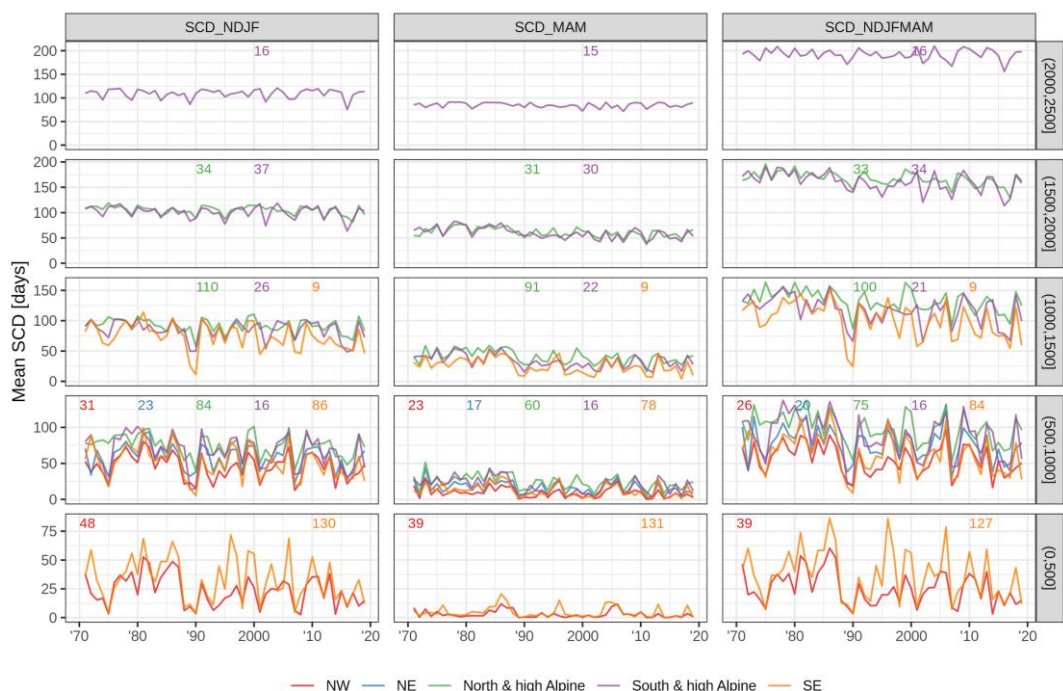


Figure C4: Time series of mean seasonal snow cover duration (SCD) indices averaged by 500 m elevation bands. The rows indicate elevation band and the columns the index. The season is indicated in the columns with the first letter of the included months (e.g. NDJF is November, December, January, and February). The small numbers at the top of each panel denote the number of stations included in the average. Lines are only shown if more than 5 stations were available.

Table C1: Overview of long-term (1971 to 2019) trends in mean seasonal snow depth indices. Summaries are shown by index, region, and 1000 m elevation bands (0 to 1000, 1000 to 2000, and 2000 to 3000 m). Cell values are the number of stations (#), the mean trend (mean, in cm decade⁻¹), and percentages of significant negative (sig-) and positive (sig+) trends; the remaining percentage (not shown) corresponds to the total of non-significant negative and positive trends. Empty cells denote no station available (for # and mean), and no stations with significant negative or positive trends (sig- and sig+). Trends were considered significant if $p < 0.05$. See also Fig. C1. A version of the table with 500 m bands instead of 1000 m is available in the supplementary material (Table S6).

Index	Region	Elevation: (0,1000] m				Elevation: (1000,2000] m				Elevation: (2000,3000] m			
		#	mean	sig-	sig+	#	mean	sig-	sig+	#	mean	sig-	sig+
meanHS DJF	NW	78	-0.38	26.9%									
	NE	25	-0.26	8.0%		1	1.36						
	N&hA	87	-1.64	14.9%		154	-2.09	7.8%		4	-4.28		
	S&hA	19	-3.57	42.1%		74	-3.56	17.6%		17	-0.07	5.9%	
	SE	222	-0.95	22.1%		10	-2.94	50.0%					
meanHS MAM	NW	62	-0.12	9.7%									

<u>Index</u>	<u>Region</u>	<u>Elevation: (0,1000] m</u>				<u>Elevation: (1000,2000] m</u>				<u>Elevation: (2000,3000] m</u>			
		<u>#</u>	<u>mean</u>	<u>sig-</u>	<u>sig+</u>	<u>#</u>	<u>mean</u>	<u>sig-</u>	<u>sig+</u>	<u>#</u>	<u>mean</u>	<u>sig-</u>	<u>sig+</u>
	<u>NE</u>	<u>18</u>	<u>-0.45</u>	<u>11.1%</u>									
	<u>N&hA</u>	<u>61</u>	<u>-1.56</u>	<u>47.5%</u>		<u>122</u>	<u>-3.74</u>	<u>42.6%</u>		<u>3</u>	<u>-4.45</u>		
	<u>S&hA</u>	<u>16</u>	<u>-1.34</u>	<u>43.8%</u>		<u>52</u>	<u>-5.38</u>	<u>69.2%</u>		<u>16</u>	<u>-6.73</u>	<u>31.2%</u>	
	<u>SE</u>	<u>209</u>	<u>-0.24</u>	<u>7.2%</u>	<u>0.5%</u>	<u>9</u>	<u>-1.82</u>	<u>33.3%</u>					
<u>meanHS_NDJFMAM</u>	<u>NW</u>	<u>65</u>	<u>-0.23</u>	<u>41.5%</u>									
	<u>NE</u>	<u>21</u>	<u>-0.31</u>	<u>9.5%</u>									
	<u>N&hA</u>	<u>76</u>	<u>-1.44</u>	<u>32.9%</u>		<u>133</u>	<u>-2.77</u>	<u>27.1%</u>		<u>3</u>	<u>-4.96</u>		
	<u>S&hA</u>	<u>16</u>	<u>-2.15</u>	<u>56.2%</u>		<u>55</u>	<u>-4.38</u>	<u>50.9%</u>		<u>17</u>	<u>-2.91</u>	<u>23.5%</u>	
	<u>SE</u>	<u>211</u>	<u>-0.60</u>	<u>27.0%</u>		<u>9</u>	<u>-2.13</u>	<u>55.6%</u>					
<u>maxHS_NDJFMAM</u>	<u>NW</u>	<u>65</u>	<u>-1.15</u>	<u>16.9%</u>									
	<u>NE</u>	<u>21</u>	<u>-0.82</u>	<u>4.8%</u>									
	<u>N&hA</u>	<u>76</u>	<u>-3.99</u>	<u>19.7%</u>		<u>133</u>	<u>-5.19</u>	<u>20.3%</u>		<u>3</u>	<u>-8.11</u>		
	<u>S&hA</u>	<u>16</u>	<u>-8.87</u>	<u>75.0%</u>		<u>55</u>	<u>-10.33</u>	<u>56.4%</u>		<u>17</u>	<u>-9.37</u>	<u>41.2%</u>	
	<u>SE</u>	<u>211</u>	<u>-2.78</u>	<u>27.0%</u>		<u>9</u>	<u>-6.59</u>	<u>55.6%</u>					

1205 **Code and data availability**

Code and most of the data are available as supplementary material at a public repository (Matiu et al., 2020). See also Sec. 2.6 and Table C1 for more details.

1210 **Table C2: Overview of long-term (1971 to 2019) trends in mean seasonal snow cover duration indices. Summaries are shown by**
index, region, and 1000 m elevation bands (0 to 1000, 1000 to 2000, and 2000 to 3000 m). Cell values are the number of stations (#),
the mean trend (mean, in days decade⁻¹), and percentages of significant negative (sig-) and positive (sig+) trends; the remaining
percentage (not shown) corresponds to the total of non-significant negative and positive trends. Empty cells denote no station
available (for # and mean), and no stations with significant negative or positive trends (sig- and sig+). Trends were considered
1215 **significant if $p < 0.05$. See also Fig. C2. A version of the table with 500 m bands instead of 1000 m is available in the supplementary**
material (Table S7).

Index	Region	Elevation: (0,1000] m				Elevation: (1000,2000] m				Elevation: (2000,3000] m			
		#	mean	sig-	sig+	#	mean	sig-	sig+	#	mean	sig-	sig+
SCD_NDJF	NW	79	-2.44	29.1%									
	NE	25	-1.91	16.0%		1	4.98		100.0%				
	N&hA	85	-3.19	36.5%		144	-2.22	35.4%		3	0.00		
	S&hA	16	-3.71	6.2%		63	-2.11	28.6%		17	-0.25		
	SE	216	-3.59	25.5%		9	-5.17	55.6%					
SCD_MAM	NW	62	-0.83	22.6%									
	NE	18	-2.03	55.6%									
	N&hA	61	-2.59	59.0%		122	-3.04	66.4%					
	S&hA	16	-2.88	75.0%		52	-4.07	78.8%		16	-0.58	12.5%	
	SE	208	-0.98	19.2%		9	-3.54	66.7%					
SCD_NDJFMAM	NW	65	-3.29	35.4%									
	NE	21	-3.87	28.6%									
	N&hA	76	-5.49	57.9%		133	-5.29	72.2%		3	0.00		
	S&hA	16	-6.59	50.0%		55	-6.38	72.7%		17	-0.92	11.8%	
	SE	211	-4.64	32.2%		9	-9.01	100.0%					

Code and data availability

All computations were performed with R statistical software version 4.0.2 (RCoreTeam, 2008). Colors for the figures were taken from scientific color scales (Crameri, 2019) and colorbrewer. Code is available at a repository (Matiu et al., 2020), which includes scripts to read in the different data sources, perform all data pre-processing, quality checks, gap filling, and do all statistical analyses.

Most data providers agreed to share their data: see Table B3 for the availability of daily and monthly values. For the full data set, please contact the main authors (MM or AC); the usage is generally free for research purposes, though explicit consent is required from some data providers, which want to keep track of the usage of the data. The shareable data is available at an open repository (Matiu et al., 2020).

Author contribution

Conceptualization: MM, AC, GB, CM, SM, WS; Data curation: MM, AC, GB, CMC, CM, DCB, GC, MV, WB, PC, GM, SCS, AC, RC, AD, MF, MG, LM, JMS, AS, AT, SU, VW; Formal analysis: MM, AC; Funding acquisition: MM; Investigation: MM; Methodology: MM, AC, CM, SM, WS; Resources: MZ; Software: MM, AC, CMC; Supervision: MM, MZ; Validation: MM, AC; Visualization: MM; Writing – original draft preparation: MM, AC; Writing – review & editing: MM, AC, GB, CMC, CM, SM, WS, GC, LDG, SK, BM, GR, ST, MV, PC, IG, GM, CN, SCS, US, MW, LG.

Competing interests

The authors declare that they have no conflict of interest.

Acknowledgements

We thank the reviewers (two anonymous and Ross Brown) for their comments, which have greatly improved the manuscript.

This project has received funding from the European Union's Horizon 2020 research and innovation programme under the Marie Skłodowska-Curie grant agreement No 795310. This work has benefited from funding from the European Union's Horizon 2020 research and innovation programme under grant agreement No 730203. CNRM/CEN is a member of LabEX OSUG@2020. G.C. acknowledges the support of the Stiftungsfonds für Umweltökonomie und Nachhaltigkeit GmbH (SUN) and likewise the support from the DFG (Deutsche Forschungsgemeinschaft) Research Group FOR2793/1 "Sensitivity of High Alpine Geosystems to Climate Change since 1850 (SEHAG)" grant CH981/3.

We acknowledge the E-OBS dataset from the EU-FP6 project UERRA (~~<https://www.uerra.eu>~~<https://www.uerra.eu>) and the Copernicus Climate Change Service, and the data providers in the ECA&D project (~~<https://www.ecad.eu>~~<https://www.ecad.eu>). For providing us with station data, we are grateful to Günther Geier from the meteorological office and avalanche warning from the province of Bolzano, to Sara Ratto from the Centro Funzionale della Regione Autonoma Valle d'Aosta, and to Gregor Vertačnik from the meteorological office of the Slovenian Environmental Agency.

- Aschauer, J., Bavay, M., Begert, M. and Marty, C.: Comparing methods for gap filling in historical snow depth time series, EGU General Assembly 2020, Online, 4–8 May 2020, EGU2020-17211, doi:<https://doi.org/10.5194/egusphere-egu2020-17211>, 2020.
- 1260 Auer, I., Böhm, R., Jurković, A., Orlik, A., Potzmann, R., Schöner, W., Ungersböck, M., Brunetti, M., Nanni, T., Maugeri, M., Briffa, K., Jones, P., Efthymiadis, D., Mestre, O., Moisselin, J.-M., Begert, M., Brazdil, R., Bochnicek, O., Cegnar, T., Gajić-Čapka, M., Zaninović, K., Majstorović, Ž., Szalai, S., Szentimrey, T. and Mercalli, L.: A new instrumental precipitation dataset for the greater alpine region for the period 1800–2002, *International Journal of Climatology*, 25(2), 139–166, doi:10.1002/joc.1135, 2005.
- 1265 Auer, I., Böhm, R., Jurkovic, A., Lipa, W., Orlik, A., Potzmann, R., Schöner, W., Ungersböck, M., Matulla, C., Briffa, K., Jones, P., Efthymiadis, D., Brunetti, M., Nanni, T., Maugeri, M., Mercalli, L., Mestre, O., Moisselin, J.-M., Begert, M., Müller-Westermeier, G., Kveton, V., Bochnicek, O., Stastny, P., Lapin, M., Szalai, S., Szentimrey, T., Cegnar, T., Dolinar, M., Gajic-Capka, M., Zaninovic, K., Majstorovic, Z. and Nieplova, E.: HISTALP—historical instrumental climatological surface time series of the Greater Alpine Region, *International Journal of Climatology*, 27(1), 17–46, doi:10.1002/joc.1377, 2007.
- 1270 Bach, A. F., Schrier, G. van der, Melsen, L. A., Tank, A. M. G. K. and Teuling, A. J.: Widespread and Accelerated Decrease of Observed Mean and Extreme Snow Depth Over Europe, *Geophysical Research Letters*, 45(22), 12,312–12,319, doi:10.1029/2018GL079799, 2018.
- 1275 Bazile, E., Abida, R., Verelle, A., Le Moigne, P. and Szczypka, C.: MESCAN-SURFEX surface analysis, deliverable D2.8 of the UERRA project. Technical Report European Commission. [online] Available from: <http://uerra.eu/publications/deliverable-reports.html>, 2017.
- Beniston, M.: Impacts of climatic change on water and associated economic activities in the Swiss Alps, *Journal of Hydrology*, 412–413, 291–296, doi:10.1016/j.jhydrol.2010.06.046, 2012a.
- Beniston, M.: Is snow in the Alps receding or disappearing?, *WIREs Climate Change*, 3(4), 349–358, doi:10.1002/wcc.179, 2012b.
- 1280 Beniston, M. and Stoffel, M.: Assessing the impacts of climatic change on mountain water resources, *Science of The Total Environment*, 493, 1129–1137, doi:10.1016/j.scitotenv.2013.11.122, 2014.
- 1285 Beniston, M., Farinotti, D., Stoffel, M., Andreassen, L. M., Coppola, E., Eckert, N., Fantini, A., Giacona, F., Hauck, C., Huss, M., Huwald, H., Lehning, M., López-Moreno, J.-I., Magnusson, J., Marty, C., Morán-Tejeda, E., Morin, S., Naaim, M., Provenzale, A., Rabatel, A., Six, D., Stötter, J., Strasser, U., Terzago, S. and Vincent, C.: The European mountain cryosphere: a review of its current state, trends, and future challenges, *The Cryosphere*, 12(2), 759–794, doi:<https://doi.org/10.5194/tc-12-759-2018>, 2018.
- Bormann, K. J., Brown, R. D., Derksen, C. and Painter, T. H.: Estimating snow-cover trends from space, *Nature Climate Change*, 8(11), 924–928, doi:10.1038/s41558-018-0318-3, 2018.
- 1290 Brown, R. D. and Petkova, N.: Snow cover variability in Bulgarian mountainous regions, 1931–2000, *International Journal of Climatology*, 27(9), 1215–1229, doi:<https://doi.org/10.1002/joc.1468>, 2007.

- Brunetti, M., Maugeri, M., Monti, F. and Nanni, T.: Temperature and precipitation variability in Italy in the last two centuries from homogenised instrumental time series, *International Journal of Climatology*, 26(3), 345–381, doi:10.1002/joc.1251, 2006.
- 295 Buchmann, M., Begert, M., Brönnimann, S. and Marty, C.: Evaluating the robustness of snow climate indicators using a unique set of parallel snow measurement series, *International Journal of Climatology*, n/a(n/a), doi:https://doi.org/10.1002/joc.6863, n.d.
- Cornes, R. C., Schrier, G. van der, Besselaar, E. J. M. van den and Jones, P. D.: An Ensemble Version of the E-OBS Temperature and Precipitation Data Sets, *Journal of Geophysical Research: Atmospheres*, 123(17), 9391–9409, doi:10.1029/2017JD028200, 2018.
- 1300 Crameri, F.: Scientific Colour Maps, Zenodo, DOI: 10.5281/zenodo.3596401., 2019.
- Crespi, A., Brunetti, M., Lentini, G. and Maugeri, M.: 1961–1990 high-resolution monthly precipitation climatologies for Italy, *International Journal of Climatology*, 38(2), 878–895, doi:10.1002/joc.5217, 2018.
- 1305 Durand, Y., Giraud, G., Laternser, M., Etchevers, P., Mérindol, L. and Lesaffre, B.: Reanalysis of 47 Years of Climate in the French Alps (1958–2005): Climatology and Trends for Snow Cover, *J. Appl. Meteor. Climatol.*, 48(12), 2487–2512, doi:10.1175/2009JAMC1810.1, 2009.
- Esposito, A., Engel, M., Ciccazzo, S., Daprà, L., Penna, D., Comiti, F., Zerbe, S. and Brusetti, L.: Spatial and temporal variability of bacterial communities in high alpine water spring sediments, *Research in Microbiology*, 167(4), 325–333, doi:10.1016/j.resmic.2015.12.006, 2016.
- 1310 Gobiet, A., Kotlarski, S., Beniston, M., Heinrich, G., Rajczak, J. and Stoffel, M.: 21st century climate change in the European Alps—A review, *Science of The Total Environment*, 493, 1138–1151, doi:10.1016/j.scitotenv.2013.07.050, 2014.
- Golzio, A., Crespi, A., Bollati, I. M., Senese, A., Guglielmina, A. D., Pelfini, M. and Maugeri, M.: High-Resolution Monthly Precipitation Fields (1913–2015) over a Complex Mountain Area Centred on the Forni Valley (Central Italian Alps), *Advances in Meteorology*, 2018, e9123814, doi:https://doi.org/10.1155/2018/9123814, 2018.
- 1315 Haberkorn, A.: European Snow Booklet – an Inventory of Snow Measurements in Europe, *EnviDat*, doi:https://doi.org/10.16904/envidat.59, 2019.
- Hock, R., Rasul, G., Adler, C., Cáceres, B., Gruber, S., Hirabayashi, Y., Jackson, M., Kääb, A., Kang, S., Kutuzov, S., Milner, A., Molau, U., Morin, S., Orlove, B. and Steltzer, H.: High Mountain Areas, in *IPCC Special Report on the Ocean and Cryosphere in a Changing Climate*, edited by H.-O. Pörtner, D. C. Roberts, V. Masson-Delmotte, P. Zhai, M. Tignor, E. Poloczanska, K. Mintenbeck, A. Alegría, M. Nicolai, A. Okem, J. Petzold, B. Rama, and N. M. Weyer, In press., 2019.
- 1320 IPCC: Summary for Policymakers, in *IPCC Special Report on the Ocean and Cryosphere in a Changing Climate*, edited by H.-O. Pörtner, D. C. Roberts, V. Masson-Delmotte, P. Zhai, M. Tignor, E. Poloczanska, K. Mintenbeck, A. Alegría, M. Nicolai, A. Okem, J. Petzold, B. Rama, and N. M. Weyer, In press., 2019.
- Isotta, F. and Frei, C.: APGD: Alpine precipitation grid dataset, , doi:10.18751/CLIMATE/GRIDDATA/APGD/1.0, 2013.
- 1325 Isotta, F. A., Frei, C., Weilguni, V., Perčec Tadić, M., Lassègues, P., Rudolf, B., Pavan, V., Cacciamani, C., Antolini, G., Ratto, S. M., Munari, M., Micheletti, S., Bonati, V., Lussana, C., Ronchi, C., Panettieri, E., Marigo, G. and Vertačnik, G.: The climate of daily precipitation in the Alps: development and analysis of a high-resolution grid dataset from pan-Alpine rain-gauge data, *Int. J. Climatol.*, 34(5), 1657–1675, doi:10.1002/joc.3794, 2014.

- Keller, F., Goyette, S. and Beniston, M.: Sensitivity Analysis of Snow Cover to Climate Change Scenarios and Their Impact on Plant Habitats in Alpine Terrain, *Climatic Change*, 72(3), 299–319, doi:10.1007/s10584-005-5360-2, 2005.
- 1330 Klein, G., Vitasse, Y., Rixen, C., Marty, C. and Rebetez, M.: Shorter snow cover duration since 1970 in the Swiss Alps due to earlier snowmelt more than to later snow onset, *Climatic Change*, 139(3–4), 637–649, doi:10.1007/s10584-016-1806-y, 2016.
- [Kreyling, J. and Henry, H. A. L.: Vanishing winters in Germany: soil frost dynamics and snow cover trends, and ecological implications, *Climate Research*, 46\(3\), 269–276, doi:10.3354/cr00996, 2011.](#)
- 1335 Laternser, M. and Schneebeli, M.: Long-term snow climate trends of the Swiss Alps (1931–99), *International Journal of Climatology*, 23(7), 733–750, doi:10.1002/joc.912, 2003.
- Lejeune, Y., Dumont, M., Panel, J.-M., Lafaysse, M., Lapalus, P., Gac, E. L., Lesaffre, B. and Morin, S.: 57 years (1960–2017) of snow and meteorological observations from a mid-altitude mountain site (Col de Porte, France, 1325 m of altitude), *Earth System Science Data*, 11(1), 71–88, doi:https://doi.org/10.5194/essd-11-71-2019, 2019.
- 1340 Lencioni, V., Marziali, L. and Rossaro, B.: Diversity and distribution of chironomids (Diptera, Chironomidae) in pristine Alpine and pre-Alpine springs (Northern Italy), *Journal of Limnology*, 70(s1), 106–121, doi:10.4081/jlimnol.2011.s1.106, 2011.
- Leporati, E. and ~~Luea, M~~[Mercalli, L.](#): Snowfall series of Turin, 1784–1992: climatological analysis and action on structures, *Annals of Glaciology*, 19, 77–84, doi:10.3189/S0260305500011010, 1994.
- 1345 López-Moreno, J. I., Soubeyroux, J. M., Gascoin, S., Alonso-Gonzalez, E., Durán-Gómez, N., Lafaysse, M., Vernay, M., Carmagnola, C. and Morin, S.: Long-term trends (1958–2017) in snow cover duration and depth in the Pyrenees, *International Journal of Climatology*, n/a(n/a), doi:10.1002/joc.6571, 2020.
- Mallucci, S., Majone, B. and Bellin, A.: Detection and attribution of hydrological changes in a large Alpine river basin, *Journal of Hydrology*, 575, 1214–1229, doi:10.1016/j.jhydrol.2019.06.020, 2019.
- 1350 Marcolini, G., Bellin, A. and Chiogna, G.: Performance of the Standard Normal Homogeneity Test for the homogenization of mean seasonal snow depth time series, *International Journal of Climatology*, 37(S1), 1267–1277, doi:10.1002/joc.4977, 2017a.
- Marcolini, G., Bellin, A., Disse, M. and Chiogna, G.: Variability in snow depth time series in the Adige catchment, *Journal of Hydrology: Regional Studies*, 13, 240–254, doi:10.1016/j.ejrh.2017.08.007, 2017b.
- 1355 [Marcolini, G., Koch, R., Chimani, B., Schöner, W., Bellin, A., Disse, M. and Chiogna, G.: Evaluation of homogenization methods for seasonal snow depth data in the Austrian Alps, 1930–2010, *International Journal of Climatology*, 39\(11\), 4514–4530, doi:https://doi.org/10.1002/joc.6095, 2019.](#)
- Marty, C.: Regime shift of snow days in Switzerland, *Geophysical Research Letters*, 35(12), doi:10.1029/2008GL033998, 2008.
- 1360 Marty, C. and Blanchet, J.: Long-term changes in annual maximum snow depth and snowfall in Switzerland based on extreme value statistics, *Climatic Change*, 111(3), 705–721, doi:10.1007/s10584-011-0159-9, 2012.
- Marty, C., Tilg, A.-M. and Jonas, T.: Recent Evidence of Large-Scale Receding Snow Water Equivalents in the European Alps, *J. Hydrometeor.*, 18(4), 1021–1031, doi:10.1175/JHM-D-16-0188.1, 2017.

- 1365 Matiu, M., Crespi, A., Bertoldi, G., Carmagnola, C. M., [Marty, C.](#), Morin, S., [Schöner, W.](#), Cat Berro, D., Chiogna, G., [De Gregorio, L.](#), Kotlarski, S., [Majone, B.](#), [Resch, G.](#), [Terzago, S.](#), Valt, M., Beozzo, W., Cianfarra, P., Gouttevin, I., [Marcolini, G.](#), [Notarnicola, C.](#), [Petitta, M.](#), Scherrer, S. [C.](#), [C.](#), [Strasser, U.](#), [Winkler, M.](#), [Zebisch, M.](#), Cicogna, A., [Cremonini, R.](#), [Debernardi, A.](#), [Faletto, M.](#), Gaddo, M., [Giovannini, L.](#), [Mercalli, L.](#), Soubeyroux, J.-M., Sušnik, A., Trenti, A., Urbani, S. and Weilguni, V.: Snow cover in the European Alps: Station observations of snow depth and depth of snowfall (Version v1.0) [Data set], Zenodo, doi:10.5281/zenodo.40641294064128, 2020.
- 1370 Micheletti, S.: Cambiamenti Climatici in Friuli-Venezia-Giulia, Neve e Valanghe, 63 [online] Available from: <https://issuu.com/aineva7/docs/nv63>, 2008.
- Najafi, M. R., Zwiers, F. and Gillett, N.: Attribution of the Observed Spring Snowpack Decline in British Columbia to Anthropogenic Climate Change, *J. Climate*, 30(11), 4113–4130, doi:10.1175/JCLI-D-16-0189.1, 2017.
- 1375 Nitu, R., Roulet, Y.-A., Wolff, M., Earle, M., Reverdin, A., Smith, C., Kochendorfer, J., Morin, S., Rasmussen, R., Wong, K., Alastrué, J., Arnold, L., Baker, B., Buisán, S., Collado, J. L., Colli, M., Collins, B., Gaydos, A., Hannula, H.-R., Hoover, J., Joe, P., Kontu, A., Laine, T., Lanza, L., Lanzinger, E., Lee, G. W., Lejeune, Y., Leppänen, L., Mekis, E., Panel, J.-M., Poikonen, A., Ryu, S., Sabatini, F., Theriault, J., Yang, D., Genthon, C., Heuvel, F. van den, Hirasawa, N., Konishi, H., Motoyoshi, H., Nakai, S., Nishimura, K., Senese, A. and Amashita, K.: WMO Solid Precipitation Intercomparison Experiment (SPICE) (2012 - 2015), World Meteorological Organization (WMO). [online] Available from: <https://www.wmo.int/pages/prog/www/IMOP/publications-IOM-series.html>, 2018.
- 1380 Notarnicola, C.: Hotspots of snow cover changes in global mountain regions over 2000–2018, *Remote Sensing of Environment*, 243, 111781, doi:10.1016/j.rse.2020.111781, 2020.
- Pierce, D. W., Barnett, T. P., Hidalgo, H. G., Das, T., Bonfils, C., Santer, B. D., Bala, G., Dettinger, M. D., Cayan, D. R., Mirin, A., Wood, A. W. and Nozawa, T.: Attribution of Declining Western U.S. Snowpack to Human Effects, *J. Climate*, 21(23), 6425–6444, doi:10.1175/2008JCLI2405.1, 2008.
- 1385 [Pifferetti, M.](#), Cat Berro, D., [Mercalli, L.](#), [Ricciardi, G.](#) and [Buffa, A.](#): [La neve nella Pianura Padano-veneta: nuova cartografia 1961-2017](#), *Nimbus*, 77, 2017.
- [Pinheiro, J. C. and Bates, D. M.](#): [Mixed-effects models in S and S-PLUS](#), Springer, New York., 2000.
- 1390 Prein, A. F. and Gobiet, A.: Impacts of uncertainties in European gridded precipitation observations on regional climate analysis, *International Journal of Climatology*, 37(1), 305–327, doi:10.1002/joc.4706, 2017.
- Pulliainen, J., Luoju, K., Derksen, C., Mudryk, L., Lemmetyinen, J., Salminen, M., Ikonen, J., Takala, M., Cohen, J., Smolander, T. and Norberg, J.: Patterns and trends of Northern Hemisphere snow mass from 1980 to 2018, *Nature*, 581(7808), 294–298, doi:10.1038/s41586-020-2258-0, 2020.
- 1395 RCoreTeam: R: A language and Environment for Statistical Computing, R Foundation for Statistical Computing, Vienna, Austria., 2008.
- Resch, G., Chimani, B., Koch, R., Schöner, W. and Marty, C.: Homogenization of long-term snow observations, EGU General Assembly 2020, Online, 4–8 May 2020, EGU2020-8807, doi:<https://doi.org/10.5194/egusphere-egu2020-8807>, 2020.
- 1400 Salzmann, N. and Mearns, L. O.: Assessing the Performance of Multiple Regional Climate Model Simulations for Seasonal Mountain Snow in the Upper Colorado River Basin, *J. Hydrometeor.*, 13(2), 539–556, doi:10.1175/2011JHM1371.1, 2011.

- Scherrer, S. C. and Appenzeller, C.: Swiss Alpine snow pack variability: major patterns and links to local climate and large-scale flow, *Climate Research*, 32(3), 187–199, doi:10.3354/cr032187, 2006.
- Scherrer, S. C., Wüthrich, C., Croci-Maspoli, M., Weingartner, R. and Appenzeller, C.: Snow variability in the Swiss Alps 1864–2009, *International Journal of Climatology*, 33(15), 3162–3173, doi:10.1002/joc.3653, 2013.
- 1405 Schöner, W., Auer, I. and Böhm, R.: Long term trend of snow depth at Sonnblick (Austrian Alps) and its relation to climate change, *Hydrological Processes*, 23(7), 1052–1063, doi:10.1002/hyp.7209, 2009.
- Schöner, W., Koch, R., Matulla, C., Marty, C. and Tilg, A.-M.: Spatiotemporal patterns of snow depth within the Swiss-Austrian Alps for the past half century (1961 to 2012) and linkages to climate change, *International Journal of Climatology*, 39(3), 1589–1603, doi:10.1002/joc.5902, 2019.
- 1410 Schwaizer, G., Keuris, L., Nagler, T., Derksen, C., Luoju, K., Marin, C., Metsämäki, S., Mudryk, L., Naegeli, K., Notarnicola, C., Salberg, A.-B., Solberg, R., Wiesmann, A., Wunderle, S., Essery, R., Gustafsson, D., Krinner, G. and Trofaier, A.-M.: Towards a long term global snow climate data record from satellite data generated within the Snow Climate Change Initiative, *EGU General Assembly 2020*, Online, 4–8 May 2020, EGU2020-19228, doi:https://doi.org/10.5194/egusphere-egu2020-19228, 2020.
- 1415 Steger, C., Kotlarski, S., Jonas, T. and Schär, C.: Alpine snow cover in a changing climate: a regional climate model perspective, *Clim Dyn*, 41(3–4), 735–754, doi:10.1007/s00382-012-1545-3, 2013.
- Steiger, R. and Stötter, J.: Climate Change Impact Assessment of Ski Tourism in Tyrol, *Tourism Geographies*, 15(4), 577–600, doi:10.1080/14616688.2012.762539, 2013.
- Storch, H. von and Zwiers, F. W.: *Statistical Analysis in Climate Research*, Cambridge University Press, Cambridge., 1999.
- 1420 Taylor, M. H., Losch, M., Wenzel, M. and Schröter, J.: On the Sensitivity of Field Reconstruction and Prediction Using Empirical Orthogonal Functions Derived from Gappy Data, *J. Climate*, 26(22), 9194–9205, doi:10.1175/JCLI-D-13-00089.1, 2013.
- Terzago, S., Cassardo, C., Cremonini, R. and Fratianni, S.: Snow Precipitation and Snow Cover Climatic Variability for the Period 1971–2009 in the Southwestern Italian Alps: The 2008–2009 Snow Season Case Study, *Water*, 2(4), 773–787, doi:10.3390/w2040773, 2010.
- 1425 Terzago, S., Fratianni, S. and Cremonini, R.: Winter precipitation in Western Italian Alps (1926–2010), *Meteorol Atmos Phys*, 119(3), 125–136, doi:10.1007/s00703-012-0231-7, 2013.
- Valt, M. and Cianfarra, P.: Recent snow cover variability in the Italian Alps, *Cold Regions Science and Technology*, 64(2), 146–157, doi:10.1016/j.coldregions.2010.08.008, 2010.
- 1430 Valt, M., Cagnatti, A., Crepaz, A. and Cat Berro, D.: Variazioni Recenti del Manto Nevoso sul Versante Meridionale delle Alpi, *Neve e Valanghe*, 63 [online] Available from: <https://issuu.com/aineva7/docs/nv63>, 2008.